

**Development of a Benchmarking Methodology for
Evaluating Oxidation Ditch Control Strategies**

Abdalla A. A. Abusam

NN08201, 3029

Abdalla Abdelgadir Ahmed Abusam

**Development of a Benchmarking Methodology for
Evaluating Oxidation Ditch Control Strategies**

PROEFSCHRIFT

ter verkrijging van de graad van doctor
op gezag van de rector magnificus
van Wageningen Universiteit,
prof. dr. ir. L. Speelman,
in het openbaar te verdedigen
op maandag 17 september 2001
des namiddags te half twee in de Aula

usn 1626084

CIP-Data Koninklijke Bibliotheek, DEN HAAG

Abusam, A. A. A.

Development of a Benchmarking Methodology for Evaluating Oxidation Ditch Control Strategies/

A. A. A. Abusam

[S.I. :s.n.]

Thesis Wageningen University. – With ref. – With summary in Dutch

ISBN 90-5808-422-1

**Propositions attached to the thesis:
 "Development of a benchmarking methodology for evaluating oxidation
 ditch control strategies", by A. A. A. Abusam**

1. Oxidation ditches have many advantages over other activated sludge systems.
2. *"In modern water management models are indispensable."*
 R.H. van Waveren (1999), Wat. Sci. Tech. 39(4):13-20.
3. 10 to 15 CSTR's are adequate for modeling the effluent quality of an oxidation ditch.
4. The response surface method (RSM) leads in a systematic way to good initial guesses of complex system parameters.
5. Any horizontal (recirculation) velocity in the range of 0.25 to 0.60 m/s is often recommended to prevent settling of organic matters to the channel bottom, however, variations of the horizontal velocity within this range significantly affect the nitrogen removal process in oxidation ditches.
6. Influent step feeding will not significantly influence the internal distribution of the sludge in oxidation ditches.
7. Although it is rarely carried out, backward uncertainty analysis results in very useful information.
8. *"Employing a vacuum flush in toilets and separating these toilet flushes at source from the remaining grey sewage and urban surface runoff is sufficient to open a myriad combinatorial possibilities for the composition of a wastewater infrastructure."*
 M.B. Beck (1999), Wat. Sci. Tech. 39(4):1-11.
9. Future is for decentralized and individual household wastewater treatment systems.
10. In the near future, the ethical ramification of research on human cloning will be one of the most controversial issues.
11. For some this is the 3rd millennium, for the Egyptians it is the 7th millennium, for the Mayans it is the 9th millennium, for some others it is more than that.

Abstract

Abusam, A.A.A. (2001), Development of a benchmarking methodology for evaluating oxidation ditch control strategies, Ph.D. thesis, Wageningen University, Wageningen, The Netherlands.

The purpose of this thesis was to develop a benchmarking methodology for evaluating control strategies for oxidation ditch wastewater treatment plants. A benchmark consists of a description of the plant layout, a basic simulation model (reactor, settler, sensors and actuators models) and definitions of (controller) performance criteria. The goal was achieved by outlining the procedure for developing such a benchmark for a specific full-scale WWTP, using available process data. For other WWTP's, the same procedure can be followed.

In developing the basic simulation model, first a loop-of-CSTR's model, without back-flows, was chosen for modeling oxidation ditches because it is simple and can be used for control purposes. Based on this model, a new method for estimating the standard oxygen transfer rate (*SOTR*), under clean water conditions, was developed and tested successfully. The new method estimates the *SOTR* on the bases of the aeration constant, which is the product of $K_L a$ and volume of aerated compartment, because neither $K_L a$ nor the volume of aerated compartment can be individually identified. Under process conditions, *C*-oxidation and nitrification processes were assumed to take place in the aerated zones, whereas the denitrification process was assumed to occur in the anoxic zones. For modeling the biochemical processes, *ASM No. 1* was used, whereas for modeling the secondary settler the non-reactive double-exponential settling velocity model was used. Based on influent-effluent concentrations, it was found that hydraulics of oxidation ditches can be approximated by 10 to 15 CSTR's. The oxidation ditch model was then calibrated successfully using a novel calibration strategy, which is based on response surface analysis. Prior to a formal parameter estimation step, the response surface analysis provides insight in the parameter sensitivity and initial estimates. Because the study was limited to *C* and *N* removal processes, only models of *DO* and *N* sensors were developed. The actuators, pumps and valves, were assumed to work perfectly, that is: dynamics and time delays of these actuators were neglected.

Evaluation criteria were then developed by modifying the criteria proposed by both COST 624 Working Group and IWA Task Group on Respirometry. Modifications were mainly made in the aeration and pumping energy equations, because oxidation ditches use mechanical aerators that are different from air diffusers adopted by COST 624 and IWA Working Groups. In addition, long-term evaluation criteria were also developed.

Further, sensitivity analysis was carried out to determine parameters of *ASM No. 1* that require special attention from the benchmark user. Sensitivity analysis was carried out using the factorial sensitivity analysis methodology. The main advantage of this methodology is that more information about the interactions (non-linearities) can be obtained. Also, the effect of the various sources of uncertainty on the performance indices was investigated. Estimation of the uncertainty contribution of the various sources is very important because it enables the benchmark user to make an appropriate selection among different control strategies. It is equally important for designing experimental or monitoring programs with the aim of reducing the uncertainty.

Finally, the benchmarking procedure was described and demonstrated by using it to evaluate some basic and advanced control strategies. Basic control strategies studied were (i) splitting the influent flow between the aerated compartments, (ii) rate of activated sludge recirculated and (iii) aeration patterns. The benchmark was also used in studying the effect of the horizontal (recirculation) velocity on nitrogen removal process. Here, the horizontal velocity was considered as a manipulated control variable, to obtain maximum *TN* removal efficiency.

Keywords: wastewater, oxidation ditch, carrousel, modeling, activated sludge, *ASM No. 1*, oxygen transfer rate, aeration, parameter estimation, calibration, sensitivity analysis, uncertainty analysis, sensors, horizontal velocity, benchmark, benchmarking, control strategies, simulation.

To the memory of my parents

Acknowledgements

It is a great pleasure that now I have the chance to thank those who have contributed to this thesis. First I would like to express my sincere gratitude to my promoter, Prof. Dr. ir. Gerrit van Straten, for giving me the opportunity to pursue my doctoral studies at the Systems and Control Group and for the wonderful guidance, constructive discussions, valuable suggestions and critical readings of my work.

My deep appreciations are also due to Dr. ir. Karel J. Keesman, my co-promotor and daily supervisor, for choosing the benchmarking problem for me. I also thank him for the skillful guidance and suggestions, for the prompt advice whenever I contacted him, and for the constructive discussions of my work-plans. As a matter of fact, I am also grateful to Dr. ir. Ton van Boxtel, who introduced me to Dr. ir. Karel Keesman.

My grateful thanks are also due to Dr. ir. Henry Spanjers, my co-promotor, for all the joyful discussions we had, for his thorough comments over my writings and his sharp criticisms with "the right word at the right place", for the valuable help in reaching the relevant literature, especially the Dutch literature, and for the contacts he made for me with a number of treatment plants and water authorities.

I am deeply indebted to ir. Kees Meinema, from DHV Water, for the discussions we had, for his contribution to the writing of most of the papers, for checking the benchmarking procedure, and for the practical experiences he has put into my work.

I gratefully acknowledge the fruitful discussions by Dr John B. Copp, the coordinator of the IWA Task Group on Respirometry, who used to attend our meetings during his stay in Wageningen. I also thank him for his willingness to answer my questions even after he has returned back to Canada, through the e-mail.

I am grateful to the Board of the University of Wageningen for giving me the permission to pursue my study at Wageningen University. In particular, I would like to thanks the former Dean for international students, Ms. Jennine Herman and the coordinator of the environmental studies, ir. Dick Legger.

I also greatly appreciate the help given by DHV Water in the Netherlands, in terms of real data used in this study and financial support for presenting a paper at the Watermatex2000 conference held in Gent, Belgium. In particular, I would like to thank B.P.A. Hoitink and E.F.J. van Heijden who helped me to collect the data.

I would like also to thank ir. F.T. van Breukelen of Hoogheemraadschap van Schieland, for providing me with extra real data of the full-scale wastewater treatment plant that I have studied.

I also thank Ad de Man of Zuiveringschap Limburg for giving me the chance to present and discuss the thesis findings with the Dutch and Flemish experts.

I also would like to thank Prof. Dr. ir. P.A. Vanrollegem from the Department of Biomath., Gent University, Belgium, for the discussions, encouragements and for sending me real data that I used to test the model I proposed for the seasonal effects of temperature.

I thank my Mexican office-mate, Irineo Lopez, for the nice time we have spent either working, discussing or just talking. I also thank him for helping me to solve some of the computer problems. In the name of my family, I also would like to thank his family for the friendly relationship they have with my family.

I also would like to thank all the staff of Systems and Control Group for the friendly treatment. In particular, I would like to thank the computer system manager, Henk Veen, for solving my computer troubles. I also like to thank the "De feestcommissie": Gerard van willenburg, Ilse quirijns, Camile Hol (recently moved back to Delft Technical University) and Stephan de Graaf who used to encourage us (me and Irineo) to participate in the social activities taking place in the department. I also thank Camile Hol for making a really nice Dutch Summary (Samenvatting) out of my translation trials.

Lastly but not least, I would like to thank my wife Nagat and my daughter Razan for the continued support and encouragements. I also like to thank my brothers, sisters, relatives and friends in Sudan, USA and the Netherlands for the continued encouragements.

Table of contents

| | |
|---------------------------------------------------------------------------------------------------------------|----------|
| Abstract | iv |
| Dedication | v |
| Acknowledgements | vi |
| 1. Introduction | 1 |
| 1.1 Background | 1 |
| 1.1.1 Biological wastewater treatment plants | 1 |
| 1.1.2 Oxidation ditches | 2 |
| 1.1.3 Need for advanced control systems in biological WWTP's | 5 |
| 1.2 Defining the benchmarking problem | 6 |
| 1.3 Research objectives | 6 |
| 1.3.1 General objective | 6 |
| 1.3.2 Specific objectives | 7 |
| 1.4 Contributions of the thesis | 7 |
| 1.5 Research methodology | 7 |
| 1.6 Research focus and limitations | 8 |
| 1.7 Outline of the thesis | 8 |
| 1.8 References | 9 |
| | |
| PART 1, MODELING | |
| | |
| 2. Oxygen transfer rate estimation in oxidation ditches from clean water measurements | |
| 2.1 Abstract | 14 |
| 2.2 Introduction | 15 |
| 2.3 The proposed method | 16 |
| 2.4 Application to real data | 18 |
| 2.4.1 Brief description of the plant | 18 |
| 2.4.2 Brief description of SOTR measurements | 19 |
| 2.5 Results and discussion of the new method | 19 |
| 2.5.1 Modelling the oxidation ditch | 19 |
| 2.5.2 Estimation of K_LA and V_A | 20 |
| 2.5.3 Estimation of k and V_A | 21 |
| 2.5.4 Estimation of k only | 21 |
| 2.5.5 Estimation of SOTR | 22 |
| 2.6 Conclusions | 23 |
| 2.7 References | 24 |
| 2.8 Appendix, Main equations STORA method | 24 |
| | |
| 3. Effect of number of CSTR's on the modelling of oxidation ditches: steady state and dynamic analysis | |
| 3.1 Abstract | 25 |
| 3.2 Introduction | 25 |
| 3.3 Materials and methods | 26 |
| 3.3.1 Plant layout | 26 |
| 3.3.2 Simulation model | 26 |

| | |
|----------------------------------------------------------------------------------------------------------------------------------------------------|----|
| 3.3.3 Methods | 26 |
| 3.4 Results and discussion | 27 |
| 3.4.1 Steady state simulations | 27 |
| 3.4.2 Dynamic simulations | 28 |
| 3.5 Conclusions | 29 |
| 3.6 References | 29 |
| 4. Parameter estimation procedure for complex non-linear systems: calibration of ASM No.1 for N-removal in a full-scale oxidation ditch | |
| 4.1 Abstract | 31 |
| 4.2 Introduction | 31 |
| 4.3 Proposed procedure | 32 |
| 4.3.1 Step 1, Specify plant layout and model | 33 |
| 4.3.2 Step 2, Collect in/output and operational data | 33 |
| 4.3.3 Step 3, Estimate initial state conditions from past data | 34 |
| 4.3.4 Step 4, Use RSM to select dominant parameters | 34 |
| 4.3.5 Step 5, Apply formal parameter estimation method | 37 |
| 4.3.6 step 6, Evaluate estimation results | 38 |
| 4.4 Conclusions | 39 |
| 4.5 References | 39 |
| 4.6 Appendix A: Operational pattern of the aerators | 40 |
| 4.7 Appendix B: Directions of dominant parameters | 41 |
| 4.8 Appendix C: Evaluation of parameter uncertainty | 41 |

PART 2, MODEL ANALYSIS

| | |
|--------------------------------------------------------------------------------------------------------------------------------------------------------------|----|
| 5. Sensitivity analysis on oxidation ditches: the effect of variations in stoichiometric, kinetic and operating parameters on the performance indices | |
| 5.1 Abstract | 43 |
| 5.2 Introduction | 45 |
| 5.3 Performance indices | 46 |
| 5.4 Method | 47 |
| 5.5 Results and discussion | 49 |
| 5.5.1 First stage: Parameters main effects | 49 |
| 5.5.2 Second stage: Factorial sensitivity analysis | 50 |
| 5.6 Conclusions | 54 |
| 5.7 References | 55 |
| 6. Uncertainty analysis | |
| 6.1 Estimation of uncertainties in the performance indices of an oxidation ditch benchmark | |
| 6.1.1 Abstract | 57 |
| 6.1.2 Introduction | 58 |
| 6.1.3 Theory | 59 |
| 6.1.4 Performance indices | 60 |
| 6.1.5 Estimation of performance indices uncertainties | 62 |
| 6.1.5.1 Parameter values and input loads uncertainties | 62 |
| 6.1.5.1.1 Method | 62 |
| 6.1.5.1.2 Results and discussion | 63 |

| | |
|--------------------------------------------------------------------------------|-----|
| 6.1.5.2 Initial state uncertainties | 66 |
| 6.1.5.2.1 Methods | 66 |
| 6.1.5.2.2 Results and discussion | 67 |
| 6.1.5.3 Model structure uncertainties | 67 |
| 6.1.5.3.1 Methods | 67 |
| 6.1.5.3.2 Results and discussion | 68 |
| 6.1.5.4 Uncertainties due to seasonal changes in water temperature | 69 |
| 6.1.5.4.1 Methods | 69 |
| 6.1.5.4.2 Results and discussion | 71 |
| 6.1.6 General discussion | 72 |
| 6.1.7 Conclusions | 72 |
| 6.1.8 References | 73 |
| | |
| 6.2 Forward and backward uncertainty propagation in mathematical models | |
| 6.2.1 Abstract | 75 |
| 6.2.2 Introduction | 75 |
| 6.2.3 Theory | 76 |
| 6.2.4 Working example | 77 |
| 6.2.5 Conclusions | 83 |
| 6.2.6 References | 83 |
| | |
| PART 3, BENCHMARKING | |
| | |
| 7. Implementation of the benchmark | |
| 7.1 Introduction | 86 |
| 7.2 Components of the benchmark | 86 |
| 7.3 Step-by-step benchmarking procedure | 86 |
| 7.4 References | 91 |
| | |
| 8. Illustration of the use of the benchmark | |
| 8.1 Introduction | 93 |
| 8.2 Effect of the horizontal velocity on performance of oxidation ditches | 94 |
| 8.2.1 Abstract | 94 |
| 8.2.2 Introduction | 94 |
| 8.2.3 Simulation example | 95 |
| 8.2.4 Practical assessment | 98 |
| 8.2.5 Conclusions | 100 |
| 8.2.6 References | 100 |
| | |
| 8.3 Evaluation of control strategies used in oxidation ditch plants | |
| 8.3.1 Abstract | 102 |
| 8.3.2 Introduction | 102 |
| 8.3.3 Benchmarking a specific WWTP | 103 |
| 8.3.3.1 Plant layout | 103 |
| 8.3.3.2 Model development and validation | 103 |
| 8.3.3.3 Performance criteria | 105 |
| 8.3.3.4 Testing of the benchmark | 105 |
| 8.3.4 Implementation of the benchmark | 105 |
| 8.3.4.1 Evaluation of short-term control strategies | 106 |

| | |
|--------------------------------------------------------------------|-----|
| 8.3.4.1.1 Control strategy No. 1, splitting of the influent flow | 106 |
| 8.3.4.1.2 Control strategy No. 2, RAS | 106 |
| 8.3.4.1.3 Control strategy No. 3, aeration patterns | 107 |
| 8.3.4.2 Evaluation of long-term control strategies | 108 |
| 8.3.5 Conclusions | 111 |
| 8.3.6 References | 111 |
| 9. General discussion and conclusions | |
| 9.1 Discussion | 113 |
| 9.2 General conclusions | 115 |
| Appendix I, ASM No. 1 | 118 |
| Appendix II, Performance indices | 119 |
| Appendix III, Modelling of sensors and actuators | 127 |
| Appendix IV, Description of the benchmarked full-scale WWTP | 132 |
| Appendix V, Matlab/Simulink model of the full-scale WWTP | 134 |
| Summary | 143 |
| Samenvatting | 146 |
| Curriculum Vitae | 149 |

1. Introduction

1.1 Background

1.1.1 Biological wastewater treatment plants

Collection and treatment of wastewater disposals is generally associated with the growth of cities, which resulted from the industrial revolution (Fair and Geyer, 1958). In the 19th century, after the Great Plague in London, use of conventional biological wastewater treatment plants (WWTP's) has started. At that time, the objectives of wastewater treatment were mainly concentrated on basic public health issues such as prevention of epidemics, protection of sources of potable water, and prevention of nuisance conditions like production of nasty odours and presence of vectors (Lester, 1996). However, in the past century, the objectives have somewhat changed (Metcalf & Eddy, 1991). From about 1900 to 1970, the objectives of wastewater treatment were: (i) removal of suspended solids and floatable matters, (ii) treatment of biodegradable organics and (iii) elimination of pathogenic organisms. From about 1970 to 1980, the objectives were mainly based on aesthetic and environmental concerns. From 1980 up to now, the main concerns are removal of nutrients, like nitrogen and phosphorus, which may cause eutrophication.

Conventional wastewater treatment is a combination of physical and biological processes. It consists of the following four steps: (i) preliminary treatment: screening and grit removal (ii) primary treatment (this step is often not practised in The Netherlands): removal of 30-50% of the suspended solids (*TSS*) in a primary settling tank, (iii) secondary treatment: biological treatment, which is usually a trickling filter or an activated sludge reactor, (iv) advanced treatment: in some conventional WWTP's chlorine disinfection is applied prior to discharge to a receiving water. Although they are very efficient in removing suspended solids and organic matter (more than 85 percent), conventional WWTP's are usually very poor in removing nitrogen, phosphorus, heavy metals, nonbiodegradable organics, bacteria and viruses (Qasim, 1999). Regarding nutrients removals in conventional WWTP's, total nitrogen (*TN*) removal is about 25-55 percent, whereas total phosphorus (*TP*) removal is about 10-30 percent (Orhon and Artan, 1994).

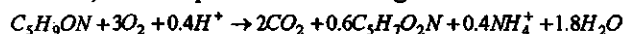
In the last few decades, knowledge and public awareness about water pollution problems have significantly increased. Due to that, environmental problems, such as: eutrophication, depletion of oxygen and toxicity to fish, have been associated with discharges of WWTP's into the receiving waters. It has been found that elimination of only the organic matter in discharges of WWTP's will not prevent the eutrophication problem, as nitrogen and phosphorus still can support biomass growth (Orhon and Artan, 1994). Hence advanced treatment processes like biological nitrogen removal and biological/chemical phosphorus removal have been introduced in WWTP's.

Biological nitrogen removal is a two-step process: nitrification followed by denitrification. In the nitrification process ammonia and organic nitrogen are converted to nitrate, whereas in the denitrification process nitrate is converted to nitrogen gas. Table 1

presents the typical reactions of organic matter oxidation and nitrogen removal processes that take place in biological WWTP's.

Table 1, Typical reactions in biological WWTP's (Rittman and Langeland, 1985).

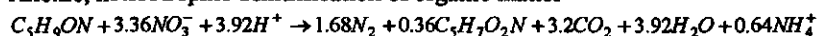
Aerobic, heterotrophic oxidation of organic matter



Aerobic, autotrophic oxidation of ammonium



Anoxic, heterotrophic denitrification of organic matter



Note, C_5H_9ON represents organic matter. $C_5H_7O_2N$ represents bacteria.

In comparison to physical or chemical removal processes, biological removal of nitrogen has the following main advantages: (i) moderate costs, (ii) high removal efficiency, and (iii) high process stability and reliability (Metcalf & Eddy, 1991). For achieving efficient biological nitrogen removal, many reactor configurations have been proposed. These configurations can broadly be classified as single-sludge systems and multi-sludge systems. In a single-sludge system, simultaneous carbon oxidation, nitrification and denitrification processes are accomplished with the same sludge, whereas in a multi-sludge system, the nitrification and denitrification processes occur in separate reactors with different biomass populations. However, both single- and multi-sludge systems can further be subdivided into pre-denitrification systems, where no external carbon source is used, and post-denitrification systems, where external carbon source is added to the system. Oxidation ditches and sequential batch reactors (SBR's) are good examples of single-sludge systems.

1.1.2 Oxidation ditches

Oxidation ditches are variants of the activated sludge system. They are single-sludge wastewater treatment systems. This means that they are capable of achieving carbon oxidation, nitrification and denitrification in single biomass slurry. Due to presence of aerobic, anoxic and anaerobic zones, in fact, oxidation ditches are capable of achieving not only C and N removals, but also P removal (WEF, 1998). However, this thesis focuses on C and N removals, only.

Since its original application in The Netherlands, the oxidation ditch has become a significant wastewater treatment technique all over the world (Huang and Drew, 1985). In the Netherlands, the oxidation ditch is the most widely used wastewater treatment system (CBS, 2000). An oxidation ditch continuously recirculates the mixed liquor

through a closed-loop, oval-shaped channel equipped with mechanical aerators (rotors) that are usually placed in series along the channel. Mechanical aerators are used to introduce oxygen into the system, and to provide sufficient horizontal velocity that prevents the organic solids from settling in the channel bottom surface. Typically, the horizontal velocity is between 0.25 and 0.35 m/s (Metcalf & Eddy, 1991).

The original version of oxidation ditches, as developed by Pasveer in the 1950s in The Netherlands, has a channel depth of about 1.5 m, equipped with brush aerators, and internal secondary settler (Pasveer, 1971). This first version of oxidation ditches is basically developed for use in a small community. For use in a larger community (e.g. > 100 000 p.e.), this type of oxidation ditch is found to be economically not feasible. Due to the shallow depth (1.5 m), a large surface area and a high number of aerators that are required.

In 1968, DHV Water BV has developed a new version of oxidation ditches, the so-called carousel oxidation ditch, which is economically a feasible system for use in large communities of up to 500 000 p.e. (Koot and Zepers, 1972). The carousel channel has a depth of 4 to 5 m. Thus it occupies less surface area than the original version of oxidation ditches developed by Pasveer in the 1950's. Further, the deep channel of the carousel allows installation of vertically mounted aerators that are more efficient than the horizontally mounted brush rotors. In addition, vertically mounted mechanical aerators add more control flexibility to the system, as various operating settings can easily be achieved by changing the number of aerators in use, the rotational speed, and/or the immersion depth.

At almost the same time as the carousel, the orbal system (a multi-channel oxidation ditch system) was also developed in South Africa (Drews *et al.*, 1972). The orbal system consists of a number of concentric oval aeration channels connected in series, followed by a secondary settler. The settler is actually surrounded by the aeration channels. The aeration mechanism of the orbal system consists of a number of perforated disks, which are partly immersed and rotate around horizontal axes. Increasing or decreasing the number of the discs controls oxygen input into the orbal system.

Recently, DHV Water BV has proposed a new version of the carousel, the so-called carousel-2000. *TN* removal efficiency of this system is expected to be higher than that of the other oxidation ditch systems, as a separated denitrification compartment will be allocated within the ditch (DHV Water, 1993). A similar modification has also been suggested by Sen *et al.*, (1992), who proposed aerating only the first half of the ditch while leaving the second half anoxic, in order to achieve high *TN* and *TP* removal efficiencies. In small oxidation ditches (e.g. under 4000 p.e.), intermittent aeration has also been successfully applied for achieving high *TN* removal (Inomae *et al.*, 1987; Araki *et al.*, 1990).

In comparison to other activated sludge systems, oxidation ditches have many advantages. First, alternating aerobic and anoxic zones exist along the ditch, due to the location of the aerators in series along the ditch channel. Consequently, simultaneous

removal of organic and nitrogenous matter occurs repeatedly in oxidation ditches. Given that only 10 to 30 minutes are usually needed for recirculating the wastewater around the ditch, biomass undergoes a rapid change of aerobic and anoxic conditions, which, in turn, stimulates growth of various types of microorganism in the oxidation ditches. Heterotrophic and autotrophic bacteria grow in the aerated zones, whereas denitrifying bacteria grow in the anoxic zones. Therefore, C-oxidation and nitrification take place in the aerated zones, whereas the denitrification process occurs in the anoxic zone. However, this is not the only explanation for the efficient denitrification process occurring in oxidation ditches. Because the travel time between the aerators is usually a fraction of the total travel time (10-30 minutes), bacteria have only a few minutes to shift from aerobic to anoxic conditions and vice versa. For this reason, researchers like Applegate *et al.*, (1980) and Rittman and Langeland (1985) argue that the most likely explanation of the simultaneous nitrification-denitrification processes taking place in oxidation ditches is that denitrification occurs continuously in the anoxic microzones within the biological floc. In general, due to the efficient nitrification and denitrification processes, which simultaneously take place in oxidation ditches, TN in the effluent is expected to be as low as 3 mg/l (Orhon and Artan, 1994).

Secondly, oxidation ditches produce less excess sludge. Because they usually work at an extended aeration mode (i.e. high sludge residence time and low food to micro-organism ratio), oxidation ditches yield a well-stabilised sludge that has little odour problems (Van der Geest and Witvoet, 1977). This sludge is usually ready for land application. If necessary, however, various chemical treatment or storage with or without dewatering can be used for reducing significantly the amount of pathogenic organisms prior to land applications (Novak *et al.*, 1984). Note that removal of toxic compounds and heavy metals is usually more important than reduction of pathogenic organisms or vectors.

Thirdly, due to the high internal recirculation rate, oxidation ditches have good mixing and good buffer against shock loads. Wastewater is usually circulated around the ditch in 10 to 30 minutes (Rittman and Langeland, 1985). The exact time needed for completing one cycle depends on the number of aerators and the dimensions of the ditch. High internal recirculation coupled with the high turbulence induced near the aerators result in a good mixing of the ditch contents.

Fourthly, construction of oxidation ditches usually is relatively cheap. The size of the oxidation ditch is usually less than the size of an up-graded multi-stage conventional WWTP that can achieve the same degree of nutrient removal as oxidation ditches. Upgrading of a conventional WWTP is usually achieved by addition of at least two more reactors (anoxic and anaerobic reactors) in pre- or post denitrification modes. Furthermore, unlike post-denitrification systems, oxidation ditches do not need external C-source, as the influent wastewater will be used as a C-source. This simply means additional saving in the capital costs by not installing C-source feeding equipments.

Finally, operation of oxidation ditches costs relatively less than the operation of other conventional WWTP's. The high rate of nitrate recirculation in oxidation ditches usually leads to a significant reduction in the amount of oxygen needed for oxidation, as nitrate,

instead of oxygen, is used as a terminal electron acceptor in the denitrification processes. Furthermore, manpower requirements are minimal and limited to usual cleanings, maintenance, and monitoring procedures (Petersen *et al.*, 1993).

1.1.3 Need for advanced control in WWTP's

The growing interest in the use of advanced control techniques in biological wastewater plants is mainly motivated by the process complexity and the strict effluent standards (Lindberg, 1997; Andrews 1998; Olsson and Newell, 1998; Lukasse, 1999). Activated sludge processes are quite complex. Many factors affect the performance of activated sludge systems. Examples of these factors are: organic and inorganic loading, sludge viability, oxygen uptake rate, mixing, detention time, sludge settling properties and solids level in the clarifier. Optimum performance of these systems usually requires monitoring and manipulating of certain process variables such as: *F/M* ratio, oxygen input, recycled activated sludge (*RAS*) flow, waste activated sludge (*WAS*) flow, and sludge blanket depth of the secondary settler (Eckenfelder *et al.*, 1986). Biological nutrient removing plants, like oxidation ditches, have even more complex processes. Nitrogen removal processes (nitrification and denitrification) are sensitive to many process and environmental variables such as: *DO*, *pH*, temperature and the presence of inhibitors. In order to optimize the performance of these complex processes, and to achieve the strict effluent standards, therefore, the use of advance control techniques can be beneficial.

The use of advanced control systems in WWTP's has even more benefits than to optimise the process and to help to achieve the standards. For example, it also helps to increase the amount of wastewater processed per unit capacity, and to minimise the number of operating personnel and to increase their productivity. Although the use of advanced control systems in WWTP's has significant benefits, it is constrained by the following main factors: (i) most of the plant operators do not have adequate training in instrumentation and control, (ii) there is a communication problem between the environmental engineers and control engineers, (iii) there is a lack of reliable on-line sensors and (iv) there is a lack of experimental proof of the proposed control strategies. For more information about the benefits and constraints of the use of advanced control techniques in WWTP's see for example Olsson and Newell (1998). Development of benchmarks, such as in this thesis, helps to alleviate some of the constraints that hinder the application of advanced control systems in WWTP's.

Literature reviews carried out by Lindberg (1997) and Weijers (2000) show that control strategies proposed for use in oxidation ditch plants are the same as those proposed for other activated sludge systems. This simply means that there is no control strategy that addresses the special features of oxidation ditches, such as the effect of the coupling of oxygen input and horizontal velocity (flow recirculation) on the nitrogen removal processes. This thesis tries to address some of the particular features of oxidation ditches. In section 8.2 of this thesis, the effect of the horizontal velocity, which is considered as a control variable, is studied for nitrogen removal processes.

1.2 Defining the benchmarking problem

Due to the increased public awareness of the problem of water pollution, effluent standards for WWTP are becoming more and more stringent (EC, 1999; UNEP, 1999). This trend is expected to continue in the future (Olsson and Newell, 1998). As argued in the previous section, to achieve these strict standards, at minimum costs, advanced control is necessary. Therefore, numerous control strategies have been recently proposed (Lindberg, 1997; Lukasse, 1999; Singman, 1999; Weijers, 2000). However, few of these control strategies have been thoroughly evaluated, either in practical tests or in computer simulations (Alex *et al.*, 1999; Pons *et al.*, 1999).

Comprehensive evaluation of proposed control strategies is obviously not a trivial task. Due to time and money limitations, evaluation of all the proposed control strategies by carrying out practical tests is clearly impossible. Thus computer simulations offer a useful approach to solve this problem. However, this approach requires development of a standard simulation procedure in conjunction with standard evaluation criteria. That is, development of a whole benchmarking methodology that can be used in evaluating all proposed control strategies. In this direction, both the European Concerted Action Programme (COST) 624 and the IWA Working Task on Respirometry have proposed benchmarking as a tool to evaluate the performance of activated sludge WWTP's (Keesman *et al.*, 1997; Pons *et al.*, 1999; Copp, 2000).

The term *benchmark* is frequently used in civil engineering, particularly in surveying, and also in computer technology. In surveying, a benchmark is a point with a known reduced level (height relative to sea water surface), relative to which levels of other points will then be measured. In computer technology, a benchmark is a reference performance to which the relative performance of hardware or software can be assigned. A dictionary definition of benchmark is "A reference value against which a measurement or a series of measurements may be compared" Parker (1994). COST 624 defines the benchmark as "protocol to obtain a measure of performance of control strategies for activated sludge plants based on numerical, realistic simulations of the controlled plant". According to this last mentioned definition, the benchmark consists of a description of the plant layout, a simulation model and definitions of (controller) performance criteria.

1.3 Research objectives

1.3.1 General objective

The main goal of this research is to develop a benchmarking methodology that can be used in evaluating existing or new control strategies proposed for full-scale oxidation ditch WWTP's.

1.3.2 Specific objectives

- (i) Develop, on basis of the available real process data, a simple, acceptable and realistic model that adequately describes both the biochemical processes and the hydraulics, and is suitable for controller design.
- (ii) Develop performance evaluation criteria for oxidation ditches.
- (iii) Conduct sensitivity analysis to specify model parameters that need special attention from the benchmark user.
- (iv) Carry out uncertainty analysis to quantify the possible effect of the various uncertainty sources on the performance indices.
- (v) Test the applicability of the benchmark.
- (vi) Illustrate the implementation of the benchmark, by evaluating a number of control strategies.

1.4 Contribution of the thesis

By developing the benchmarking methodology, this thesis will contribute to (i) bridging the gap that exists between control theory and its application in the field of wastewater treatment, (ii) promoting the acceptance of existing control strategies and (iii) enhancing the development of new control strategies. In particular, carrying out items (ii) and (iii) of the specific objectives, mentioned above, will constitute a major innovation over the known benchmarking procedures (see for example COST (2000)).

1.5 Research methodology

As mentioned before, the objective of the research is to develop a methodology for evaluating control strategies used in oxidation ditch WWTP's. This objective is achieved by outlining the procedure for developing such a benchmark for a specific full-scale WWTP, using the available operational data. For other WWTP's, the same procedure can be followed. The oxidation ditch plant, from which the operational data used in this thesis were obtained, is a 300 000 p.e. carousel WWTP situated in Rotterdam, The Netherlands. Description of this treatment plant, with its existing control strategy, is given in the Appendix IV. It must be emphasized that this plant will not be a reference case (benchmark). Rather, the procedure developed here can be used in benchmarking any specific oxidation ditch WWTP.

The benchmarking methodology followed here is different from that proposed by COST 624 and the IWA Task Group on Respirometry. These groups have proposed to develop benchmarks for hypothetical WWTP's with typical design capacities. Further, they use typical influent and operational data for developing these benchmarks. In contrast, throughout this thesis real data have been used. Thus, the benchmarking approach followed here is more realistic and suitable for adaptation to other real WWTP's. Adjustments for other oxidation ditches is mainly regarding the aeration and the

hydraulics. In chapter 2, a method for modeling the aeration, using a loop-of-CSTR's model, in terms of the aeration constant ($k = K_L a \cdot V_A$) is presented. Here V_A is the effectively aerated volume around an aerator. In chapter 3, the adequate number of CSTR's needed for modeling an oxidation ditch is investigated.

1.6 Research focus and limitations

The research is focused on benchmarking control strategies used in oxidation ditch plants that perform only carbon oxidation and nitrogen removal. Therefore, phosphorus removal is considered to be beyond the scope of this research. For this reason, the first version of activated sludge models, *ASM No. 1* (Henze *et al.*, 1987), is considered to be sufficient for modeling biochemical processes taking place in the ditch. In addition, the study is limited to oxidation ditches that treat mainly domestic wastewater. Therefore, oxidation ditches used for other purposes, e.g. for treating industrial wastewater, were not studied. The secondary settler was modelled as a non-reactive settler, using the 10-layer one dimensional settler model with the double exponential settling velocity function (Takács *et al.*, 1991). So the emphasis of this study was on the biological processes taking place in the aeration tank.

1.7 Outlines of the thesis

In this thesis, each chapter can be read independently, because they are presented as they have been (or will be) published.

The chapters are grouped into three parts. The first part (chapters 2, 3 and 4) deals with the modeling issue of oxidation ditch plants. The loop-of-CSTR's model, without back flows, was chosen for modeling oxidation ditches because it is simple, realistic, and can be easily incorporated within control algorithms. Chapter 2 investigates the use of the loop-of-CSTR's model for modeling oxidation ditches under clean water conditions, and estimates the ditch hydraulics and aeration. Chapter 3 studies the effect of number of CSTR's on modeling oxidation ditches based on influent-effluent concentrations. Chapter 4 presents a new calibration methodology, which can be used in calibrating non-linear systems like the oxidation ditch systems. The methodology that is based on *elliptical* analysis of response surfaces, is used in calibrating a loop-of-CSTR's model used for modeling a real full-scale oxidation ditch plant, under process conditions. According to the existing calibration methods (see for example STOWA (2000)), which assume that $K_L a$ is known in advance, first sludge production will be calibrated, then ammonia and finally nitrate. In contrast, the new method allows a simultaneous calibration of the three above-mentioned functions plus the aeration.

The second part of the thesis (chapters 5 and 6) analyses the performance of the developed loop-of-CSTR's model. In this part, sensitivity and uncertainty analysis were carried out to assess the reliability and applicability of the developed model, using *elliptical* analysis. Chapter 5 deals with the sensitivity analysis. That is, assessing the

effect of parameter variations on the performance indices. Chapter 6 is devoted to uncertainty analysis. In this chapter, the effect of various uncertainty sources on the performance indices is quantified (see section 6.1). In chapter 6, also a novel backward uncertainty propagation method is illustrated with a working example (see section 6.2). Backward uncertainty propagation gives essential information for reduction of the predefined parameter uncertainty region and parameters dominating specific phenomena.

The third part of the thesis provides the benchmarking procedure and illustrates the use of the benchmark. In chapter 7, components of the benchmark are defined and the step-by-step benchmarking procedure is outlined. In chapter 8, the use of the benchmark is illustrated. In section 8.2, the benchmark is used for evaluating the effect of the horizontal velocity on the performance of oxidation ditches. Here, the horizontal velocity is considered as a control variable, from *TN* removal efficiency point of view. In oxidation ditches, oxygen input and flow recirculation (horizontal velocity) are coupled, due to the use of mechanical aerators. At high horizontal velocity, high amounts of nitrate and dissolved oxygen will be recirculated from aerobic zones to the anoxic zones. Consequently, nitrogen removal processes will significantly deteriorate. In section 8.3, the usefulness of the benchmark is illustrated by using it to evaluate some basic and advanced control strategies. Finally, chapter 9 ends the thesis with overall discussion, conclusions and recommendations for future research.

1.8 References

Alex, J., J.-F. Béteau, J.B. Copp, C. Hellings, U. Jeppsson, S. Marsili-Libelli, M.N. Pons, H. Spanjers, and H. Vanhooren (1999), Benchmark for evaluating control strategies in wastewater treatment plants, ECC'99 (European control conference), Karlsruhe August 31 – September 3, 1999.

Araki, H., K. Koga, K. Inomae, T. Kusuda, and Y. Awaya (1990), Intermittent aeration for nitrogen removal in small oxidation ditches, *Wat. Sci. Tech.* 22(3-4):131-138.

Andrews, J.F. (1998), Dynamics and control of wastewater treatment systems: an overview, in dynamics and control of wastewater systems, *Water Quality library*, Vol. 6, 2nd edition, edited by: M.W. Barnett, M.K. Stenstrom, and J.F. Andrews, Technomic Publishing Company, Inc.

Applegate, C.S., B. Wilder, and J.R. De Shaw (1980). Total nitrogen removal in a multi-channel oxidation system, *JWPCF* 52:568-579

CBS (2000), *Waterkwaliteitsbeheer: zuivering van afvalwater, 1998*, Centraal Bureau voor Statistiek, Voorburg/Heerlen (in Dutch).

Copp, J.B. (2000), Defining a simulation benchmark for control strategies, *Water21*, 1(1):44-49.

- COST (2000), www.ensic.u-nancy.fr/COSTWWTP/Benchmark/Benchmark1.htm.
- DHV Water (1993), dossier G8112 - 10-001, DHV Water BV, Amersfoort, The Netherlands
- Drews, R.J.L.C., W.M. Malan, P.G.J. Meiring, and B. Moffatt (1972), The orbital extended aeration activated sludge plant, *J. WPCF* 7:1183-1193.
- EC (1999), Implementation of Council Directive 91/271/EEC of 21 May 1991 concerning urban waste water treatment, as amended by Commission Directive 98/15/EC of 27 February 1998: summary of the measures implemented by the member states and assessment of the information received pursuant to article 17 and 13 of the Directive, European Commission, Office for Official Publications of the European Communities, Luxembourg.
- Eckenfelder, W.W., D.L. Ford, P.W. Landford, G. Shell, and D.L. Sullivan (1986), Operation, control, and management of activated sludge plants, Department of Civil and Environmental Engineering, Vanderbilt University, Nashville, Tennessee, USA.
- Fair, G.M. and J.C. Geyer, (1958), Elements of water supply and wastewater disposal, 5th ed, John Wiley & Sons, Inc.
- Henze, M., C.P.L. Grady, jr, W. Gujer, G. van R. Marais and T. Matsuo (1987), Activated sludge model no. 1, IAWQ scientific and Technical Report no. 1, IAWQ, London, U.K.
- Huang, J.Y.C. and D.M. Drew (1985), Investigation of the removal of nitrogen in an oxidation ditch, *J. WPCF* 57(2):151-156.
- Inomae, K., H. Araki, K. Koga, Y. Awaya, T. Kusuda, and Y. Matsuo (1987), Nitrogen removal in oxidation ditch with intermittent aeration, *Wat. Sci. Tech.* 19:209-218.
- Keesman, K.J., H. Spanjers, P. Vanrolleghem, and J. Alex (1997), Benchmarks for control strategies in activated sludge plants, TMR Research Proposal No. ERB4061PL970020, Wageningen, The Netherlands.
- Koot, A.C.J. and J. Zepers, (1972), Carrousel, a new type of aeration-system with low organic load, *Wat. Res.* 6:401-406.
- Lester, J.N. (1996), sewage and sewage sludge treatment, in *Pollution: causes, effects and control*, 3rd ed., edited by R.M. Harrison, the royal society of chemistry information services.
- Lindberg, C-F. (1997), Control and estimation strategies applied to the activated sludge process, Ph.D. thesis, Uppsala University, Sweden.

Lukasse, L.J.S. (1999), Control and identification in activated sludge processes, Ph.D. thesis, Wageningen University, The Netherlands.

Metcalf & Eddy (1991), Wastewater engineering: treatment, disposal and reuse, 3rd ed, McGraw-Hill.

Novak, J.T., M.P. Eichelberger, S.K. Banerij, and J. Yaun (1984), Stabilisation of sludge from an oxidation ditch, J. WPCF 56(8):950-954.

Olsson, G. and B. Newell, (1998), Wastewater treatment systems: modeling, diagnosis, and control, IWA Publishing, London, UK.

Orhon, D. and N. Artan (1994), Modeling of activated sludge systems, Technomic Publishing Company, Inc. Lancaster, Pennsylvania, USA.

Parker, S.P. (1994), McGraw-Hill Dictionary of Scientific & Technical Terms, 5th edition.

Pasveer, A. (1971), Verdere ontwikkeling. Het oxydenitroproces, H₂O 4(22):499-504, (in Dutch).

Petersen, G., H. Nour El-Din, and E. Bundgaard (1993), Second generation of oxidation ditches: advanced technology in simple design, Wat. Sci. Tech. 27(9):105-113.

Pons, M.N., H. Spanjers and U. Jeppsson, Towards a benchmark for evaluating control strategies in wastewater treatment plants by simulations, Escape 9 (European symposium on computer aided process engineering-9), Budapest (1999).

Qasim, S.R. (1999), Wastewater treatment plants: planning, design and operation, 2nd ed, Technomic Publishing CO., Inc.

Rittman, B.E. and W.E. Langeland (1985), Simultaneous denitrification with nitrification in single-channel oxidation ditches, J. WPCF 57(4):300-308.

Takács, I., G.G. Patry and D. Nolasco (1991). A dynamic model of the clarification-thickening process, Wat. Res. 25(10):1263-71.

Sen, D., C.W. Randall, T.J. Grizzard and D.R. Rumke (1992), Process design and operation modifications of oxidation ditches for biological nutrient removal, Wat. Sci. Tech. 25(4-5):249-256.

Singman, J. (1999), Efficient control of wastewater treatment plants – a benchmark study, M.Sc. thesis, Uppsala University, Sweden.

STOWA (2000), SIMBA-protocol, richtlijnen voor het dynamisch modelleren van actiefslibsystemen, STOWA, 2000-16 (in Dutch).

Van der Geest, A.T. and W.C. Witvoet, (1977), Nitrification and denitrification in a carousel system, Prog. Wat. Tech. 8(4/5):654-660.

UNEP (1999), Global environment outlook 2000, United Nations Environment Programme, Earthscan Publication Ltd, London.

WEF (1998), Biological and chemical systems for nutrient removal, A special publication, Municipal subcommittee of the technical practice committee, Water Environment Federation (WEF), USA.

Weijers, S. (2000), Modeling, identification and control of activated sludge plants for nitrogen removal, Ph.D. thesis Eindhoven University of Technology, The Netherlands.

PART 1
MODELING

2. Oxygen transfer rate estimation in oxidation ditches from clean water measurements[†]

2.1 Abstract

Standard methods for the determination of oxygen transfer rate are based on assumptions that are not valid for oxidation ditches. This paper presents a realistic and simple new method to be used in the estimation of oxygen transfer rate in oxidation ditches from clean water measurements. The new method uses a loop-of-CSTR's model, which can be easily incorporated within control algorithms, for modeling oxidation ditches. Further, this method assumes zero oxygen transfer rates (K_{La}) in the unaerated CSTR's. Application of a formal estimation procedure to real data revealed that the aeration constant ($K_{La} \cdot V_A$, where V_A is the volume of the aerated CSTR), can be determined significantly more accurately than K_{La} and V_A . Therefore, the new method estimates k instead of K_{La} . From application to real data, this method proved to be more accurate than the commonly used Dutch standard method (STORA, 1980).

Key words: oxygen transfer rate, aeration, K_{La} , oxidation ditch, carousel.

Nomenclature

C_i : DO concentration in outflow of the i^{th} CSTR (mg/l).

C_{i-1} : DO concentration in the inflow of the i^{th} CSTR (mg/l).

COD: chemical oxygen demand (mg/l).

C_s : DO saturation concentration (mg/l).

CSTR: completely stirred tank reactor.

DO: dissolved oxygen.

J : objective function.

k : aeration constant, $K_{La} \cdot V_A$, (m^3/min)

k_{10} : aeration constant at 10°C (m^3/min).

K_{La} : overall oxygen transfer rate (min^{-1}). Note that here K_{La} is calculated for the assumed aerated volume and not for the whole ditch.

m : number of aerators.

N : number of observation samples instances.

n : number of compartments (CSTR's).

OC_{10} : aerator oxygenation capacity at 10°C .

OTR: oxygen transfer rate ($\text{kg O}_2/\text{h}$).

q : water flow (m^3/min).

rpm: revolution per minute.

SOTR: standard oxygen transfer rate ($\text{kg O}_2/\text{h}$).

t : time (min.).

V_A : volume of the aerated CSTR (m^3).

V_{mixed} : mixed volume around the aerator (m^3).

V_{NA} : volume of the non-aerated CSTR (m^3).

V_{TOT} : total volume of the oxidation ditch (m^3).

[†] A slightly modified version published by A. Abusam, K.J. Keesman, K. Meinema and G. van Straten in Wat. Res. 35(8):2058-2064.

$$V_n = V_{TOT}/n$$

X : sensitivity matrix.

y : measured DO concentration (mg/l).

τ : index that indicates whether the CSTR is aerated ($\tau=1$) or unaerated ($\tau=0$).

θ : parameter vector

cov θ : covariance matrix of θ .

ε : residual i.e. measured DO - estimated DO (mg/l).

σ_ε^2 : residual variance (mg^2/l^2).

Δp : difference in atmospheric pressure (kPa).

χ : correction factor used by STORA.

2.2 Introduction

Accurate estimation of the oxygen transfer rate (*OTR*) in an activated sludge reactor is essential not only for ensuring that the aerators meet the design specifications, but it is also crucial for the optimum design and operation of the reactor. A variety of methods are used in determining *OTR* in an aeration tank. Examples are clean-water-tests, process-condition tests, radioactive and non-radioactive tracer techniques, dissolved oxygen (*DO*) mass balance procedures and off-gas methods. All these methods are standardised to provide what is known as the standard methods for estimating the oxygen transfer rate of an aeration system. Standard methods are commonly known as clean-water-tests and process-condition tests (Boyle and Paulson, 1979; Kayser, 1979).

However, all these standard methods are based on the assumptions that the reactor is completely mixed and $K_L a$ is uniformly distributed along the aeration tank. For a number of reasons, these assumptions are not valid for oxidation ditches. First, $K_L a$ is not the same all over the ditch. For instance, a few meters away from the aerator, $K_L a$ is practically zero. Second, the flow pattern in an oxidation ditch cannot be considered as a completely mixed flow pattern. In fact, it is a mixture of a completely mixed and plug flow pattern.

In an attempt toward an accurate estimation of the oxygen transfer rate in oxidation ditches, the Dutch standard method (STORA, 1980) distinguishes between the total volume of the oxidation ditch (V_{TOT}) and the mixed volume around the aerator (V_{mixed}) - see the Appendix. Differentiation between V_{mixed} and V_{TOT} makes this method look more realistic than the other methods in calculating the *OTR* in oxidation ditches. However, like the other standard methods, the Dutch standard method estimates $K_L a$ from the completely mixed batch reactor model. Further, it assumes that V_{mixed} equals the design volume of the aerated compartment. That is, V_{mixed} is a constant volume. In fact, V_{mixed} changes with the change in the aerator operating conditions, like the rotational speed and immersion depth. Recent attempts for more accurate estimation of *OTR* in oxidation ditches have been made by Dudley (1995). He proposed a procedure based on a first-order partial-differential equation for estimating the *OTR* in oxidation ditches under process conditions. However, the proposed model is relatively complicated and can not be easily used for controller design.

The objective of this paper is to present a new method for estimating the *OTR* in oxidation ditches from clean water measurements. The new method uses a loop-of-*CSTR*'s model, which can be easily incorporated within control algorithms. Further, the new method assumes that K_{La} in the unaerated *CSTR*'s is zero. According to this new method, k will be estimated instead of K_{La} , where k is defined as $K_{La} \cdot V_A$. Besides being simple and realistic, this new method directly gives an accurate estimate of the aeration constant (k), with corresponding estimation error that can be used in an oxidation ditch plant model. Consequently, the new method enables more accurate estimation of the *SOTR* (i.e. *OTR* at maximum deficit, C_s). That is, the proposed method will help in getting a better understanding of the biochemical processes taking place in the oxidation ditch.

The outline of this paper is as follows. In section 2, the proposed estimation procedure will be described. Then the results of applying this procedure to real data will be presented and discussed in section 3. Finally, in section 4, the paper will end with some conclusions and recommendations.

2.3 The proposed method

The proposed method can be summarised in the following three steps:

Step 1: model the oxidation ditch as a loop of aerated and unaerated *CSTR*'s.

As will be shown in section (3.3.4), any number of *CSTR*'s, greater than twice the number of aerators, can be used.

Step 2: estimate relevant aeration parameters, using a formal estimation procedure.

Assumptions:

- The number of the aerators in the oxidation ditch is 'm'.
- All aerators have the same aeration capacity and are working under the same operating conditions (i.e. the same rotational speed and immersion depth).
- K_{La} is zero for the unaerated *CSTR*'s.
- Given measured temperature data, literature values can be used for the saturated dissolved oxygen concentration (C_s).

Originally, the idea was to estimate K_{La} and V_A as follows:

In clean water tests, the biochemical oxygen uptake rate is zero. Therefore, the *DO* concentration in the aerated and unaerated *CSTR* can be described as:

For the aerated *CSTR*:

$$\frac{dC_i(t)}{dt} = \frac{q(t)}{V_A} \cdot (C_i(t) - C_{i-1}(t)) + K_{La} \cdot (C_s - C_i(t)) \quad (1)$$

For the **unaerated** CSTR:

$$\frac{dC_i(t)}{dt} = \frac{q(t)}{V_{NA}} \cdot (C_{i-1}(t) - C_i(t)) \quad (2)$$

where V_{NA} is defined as:

$$V_{NA} = (V_{TOT} - m \cdot V_A) / (n - m) \quad (3)$$

with $m \leq n$ and 'n' the total number of CSTR's used in describing the oxidation ditch. Because of the loop nature of the ditch: $C_{i=0}(t) = C_{i=n}(t)$. In these equations (1-3) the unknowns are K_{LA} and V_A , which need to be estimated from measured data.

Given that $q(t)$, $C_{i-1}(t)$, $C_i(t)$ and C_S are known, the optimisation problem for the estimation of K_{LA} and V_A can be formulated as:

$$\hat{\theta} := [\hat{K}_{LA}, \hat{V}_A]^T = \arg \min J(\theta) \quad (4)$$

The objective function $J(\theta)$ is defined as:

$$J(\theta) = \sum_{k=1}^N [y(t_k) - C(t_k|\theta)]^2 = \sum_{k=1}^N [\varepsilon(t_k|\theta)]^2 \quad (5)$$

where $y(t_k)$ and $C(t_k|\theta)$ denote the measured and predicted DO concentration at the measuring point (see Fig. 1) at time instant t_k with $k = 1, \dots, N$. The covariance matrix associated with the estimated parameter vector ($\hat{\theta}$) is given by:

$$\text{cov } \hat{\theta} = \hat{\sigma}_\varepsilon^2 (X^T \cdot X)^{-1} \quad (6)$$

where X is the locally available Jacobi matrix with the elements

$$X(k, j) = \frac{d\varepsilon(t_k|\hat{\theta})}{d\hat{\theta}_j} \quad \text{for } j = 1, \dots, p \quad \text{and } k = 1, \dots, N. \quad (7)$$

Furthermore, $\hat{\sigma}_\varepsilon^2$ is the residual variance defined by

$$\hat{\sigma}_\varepsilon^2 = \frac{1}{N - p} \sum_{i=1}^N [\varepsilon(t_i|\hat{\theta})]^2 \quad (8)$$

However, application to real data has clearly indicated that neither K_{LA} nor V_A can be accurately estimated, due to the hyperbolic relationship between them (see section 3.4.1). Therefore, it has been decided to choose V_A arbitrarily. Furthermore, for simplicity, V_A was considered to be equal to V_{NA} . That is to say, a loop-of-equal CSTR's model was used. Consequently, the following equation will be used, instead of Eqn. 1 and 2, for describing the DO concentrations in both the aerated and unaerated CSTR's.

$$\frac{dC_i(t)}{dt} = \frac{q(t)}{V_n} \cdot (C_i(t) - C_{i-1}(t)) + \frac{k}{V_n} \cdot (C_S - C_i(t)) \cdot \tau_i \quad (9)$$

where $V_n = V_{TOT}/n$, $\tau_i = 1$ in an aerated compartment and $\tau_i = 0$ in a non-aerated compartment, and $C_{i=0}(t) = C_{i=n}(t)$, as before.

Note that in Eqn. 9, k is the only unknown to be estimated from measured data.

Step 3: estimate the *SORT*

After estimating k from the measured data, using Eqn. 9, *SOTR* can be estimated as follows:

$$SOTR = k \cdot C_s \quad (10)$$

In this equation, it is suggested to use literature values for C_s . As will be seen later, clean water tests are usually too limited to estimate C_s accurately.

2.4 Application to real data

The new method was applied to clean water measurements carried out by the DHV Water BV, in 1994, at the carrousel in Botlek, The Netherlands.

2.4.1 Brief description of the plant

The main features of the carrousel and its aerators are as follows:

Carrousel characteristics:

Width = 7.5 m.

Length = 210 m.

Water depth (at zero submergence) = 4.19 m.

Water volume (at zero submergence) = 6432 m³.

Aerators characteristics:

Number = 3.

Type: Landy-F.

Diameter = 2900 mm.

Measured speed = 24.4/32.6 rpm.

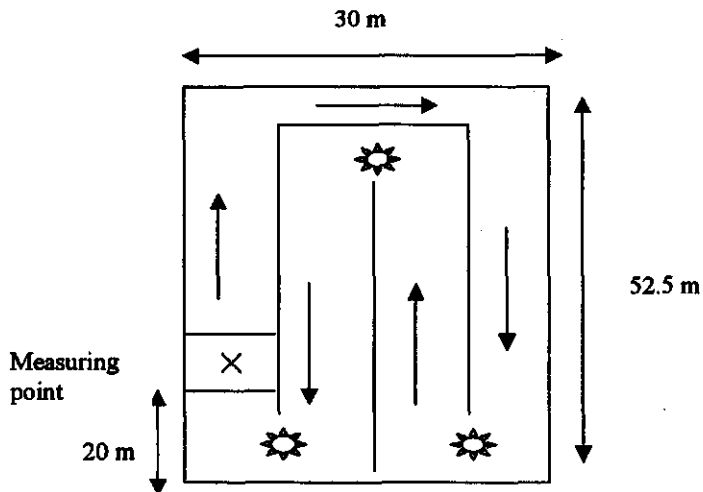


Fig. 1, Relative position of the aerators and the measuring point

2.4.2 Brief description of SOTR measurements

In order to determine the standard oxygen transfer rate (*SOTR*) of the aerators in the carousel, six experiments, according to the Dutch standard method (STORA, 1980), were carried out by previous investigators, in August 1994, as follows. The carousel was first closed, and then it was filled with suitable clean water (16 mg *COD/l*). After that, bleaching chloride was added at a rate of 5 g chloride/m³, in order to prevent the growth of algae. For dropping the *DO* concentration to zero, sodium sulphite and cobalt sulphate – as catalysts – were pumped into the carousel. After maintaining 0 mg *DO/l*, for about 10 minutes, all the aerators were put in operation at the same moment and at the same rotational speed and immersion depth. Increase in *DO* concentration was measured by the *DO* electrode, which was situated at about 20 m downstream of one of the aerators (see Fig.1), and automatically recorded. Based on this recorded information, a fixed time interval was determined for samples to be taken for chemical determination of *DO* concentration according to the Winkler method. Water samples were taken at a depth of about 2 m at the measuring point. By changing the rotational speed and submergence depth of the aerators, six sets of single measurements were obtained. These sets of measurements were called A1, A2, B1, B2, C1 and C2, respectively. For each of these sets, the circulation velocity was calculated from the readings of a current meter (Ott-propeller). Based on the results of these experiments (Table 1), it had been concluded that the aerators do not meet the specifications, despite difference in immersion depth and rotational speed between specifications and experiments.

Table 1, Results of the *SOTR* measurements carried at the carousel in August 1994, according to the Dutch standard method (STORA, 1980).

| Measuring points | Measurement results | | | | | | Specifications | | |
|------------------------------------|---------------------|------|------|------|------|------|----------------|------|------|
| | A1 | A2 | B1 | B2 | C1 | C2 | | | |
| Temperature (°C) | 22.8 | 22.9 | 22.5 | 22.7 | 23.0 | 22.3 | | | |
| Pressure (mm Hg) | 763 | 762 | 763 | 760 | 759 | 753 | | | |
| Rotor speed (rpm) | 24.5 | 24.5 | 32.6 | 32.6 | 32.6 | 32.6 | 24.1 | 32.3 | 32.3 |
| Immersion depth (cm) | 3.5 | 4.7 | 4.0 | 5.3 | 20.3 | 18.7 | 2.5 | 2.5 | 5.5 |
| <i>SOTR</i> (kg O ₂ /h) | 47 | 48 | 93 | 98 | 101 | 102 | 53 | 107 | 113 |

2.5 Results and discussion of the new method

2.5.1 Modeling the oxidation ditch

Initially the oxidation ditch was modelled as a loop of 20 equal *CSTR*'s, using Eqn. (9). However, as will be shown in section (3.3.4), models that consist of different number of

CSTR's (6, 15, 20 and 30 equal CSTR's) were also used for investigating the effect of the number of CSTR's on the estimation of the aeration constant (k).

2.5.2 Estimation of K_{La} and V_A

The experimental results were re-used to estimate relevant aeration parameters with the proposed model-based method. Using a non-linear least squares optimisation technique, attempts were first made to solve the estimation problem (Eqn. 4 and 5) for a loop-of-20-CSTR's model. However, these attempts failed as V_A was found to be practically unidentifiable. It was found that whenever the initial guesses were changed, new values for K_{La} and V_A were obtained. The contour plot shown in Fig.2 clearly shows that

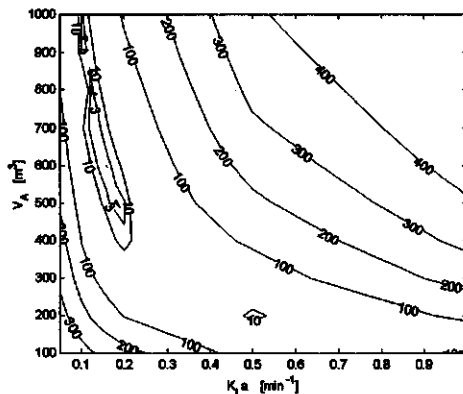


Fig. 2, Sum of squares of error for A1, K_{La} vs. V_A

there is more than one possible solution for this estimation problem. In addition, this contour plot hints that

the product $K_{La} \cdot V_A$ is about a constant. Notice that eigenvalue decomposition of the covariance matrix, as e.g. suggested by Lukasse et al. (1996), does not suffice to reveal this non-linear type of relationship between parameters. Hence, graphical representation of the estimation results can be very helpful.

Investigation of the covariance matrix, $\text{cov } \hat{\theta} = \begin{bmatrix} 0.0020 & -8.5978 \\ -8.5978 & 36505.48 \end{bmatrix}$, calculated at one

of these possible solutions ($V_A = 633 \text{ m}^3$ and $K_{La} = 0.15 \text{ min}^{-1}$), reveals the following. As can be seen from this covariance matrix, the standard deviations of V_A (191.1 m^3) and K_{La} (0.045 min^{-1}) are about 1/3 of their estimated values. From this it can be concluded that neither K_{La} nor V_A can be accurately estimated from the given data.

2.5.3 Estimation of k and V_A

Based on these results, attempts were made to estimate the relevant parameters in other combinations, e.g. as V_A and k ($K_L a \cdot V_A$). The contour plot shown in Fig.3, illustrates that k is about 90 m^3/min , while V_A takes a whole range of values. Clearly, k can be estimated more accurately than V_A .

The covariance matrix for $\hat{\theta} = [95.4, 700]^T$,

$$\text{cov } \hat{\theta} = \begin{bmatrix} 0.5620 & -18.6488 \\ -18.6488 & 2018.46 \end{bmatrix}$$

confirms that k (standard deviation of 0.7497 m^3/min , coefficient of variation < 1%) can be determined more accurately than V_A (standard deviation of 44.93 m^3 , coefficient of variation about 6%).

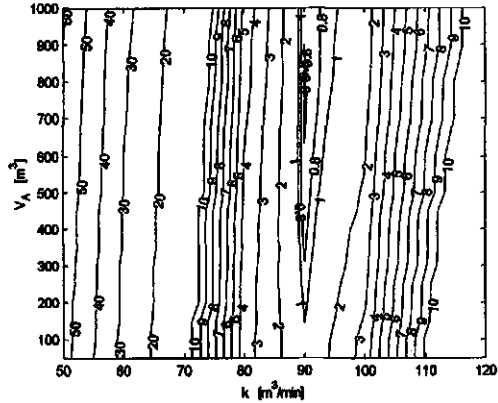


Fig. 3, Sum of squares of errors for A1, k vs. V_A

2.5.4 Estimation of k only

From the previous results, it can be concluded that V_A can not be accurately estimated. Therefore, V_A can be chosen more or less arbitrary. To test the effect of the arbitrary chosen value of V_A , the aeration constant (k) was estimated at different values of V_A that were obtained by changing the number of *CSTR*'s (6, 15, 20 and 30). For simplicity, V_A was considered to be equal to V_{NA} . Thus a loop-of-equal *CSTR*'s model was used. Consequently, the *DO* concentrations in the carousel are described by Eqn. 9.

Values of k found from solving Eqn. 9 are presented in Table 2. This table shows the effects of change in the number of *CSTR*'s, in the range from 6 to 30 *CSTR*'s, on the estimated aeration constant (k). It is worth mentioning here that the effect of number of *CSTR*'s less than six has not been studied because the number of aerators in the carousel is three. As expected, results presented in Table 2 show that the number of *CSTR*'s has no significant effect on the estimated value of the aeration constant (k).

Table 2, Estimated k , aeration constant, (m^3/min)

| # <i>CSTR</i> 's | A1 | A2 | B1 | B2 | C1 | C2 |
|------------------|------|------|-------|-------|-------|-------|
| 6 | 96.0 | 87.4 | 147.3 | 167.9 | 177.6 | 231.3 |
| 15 | 95.3 | 86.8 | 146.5 | 167.4 | 176.8 | 231.0 |
| 20 | 95.9 | 87.3 | 147.6 | 168.7 | 178.2 | 233.0 |
| 30 | 96.6 | 85.9 | 148.7 | 169.8 | 179.5 | 235.2 |

2.5.5 Estimation of *SOTR*

On the basis of these estimation results, Eqn. 9 can be used to calculate the standard oxygen transfer rate (*SOTR*), with C_s found from literature (at 10 °C: 11.3 mg/l). Furthermore, k can explicitly be corrected for temperature according to STORA (1980) as:

$$k_{10} = k_T \cdot (1.019)^{10-T} \quad (10)$$

Table 3 compares the *SOTR* values estimated according to the new method with those found according to STORA (1980). This table shows that both the new method and STORA method lead to the same conclusion that the aerators do not satisfy the specifications (107 kg O₂/h) at immersion depth equal to 2.5 cm. However, results obtained by the new method show that the specifications could be met at about 18 cm submergence depth (experiment C2).

Table 3, Estimated *SOTR* (kg O₂/h) - at 10 °C and 101.3 kPa: new method vs. STORA method.

| | A1 | A2 | B1 | B2 | C1 | C2 |
|----------------|----|----|----|----|-----|-----|
| The new method | 51 | 46 | 79 | 90 | 94 | 124 |
| STORA method | 47 | 48 | 93 | 98 | 101 | 102 |

Fig. 4 compares the reconstructed *DO* concentration for experiment C2 when the new method was used to that when STORA method was used. From this figure, it is clear that the new method is more accurate than the STORA method.

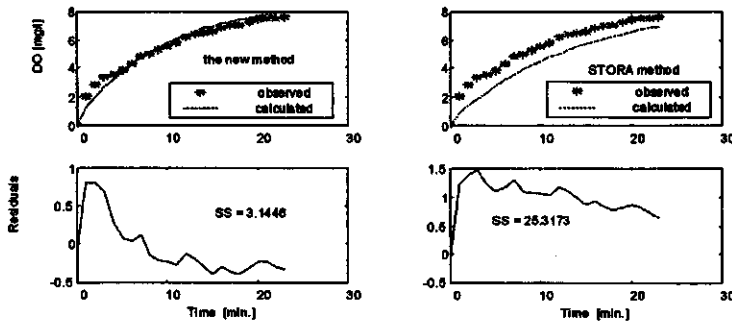


Fig. 4, Reconstruction of *DO* for experiment C2 (a) the new method (b) STORA method.

Looking at Fig. 4, it becomes clear that forcing the initial *DO* to be zero will introduce a bias. Therefore, attempts have been made to have more accurate estimate of *SOTR*, by either estimating the initial *DO* concentration ($C(t=0)$), or by starting from the second measurement ($C(t=1)$). As indicated by the residual standard deviations (given between parenthesis in Table 4), more accurate estimates of *SOTR* were obtained in both trials - for most of the sets. Furthermore, comparison of these results with those reported in Table 3 indicates that starting from the second measurement results in values close to that obtained by STORA method. These attempts clearly indicate that the initial *DO* concentration(s) needs to be accurately estimated. If the estimation results appear to be inaccurate, it is better that *DO* initial measurements not be used in the estimation of *SOTR*. However, it should be taken into account that dropping considerable part of the data, especially for a very limited amount of data, can significantly affect the estimation accuracy.

Table 4, Results of the attempts for improving the estimation of *SOTR* (kg O₂/h) - at 10 °C and 101.3 kNm⁻².

| | A1 | A2 | B1 | B2 | C1 | C2 |
|------------------------------------|----------------|----------------|----------------|----------------|-----------------|-----------------|
| starting at C(0) = 0 | 51 (0.1139) | 46 (0.3353) | 79 (0.3097) | 90 (0.1666) | 94 (0.2037) | 124 (0.3632) |
| estimating C(0) | 51 (0.1159) | 51 (0.2779) | 86 (0.2107) | 92 (0.1520) | 100 (0.1385) | 110 (0.2394) |
| starting at the second measurement | 50 (0.1099) | 46 (0.3463) | 82 (0.2344) | 91 (0.1422) | 99 (0.1107) | 100 (0.0888) |

* values between the parenthesis are the residual standard deviations (see Eqn. 8).

2.6 Conclusions

A simple and realistic method, which is based on a loop-of-*CSTR*'s model that can be easily incorporated within control algorithms, has been proposed for estimating the oxygen transfer rate (*OTR*) in oxidation ditches. From application to real measurements, this new method proved to be more accurate than the Dutch standard methods (STORA, 1980). Being able to estimate accurately *OTR*, the method will help in getting a better understanding of the biochemical processes taking place in the oxidation ditch.

As an advantage, the proposed method directly gives the estimates of the aeration constant (k), which can be used in a *CSTR* model. In addition, the standard deviation and the estimation error are also provided.

Due to the significant effect they have on the estimates of k and consequently *SOTR*, initial *DO* concentration(s) needs to be accurately estimated, otherwise it is better to neglect them.

From the formal estimation procedure, it is found that the aeration constant (k) can be estimated more accurately than V_A and K_{La} , separately. This finding can also be used for accurate estimation of *OTR* in other activated sludge systems. Application to the other systems requires only simple mathematical manipulation similar to that used in (9).

2.7 References

ASCE. Standard – The measurement of oxygen transfer in clean water, Am. Soc. Civ. Eng., New York, N.Y., USA, 1992.

Boyle, W.C., Stenstrom, M.K., Campbell, H. J. and Brenner, Jr., R. C. (1989). Oxygen transfer in clean and process water for draft tube turbine aerators in total barrier oxidation ditches, J WPCF, 61(8):1449-1463.

Boyle, W.C. and Paulson, W.L. (1979), Progress toward standardised oxygen transfer test procedures, Prog. Wat. Tech. 11(3):161-170.

DHV Water bv. Results of the extra oxygenation capacity measurements, Dossier G8316-70-100, Amersfoort, the Netherlands, August 1994. (in Dutch).

Dudley, J (1995). Process testing of aerators in oxidation ditches, Wat. Res. 29(9):2217-2219

Kayser, R. (1979). Measurements of oxygen transfer in clean water and under process conditions, Prog. Wat. Tech. 11(3):23-36.

Lukasse, L.J.S, Keesman, K.J., and van Straten, G. (1996). Grey-box identification of dissolved oxygen dynamics in activated sludge processes. In Proc. 13th IFAC World Congress, vol. N, San Francisco, pp 485-490.

Stephenson, R. V., Baumann, E. R., and Berk, W. L. (1984). Performance of surface aerators in an oxidation ditch, J. Env. Eng. Div., ASCE, 111(1):79-91.

STORA, Zuurstofvoervoermogen in beluchtingssystemen: Bepaling in rein water (reaeratiemethode), Rijswijk: STORA, 1980. (in Dutch).

2.8 Appendix: Main equations STORA method

As the other standard methods, STORA method estimates $K_L a$ from the solution of a batch reactor model (A1).

$$C(t) = C_s - (C_s - C(t=0)) \cdot (e^{-K_L a t}) \quad (A1)$$

However, STORA uses a special correction factor for calculating the oxygen transfer rate in oxidation ditches (equation A2). In this correction factor, a distinction is made between the total volume (V_{TOT}) and the mixed volume around the aerator (V_{mixed}).

$$OC_{10} = 11.3(1 + 0.01\Delta p)(2.3K_L a \cdot K_L a)(1 + (1 - \frac{n \cdot V_{mixed}}{V_{TOT}})(1.15\chi + 0.9\chi^2)) \cdot (1.09)^{10-T} \quad (A2)$$

$$\chi = \frac{V_{TOT} - n \cdot V_{mixed}}{n \cdot q} \cdot K_L a \quad (A3)$$

3. Effect of number of *CSTR*'s on the modeling of oxidation ditches: steady state and dynamic analysis[†]

3.1 Abstract

A typical oxidation ditch (200 m x 10 m x 4 m) has been modelled as a loop of 4, 6, 10, 14, 20, 24 and 30 completely stirred tank reactors (*CSTR*'s). Simulation results have shown that the number of *CSTR*'s mainly affects effluent components, S_{NO} , and S_{NH} . This effect is generally negligible, when 10 or more *CSTR*'s is used for modeling the ditch. The general conclusion drawn is that the number of *CSTR*'s required for modeling an oxidation ditch, in terms of influent and effluent concentrations, better be limited to 10-15 *CSTR*'s or to the minimum number needed for adequate modeling of the aeration configuration, since in practice the effect on S_{NO} and S_{NH} can always be compensated by an adjustment of the estimated aeration capacity. In other words, the number of aerators in the oxidation ditch mainly determines the number of *CSTR*'s needed for modeling an oxidation ditch.

Key words: oxidation ditch, carousel, modeling, *CSTR*.

3.2 Introduction

Many models have been proposed for modeling the hydrodynamics of oxidation ditches. These models range from a very simple one like a single *CSTR* model, to a relatively sophisticated one such as the 3D advection-dispersion model (see e.g. Alex *et al.*, 1999; Dudley, 1995; Stamou, 1994 and von Sperling, 1990). Sophisticated models can only be justified when they are used for design purposes, whereas for control applications simple models most often suffice. The loop-of-*CSTR*'s model is one of the most straightforward models. This type of model is simple and can easily be incorporated within control algorithms. Furthermore, it can be used for describing adequately the various aeration configurations that may take place along the oxidation ditch, because each *CSTR*'s may be used to represent a different aeration condition. Simulation packages like SIMBA 3.0⁺ are solely based on *CSTR*'s models.

The objective of this study is to investigate the effect of the number of *CSTR*'s on the predicted effluent quality of oxidation ditches modelled as a loop-of-*CSTR*'s.

The paper is organised as follows: in the next section, material and methods are described. Then, the results are presented and discussed. And finally, the paper ends with some conclusions.

[†] A slightly modified version published by A. Abusam and K.J. Keesman in Med. Fac. Landbouw. Univ. Gent, Proc. 13th FAB, 64(5a), 1999, pp 91-94.

3.3 Materials and methods

3.3.1 Plant layout

The plant studied is a typical oxidation ditch plant that achieves *C*- and *N*-removal. For this analysis only an oxidation ditch (200 m x 10 m x 4 m) plus circular secondary settler, with surface area of 1500 m² and depth of 4 m, have been studied. Further assumptions used in the study are the following: (i) the oxidation ditch has only two aerators: the first aerator is located near the inlet port of the ditch, and the other aerator is exactly placed at the middle of the ditch, (ii) DO in the aerated compartments (*CSTR*'s) is assumed to be kept constant at 2 mg/l, (iii) volume of the aerated compartment is one-twentieth of the total volume (400 m³), (iv) circulation velocity along the ditch is 0.3 m/s, (v) sludge is wasted, from the bottom of the settler, at a constant rate of 0.01925 of the inflow, and (vi) returned sludge ratio is equal to 1.

3.3.2 Simulation model

In the Matlab/Simulink environment, the oxidation ditch was modelled as a loop-of-*CSTR*'s, using *ASM No.1* (Henze *et al.* 1987) for the biochemical processes. The secondary settler was modelled as a ten-layer non-reactive settling tank, using the model developed by Takács *et al.* (1991). The number of *CSTR*'s studied is equal to 4, 6, 10, 14, 20, 24 and 30. Values of the kinetic, stoichiometric and settling parameters used in these models were the same as those suggested by the COST 624, for temperature of 15 °C (see <http://www.ensic.u-nancy.fr/COSTWWTP/Benchmark/Benchmark1.htm>).

3.3.3 Methods

A steady state simulation has been conducted for 100 days, using the average concentrations given by COST 624. Results of these simulations were then used for studying the effect of number of *CSTR*'s on effluent quality - at steady state conditions.

Using the end values of the steady state simulations as initial conditions, dynamic simulations were then carried out for another 28 days. Influent data used in the dynamic simulations were the dry weather flow provided by COST 624 Working Group. These influent data have a sampling interval equal to 15 minutes. Only the last 14 days of the dynamic simulations were used in the dynamic (frequency domain) analysis, which essentially presents the influent frequency spectrum and the amplitude plots of the transfer function estimates for the different components. In particular, the amplitudes are calculated as $|\hat{G}_s^N(e^{i\omega})|$ i.e. the absolute values of the spectral estimate $\hat{G}_s^N(e^{i\omega})$ for the different frequencies (ω) calculated from the *N* input and output data. This estimate is calculated as:

$$\hat{G}_s^N(e^{i\omega}) = \frac{\hat{\Phi}_{\phi_s^N}^N(\omega)}{\hat{\Phi}_{u_s^N}^N(\omega)} = \frac{\sum_{l=0}^N \hat{r}_s^N(l) e^{-i\omega l}}{\sum_{l=0}^N \hat{r}_u^N(l) e^{-i\omega l}} \quad (1)$$

Herein, u is the influent concentration, and \hat{y} is the corresponding simulated output of a specific component indicated by the dot. Furthermore, $\hat{\Phi}_{u,\dot{y}}^N$ is the cross spectrum of input and output, and $\hat{\Phi}_{\dot{y},\dot{y}}^N$ is the power (auto-) spectrum. These spectra can thus be calculated from $\hat{r}_{\dot{y}}^N(\omega)$ and $\hat{r}_u^N(\omega)$, the cross- and auto-correlation functions, respectively (see e.g. Jenkins and Watts, 1968).

3.4 Results and discussion

3.4.1 Steady state simulations

Fig. 1a shows the effect on the soluble components. As it will be seen from this figure, the mostly affected soluble components are S_{NO} and S_{NH} . Effect on these components can be attributed to the increase in S_O (see Fig.2), with the increase in number of *CSTR*'s. Increase in S_O has affected the rate of nitrification-denitrification processes, and consequently, S_{NH} has decreased while S_{NO} has increased (Fig.1a). Hence the effect on S_{NO} is mainly due to increase in S_O along the ditch (Fig.2). It can also be seen from Fig. 1a that beyond 10-15 *CSTR*'s there is no significant increase in S_{NO} , nor a significant decrease in S_{NH} . Therefore, we have concluded in this particular case that, regarding the

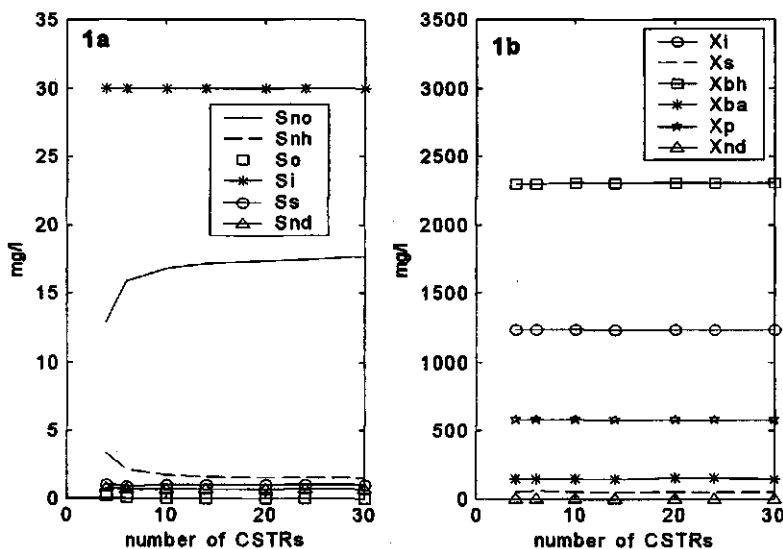


Fig. 1, (a) Effect of number of *CSTR*'s on the soluble components (b) Effect of number of *CSTR*'s on the particulate components, in steady state.

soluble components, the number of *CSTR*'s can be limited to 10 *CSTR*'s, or preferably to the number of *CSTR*'s needed for adequate modeling of the ditch, since in practice the effect on effluent S_{NO} and S_{NH} can always be compensated by an adjustment of the estimated aeration capacity.

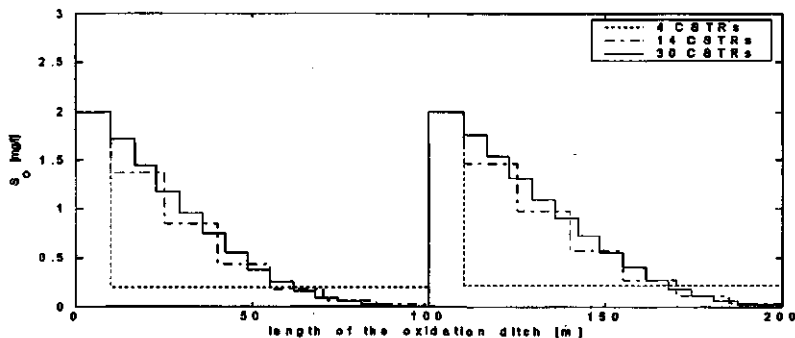


Fig. 2, S_o profile along the oxidation ditch.

Fig.1b presents the effect of number of *CSTR*'s on the particulate components. It is very clear that number of *CSTR*'s has no significant influence on the predicted concentration of the particulate components. Thus, as far as the particulate components are concerned, any number of *CSTR*'s can be used for modeling the oxidation ditch. However, the lower the number of *CSTR*'s, the less the computational time. Thus, regarding both the soluble and the particulate components it is advisable to keep the number of *CSTR*'s used for modeling an oxidation ditch at a minimum. This is as far as the steady states simulations are concerned.

3.4.2 Dynamic simulations

Influent frequency spectrum and amplitude plots for the components S_S , X_{BH} , and S_{NH} in the in- and outflow of the oxidation ditch are presented in Fig.3.a, b, c and d, respectively. It is evident from these figures that the estimates of the transfer function representing the system dynamics are very sensitive for high frequencies. It is also clear that no useful information about the system dynamics can be obtained at frequencies higher than 1 rad/15 min. due to the significant presence of high frequent noise components in the input and output (see Fig. 3b, c and d). Notice that the influent spectrum (Fig.3a) shows a peak at approximately 0.14 rad/15 min. i.e. $24 \cdot 4 \cdot 0.14 / 2\pi \approx 2 \text{ day}^{-1}$, which is, as visible in the influent data (not shown here), the approximate 2 peaks per day. At frequencies lower than 0.3 rad/15 min., there is a clear variation in the amplitude ratio due to the variation in number of *CSTR*'s. As in the steady state conditions, soluble components (S_S and S_{NH}) are more affected by the change in the number of *CSTR*'s than the particulate components (only the effect on X_{BH} is presented here). These results confirm the conclusions we have arrived to through steady state

simulations. Finally, it can also be seen from these figures that increasing the number of CSTR's have resulted in a slight reduction in the flat region of the amplitude plots (Fig.3b, c and d). This means that the effect of number of CSTR's is mainly apparent at low frequency region.

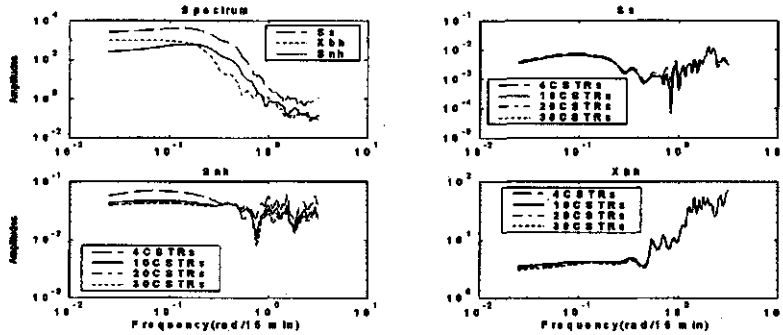


Fig. 3, (a) Amplitude spectrum of influent S_s , X_{BH} and S_{NH} , (b) Empirical Bode amplitude plot for S_s , (c) Empirical Bode amplitude plot for S_{NH} , (d) Empirical Bode amplitude plot for X_{BH} .

3.5 Conclusions

The number of CSTR's has no significant effect on the predicted effluent particulate concentration of an oxidation ditch. However, number of CSTR's mainly affects S_{NO} and S_{NH} due to increase in S_O with the increase in number of CSTR's. Beyond 10 CSTR's, there is no significant effect to increase in number of CSTR's. Thus it is recommended to limit the number of CSTR's to 10 or to the minimum number needed for adequate modeling of the ditch, since the effect on S_{NO} and S_{NH} can always be compensated by an adjustment of the estimated aeration capacity. That is, the number of aerators in the ditch mainly determines the number of CSTR's needed for adequate modeling of the oxidation ditch.

3.6 References

- Alex, J. R. Tschepetzki, U. Jumar, F. Obenaus and K. H. Rosenwinkel (1999), Analysis and design of suitable model structure for activated sludge tanks with circulating flow, Wat. Sci. Tech. 39(4): 55-61.
- Dudley, J. (1995), Process testing of aerators in oxidation ditches, Wat. Res. 29(9): 2217-2219.
- Henze, M., C.P.L. Grady, W. Gujer, G.v.R. Marais and T. Matsuo (1987), Activated Sludge Model No. 1, IAWPRC Scientific and Technical Report, No. 1, IAWPRC, London. ISSN: 1010-707X.

Stamou, A. I. (1994), Modeling of oxidation ditches using the IAWPRC Activated Sludge Model with hydrodynamic effects. *Wat. Sci. Tech.* 30(2): 185-192.

Takács, I, G.G. Patry and D. Nolasco (1991), A dynamic model of the clarification-thickening process, *Wat. Res.* 25(10): 1263-71.

von Sperling, M. (1990), Optimal management of the oxidation ditch process, Ph.D. thesis, Imperial College, U.K.

Jenkins, G.M., and D.G. Watts (1968), Spectral analysis and its applications, Holden-Day, San Francisco.

4. Parameter estimation procedure for complex non-linear systems: calibration of *ASM No. 1* for N-removal in a full-scale oxidation ditch[§]

4.1 Abstract

When applied to large simulation models, the process of parameter estimation is also called calibration. Calibration of complex non-linear systems, such as activated sludge plants, is often not an easy task. On the one hand, manual calibration of such complex systems is usually time-consuming, and its results are often not reproducible. On the other hand, conventional automatic calibration methods are not always straightforward and often hampered by local minima problems. In this paper a new straightforward and automatic procedure, which is based on the response surface method (*RSM*) for selecting the best identifiable parameters, is proposed. In *RSM*, the process response (output) is related to the levels of the input variables in terms of a first- or second-order regression model. Usually, *RSM* is used to relate measured process output quantities to process conditions. However, in this paper *RSM* is used for selecting the dominant parameters, by evaluating parameters sensitivity in a predefined region. Good results obtained in calibration of *ASM No.1* for N-removal in a full-scale oxidation ditch proved that the proposed procedure is successful and reliable.

Keywords: Calibration; carousel; modeling; oxidation ditches; parameter estimation; *ASM No. 1*.

4.2 Introduction

Activated sludge plants are typical examples of complex non-linear systems. For on-line application, there is a need for adjusting the parameters initially obtained from literature or previous experiments, such that the model output fits the available data. The process of parameter estimation, when applied to large simulation models, is also called calibration. Calibration can be done either manually (hand calibration) or through automatic optimisation algorithms. Hand calibration, which is still commonly used in practice, is a trial and error method in which values of the parameters are changed manually and the difference between the measured and predicted values is evaluated visually. Because it consumes a lot of time and the reproduction of its results is always difficult, hand calibration is used only when automatic calibration is not available.

[§] A slightly modified version published by A. Abusam, K.J. Keesman, H. Spanjers, G. van Straten and K.Meinema in Proc. 5th Int. Symp. on Systems Analysis and Computing in Water Quality Management (*Watermatex2000*), Gent, Belgium, September 18-20, 2000, PP 8.1 - 8.8, (published in *Wat. Sci. Tech.*43(7):367-376).

On the contrary, the application of automatic calibration is also not always straightforward. For instance, automatic calibration of a model with multiple output variables and more than 5-7 parameters will usually show local minima. Selecting the best identifiable parameters and finding the optimum region(s) to obtain good initial guesses are the difficult parts in the calibration procedure. In order to remedy this a method like the response surface method (*RSM*) (see for example Box and Draper, 1987) can be useful. Myers and Montgomery (1995) define *RSM* as "a collection of statistical and mathematical techniques useful for developing, improving and optimising processes." In *RSM*, the process response (output) is related to the levels of the input variables in terms of a first- or second-order regression model. In this paper, *RSM* is used as a "regional sensitivity analysis" tool, where the input variables are the parameters and the outputs the sum of squares of the residuals. As a result of this, a set of best identifiable parameters can be found, while the optimum region(s) for these parameters can also be allocated from the surface analysis of the relationships found by *RSM*. Then, within the optimum region(s), any automatic calibration method can be applied for optimising the selected set of parameters.

The objective of this paper is to present a new straightforward automatic procedure, based on *RSM*, that can be used in parameter estimation for complex non-linear systems. The structure of this paper is as follows. First, the procedure is briefly described. Then, results of applying this procedure in calibration of *ASM No.1* for *N*-removal in a full-scale oxidation ditch is presented. Finally, the paper ends with conclusions about the success and reliability of the proposed method.

4.3 Proposed procedure

Generally, *RSM* is used to relate measured process output quantities to process conditions. However, in this paper *RSM* will be used to evaluate parameters sensitivity in a predefined region and not, as is common practice, in a local point in the parameter space. On the basis of this, dominant parameters can easily be selected. In addition, optimum region(s) for these parameters can be found by carrying out a surface analysis of the predicted sum of squares of the residuals. The proposed procedure can be summarised in the following six steps: (i) specify plant layout and model, (ii) collect in/output and operational data, (iii) estimate initial state conditions from past data, (iv) use *RSM* to select dominant parameters (run, for instance, a two-level simulation experiment and select the sensitive parameters from the resulting first- or second-order meta-model), (v) apply formal parameter estimation method and (vi) evaluate estimation results. In the next sections the procedure will be illuminated to a full-scale example. The proposed procedure was applied in the calibration of *ASM No.1* for *N*-removal in a full-scale carousel type *WWTP* situated in Rotterdam, the Netherlands.

4.3.1 Step 1: Specify plant layout and model.

The plant is designed for dry weather flow of $3583 \text{ m}^3/\text{h}$ and rain flow of $12800 \text{ m}^3/\text{h}$ (301500 inhabitants at $54 \text{ g BOD}_5/\text{capita} \cdot \text{d}$). It consists of two parallel lines, each having two primary settlers, one selector, three circular secondary settlers (diameter = 529 m and depth = 2 m), one carrousel of capacity equal to 13000 m^3 (see Fig. 1) and four aerators (estimated oxygen input for each is $70.2 \text{ kg O}_2/\text{h}$ at high speed, and $40.2 \text{ kg O}_2/\text{h}$ at low

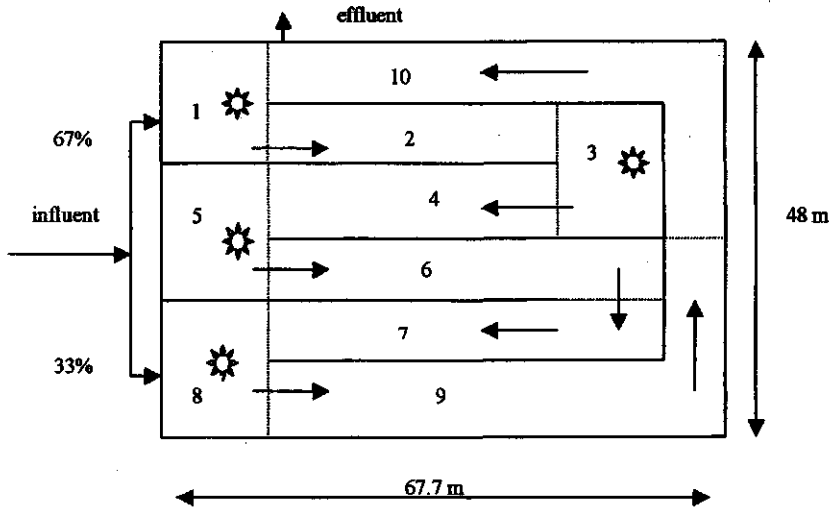


Fig. 1, Layout of the carrousel

speed). The plant was modelled as a loop of 10 equal-volume *CSTR*'s plus a secondary settler. *ASM No. 1* (Henze et al., 1987), which is considered to be the state of the art for dynamic modeling of activated sludge plants with *COD* and *N* removal, was used for modeling the biochemical processes, while the double exponential model, developed by Takács et al. (1991) was used for modeling the secondary settler. The number of *CSTR*'s was chosen on the basis of the number of aerators in the ditch and the ditch layout. This number was limited to 10 *CSTR*'s, of which four for representing the aerated compartments and six for representing the anoxic compartments. In a previous paper it has been shown that increase of number of *CSTR*'s beyond 10 does not significantly affect the predicted effluent quality of the oxidation ditch (Abusam and Keesman, 1999).

4.3.2 Step 2: Collect in/output and operational data

The calibration data set consist of 10-day measurements performed, at dry weather conditions (DHW Water, 1993), from 27 July to 7 August 1992. Variables measured were daily influent and effluent *COD_{tot}*, *TKN*, *NH₄-N*, *NO₃-N* and temperature (mean: $22.3 \text{ }^\circ\text{C}$). *COD_{tot}* and *TKN* were calculated from the settleable, colloidal and dissolved fractions.

On 29/7, 30/7, 4/8 and 7/8 volume proportional sampling was carried out every 2 hours, from which it was concluded that variations in concentration of COD_{tot} and TKN were very small over the day. Other operational data are as follows. Average daily flow equals to $48681 \text{ m}^3/\text{d}$; 67% of the carousel influent, on volume basis, is directed to the first aerator and the rest to the fourth aerator (compartment 8, in Fig. 1). Further, the rate of waste activated sludge (WAS) is $780 - 870 \text{ m}^3/\text{d}$, the rate of recycled activated sludge (RAS) is equal to the influent flow rate, the rate of internal recirculation is about 83 times the influent flow rate, and the sludge age is about 9 days.

The influent composition expressed in *ASM No.1* components were obtained using the influent characterisation values provided with the data. Provided data also included the 19 kinetic and stoichiometric parameter values, which were then used as a starting point of the procedure.

4.3.3 Step 3: Estimate initial state conditions from past data

Initial substrate and biomass concentrations were unknown. For estimating these, we have performed a 100-day steady state simulation, using the averages of the provided measurements and default parameter values (DHV Water, 1993). The aeration constant used in the steady state simulation was estimated from the given information about oxygen input (based only on COD removal) and it was equal to $150000 \text{ m}^3/\text{d}$. Note here that we have estimated the aeration constant ($k = K_{La} \cdot V_A$) because it can be estimated more accurately than K_{La} . In fact, neither K_{La} nor V_A can be identified individually due to the hyperbolic relationship between these parameters (Abusam et al., 2001).

4.3.4 Step 4: Use *RSM* to select dominant parameters

In this study, given the measurements of effluent NH_4-N and effluent NO_3-N , there are two responses; that is, the sum of squared errors for effluent NO_3-N and effluent NH_4-N . However, for total nitrogen removal, the response that needs to be analysed is the weighted sum of squared errors for both effluent NO_3-N and effluent NH_4-N . Note that COD_{tot} has not been taken into account, because it was found to be unreliable.

In order to apply *RSM*, it is wise to limit the number of computations by restricting the number of parameters to no more than 10-12. A pre-sensitivity analysis could help in performing this pre-selection. Many parameters can be tried for calibrating N -removal in such cases (Weijers et al., 1996; Keesman et al., 1996). Since our goal here is to illustrate the method, we have restricted the analysis to those parameters that can be of potential interest: η_g and η_h , K_{NO} and K_{NH} (coefficients for growth and hydrolysis under anoxic conditions, nitrate and ammonia half-saturation coefficients, respectively). Since we do not know the actual oxygen input, we will also try to estimate the aeration constant (k), which is the product of K_{La} and V_A (the actually aerated volume). As mentioned above, k can be estimated more accurately than K_{La} or V_A . However, instead of estimating k directly, we have estimated a multiplication factor ($m = k/k_0$), which we can use subsequently for the calculation of the actual aeration constant ($k = m \cdot k_0$). Here k_0 is the

initial guess for the actual aeration constant ($k_0 = 150000 \text{ m}^3/d$). Thus we have five potential parameters that need to be identified: m , K_{NO} , K_{NH} , η_g and η_h .

The next step is to design a simulation experiment such that a second-order regression-type meta-model can be fitted. As recommended by Box and Draper (1987), a two-level factorial design with cubic, star and centre portions has been chosen. The normalised second-order composite design around the nominal parameter vector has been specified as follows: cube portion: $(\pm 1, \pm 1, \pm 1, \pm 1, \pm 1)$, star portion: $(\pm \alpha, 0, 0, 0, 0)$, $(0, \pm \alpha, 0, 0, 0)$, $(0, 0, \pm \alpha, 0, 0)$, $(0, 0, 0, \pm \alpha, 0)$, $(0, 0, 0, 0, \pm \alpha)$ and centre portion: $(0, 0, 0, 0, 0)$. Here $\alpha = \sqrt{5}$, so that all points, except the centre point, are situated on a ball in the parameter space. Hence the total number of simulation runs equals to 43 ($= 2^5 + 5.2 + 1$).

Table 1 presents the coded levels for the five chosen parameters. As it can be seen from this table, values of the parameters K_{NO} and K_{NH} were limited to the ranges reported in literature, while relatively wide ranges are explored for m (indirectly the aeration constant) η_g and η_h .

Table 1, Coded level of the 5 variables

| Variables | Coded Level, x_i | | | | | x_i in terms of the variables |
|-----------|--------------------|------|-----|------|-------------|---------------------------------|
| | $-\sqrt{5}$ | -1 | 0 | +1 | $+\sqrt{5}$ | |
| m | 0.38 | 1.0 | 1.5 | 2.0 | 2.63 | $x_1 = (m-1.5)/0.5$ |
| η_g | 0.2 | 0.42 | 0.6 | 0.78 | 1.0 | $x_2 = (\eta_g-0.6)/0.18$ |
| η_h | 0.2 | 0.42 | 0.6 | 0.78 | 1.0 | $x_3 = (\eta_h-0.6)/0.18$ |
| K_{NO} | 0.28 | 0.40 | 0.5 | 0.60 | 0.72 | $x_4 = (K_{NO}-0.6)/0.1$ |
| K_{NH} | 0.64 | 0.71 | 0.8 | 0.87 | 0.96 | $x_5 = (K_{NH}-0.8)/0.08$ |

From the 43 simulation runs the following second-order regression model resulted for the weighted sum of squares ($V = \frac{V_{NO3}}{10} + V_{NH4}$):

$$\begin{aligned}
 V = & 187.8 - 611.4x_1 - 120.4x_2 + 184.0x_3 + 21.3x_4 + 34.2x_5 \\
 & (\pm 192.9) (\pm 29.8) (\pm 29.8) (\pm 29.8) (\pm 29.8) (\pm 29.8) \\
 & + 369.7x_1^2 + 63.1x_2^2 + 18.7x_3^2 + 3.9x_4^2 + 3.7x_5^2 + 165.2x_1x_2 \\
 & (\pm 46.0) (\pm 46.0) (\pm 46.0) (\pm 46.0) (\pm 46.0) (\pm 34.1) \\
 & - 130.2x_1x_3 + 42.5x_1x_4 + 30.7x_1x_5 - 6.3x_2x_3 + 37.7x_2x_4 + 35.7x_2x_5 \\
 & (\pm 34.1) (\pm 34.1) (\pm 34.1) (\pm 34.1) (\pm 34.1) (\pm 34.1) \\
 & + 37.9x_3x_4 + 36.7x_3x_5 + 36.3x_4x_5 \\
 & (\pm 34.1) (\pm 34.1) (\pm 34.1)
 \end{aligned} \tag{1}$$

where the values between the parenthesis are the standard deviations, and V_{NO_3} and V_{NH_4} are the sum of squared errors for effluent NO_3-N and effluent NH_4-N , respectively.

Comparison of the standard deviations (shown between parenthesis) and corresponding coefficients (which are the parameter sensitivity coefficients) in the model (Equation 1) indicates which parameters are sensitive and which are not (coefficient $< 2 \text{ std. dev.}$). Equation (1) shows that the sensitive parameters are only x_1 , x_2 , x_3 , x_1^2 , x_2^2 and the interactions x_1x_2 and x_1x_3 . Thus, it can be concluded that the sensitive parameters here are: x_1 , x_2 and x_3 . Consequently x_4 and x_5 are insensitive and can be set to default values.

For further analysis and evaluation of this result, the general format for this second-order model:

$$V = C + Lx + x^T Hx \quad (2)$$

will be used, where C is a scalar term, L is a column vector consisting of the coefficients of the linear terms and H is a symmetrical matrix formed from the coefficients of the quadratic terms.

Figure 2 presents the contour plots (of Equation 1) of the weighted sum of squared errors for both NO_3-N and NH_4-N , where the weighting factor is equal to 10. The factor of 10 was chosen because individual responses indicated that the sum of squared errors for NO_3-N is about 10 times higher than that for NH_4-N . In fact, this is an engineering guess.

Careful examination of Fig. 2 reveals that the optimum value of m is between 1.25 to 2.125 (x_1 : -0.5 to 1.25), optimum value of η_g is between 0.3 and 1.0 (x_2 : -1.5 to 2.24), and optimum value of η_h is between 0.2 and 0.9 (x_3 : -2.24 to 1.5). In addition to this, directions of the principal axes of the ellipses can be obtained from the eigenvalue decomposition of the matrix H for this so called meta model (see Appendix B), and the centre of the model response surface ($x_g = -H^{-1} \cdot L/2$)

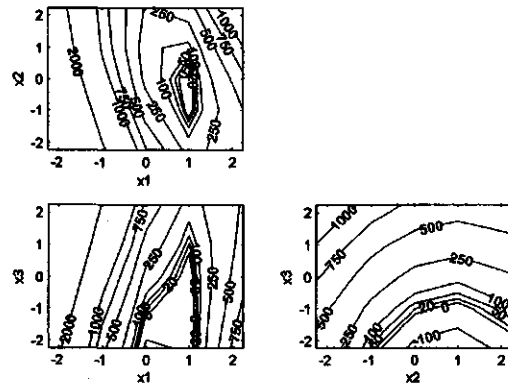


Fig. 2, Contour plots of $V_{NO_3}/10 + V_{NH_4}$ for (a) $x_1 - x_2$ (b) $x_1 - x_3$ and (c) $x_2 - x_3$

(Box and Draper, 1987) can be used as initial guess. This is especially useful when the number of parameters is large. Since it exponentially increases with the increase in number of parameters, computational time will be the real problem when the number of parameters become very high. But this problem can be solved, as suggested by Box and Draper (1987), by using the so-called fractional factorial designs instead of the full

factorial design. In the next step, this information about the optimum regions will be used within a constrained optimisation routine for estimating the parameters m , η_g and η_h .

4.3.5 Step 5: Apply formal parameter estimation method

All the 19 parameters in *ASM No.1* were set to default values obtained from DHV Water (1993), except the three best identifiable parameters: m , η_g and η_h . Values of these parameters were constrained as specified in the previous step.

Fig. 3 presents the results of the second least squares optimisation trial with the following results: $m=1.84$ ($k=1.84 \cdot 150000 = 276000 \text{ m}^3/\text{d}$), $\eta_g = 1.0$ and $\eta_h = 0.32$. Two trials of optimisation were conducted because it appeared that the parameter values of the first trial ($m = 1.89$, $\eta_g = 0.92$ and $\eta_h = 0.31$) led to significantly different initial state conditions when compared to those obtained from prior knowledge. Using these

recalculations with conditions led to a relatively poor fit. In the second trial, using the recalculated initial conditions from the first trial, however, there was no change in the fit even when the results of least-square optimisation were used again for recalculating the initial conditions. From these two trials, we noted that the estimated initial concentrations of heterotrophic and autotrophic biomass are almost the same for both trials. However, the initial concentration of the slowly biodegradable substrate (X_S) obtained from steady state simulation using the default parameters was very high (418 mg COD/l) compared to that obtained using parameters from the first trial (64 mg COD/l) or the second trial (68 mg COD/l). Hence, there was clearly a need for recalculating the initial conditions.

In order to see the effect of the initial concentration of $\text{NO}_3\text{-N}$ and $\text{NH}_4\text{-N}$, we carried out a number of simulations with different initial values for $\text{NO}_3\text{-N}$ and $\text{NH}_4\text{-N}$. Results of these simulations indicated that over a reasonable range initial nitrogen concentrations have no effect on the curve fit. From steady state simulations, however, we have noted that the predicted initial nitrogen concentration (about $9.5 \text{ mg NO}_3\text{-N/l}$ and $0.5 \text{ mg NH}_4\text{-N/l}$) is always different from the measured value ($5.21 \text{ mg NO}_3\text{-N/l}$ and $2.57 \text{ mg NH}_4\text{-N/l}$). If we again have a look at Fig. 3, we can see that nitrogen concentrations in the first day seem to be inconsistent with the rest of the data. Therefore, we indicate that nitrogen values reported for the first day may be incorrect. The reason for that is probably an experimental error.

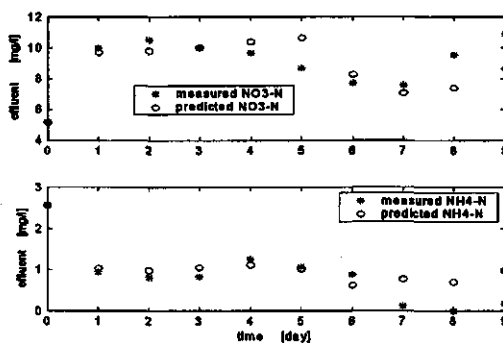


Fig. 3, Predicted and measured concentration in effluent (a) nitrate and (b) ammonia

Furthermore, the effect of the number of *CSTR*'s on the parameter estimation was evaluated. For that we have constructed two extra models that consist of 8 and 16 *CSTR*'s. Subsequently, the same formal optimisation procedure was applied. As shown in Table 2 the number of *CSTR*'s has no significant effect on the estimated values.

Table 2, Effect of number of *CSTR*'s on the parameter estimation

| Number of <i>CSTR</i> 's | m | η_R | η_h |
|--------------------------|------|----------|----------|
| 8 | 1.89 | 0.99 | 0.35 |
| 10 | 1.84 | 1.0 | 0.32 |
| 16 | 1.85 | 0.99 | 0.34 |

4.3.6 Step 6: Evaluate estimation results

First of all, evaluation of the residuals (Fig. 3) shows that the amplitude of the residual is acceptable. However, systematic errors appear indicating incorrectness of model structure and/or experimental data. The data is too short to deduce more profound conclusions. In addition, uncertainty analysis of the estimates was carried out (see also Lukasse *et al.*, 1996 and 1997). Neglecting the residual correlation structure, local parameter estimates uncertainties can be approximately found from the resulting covariance matrix:

$$\text{Cov}(\hat{\theta}_N) = \hat{\sigma}_\varepsilon^2 (J^T J)^{-1} \quad (3)$$

where J is the Jacobi matrix $\frac{d\varepsilon(t_k|\theta)}{d\theta_j}$ with $k=1, \dots, N$; $j=1, \dots, p$, and $\hat{\sigma}_\varepsilon^2$ is the variance of the residuals.

In order to evaluate the estimation uncertainty in more detail, the dominant parameter directions were investigated via eigenvalue decomposition of the covariance matrix; that is

$$M^T \text{Cov} \hat{\theta}_N M = \Lambda \quad (4)$$

where M is the orthogonal matrix of eigenvectors and Λ is a diagonal matrix with eigenvalues.

From the covariance matrix and eigenvalue decomposition results, which are presented in Appendix C, we can conclude the following. Firstly, a small value of the elements of Λ (eigenvalues) indicates that all the three parameters can be estimated with a high reliability. This is also indicated by the small standard deviations (square root of the diagonal of the covariance matrix). Secondly, the third element of Λ has the smallest value (0.0063), which indicates that η_h slightly dominates the model behaviour. Finally, there is no relatively big difference between the values of the elements in Λ . This simply means that all the three parameters are sensitive, a result that has also been found from the previous RSM analysis.

The aeration constant (k , related to m) can also be estimated roughly in another way from the average C and N removals (about 215 g COD/m^3 and 27 g N/m^3 , respectively). This provides a cross-check about the adequacy of the method. Using Equation 5, the oxygen input by one aerator at full capacity can be estimated to be $1774 \text{ kg O}_2/\text{d}$.

$$O_2 = Q(\text{COD}_{\text{ox}} \cdot (1 - Y_H) + 4.57TN) / f \quad (5)$$

where, $Q = \frac{48681}{2} \text{ m}^3/\text{d}$, $Y_H = 0.67$ and $f = 2.76$. Here f is the sum of the relative working capacity per day for all the aerators (see Appendix A). From simulations it has been found that the average oxygen deficit, around the first and second aerators, is about 7.2 g/m^3 . Thus the k (oxygen input/oxygen deficit) is about $246389 \text{ m}^3/\text{d}$. Comparison of this rough estimate ($246389 \text{ m}^3/\text{d}$) with the value obtained in step 5 ($276000 \text{ m}^3/\text{d}$) indicates that the aeration constant was estimated very accurately.

4.4 Conclusions

A new procedure was proposed for estimating parameters of a non-linear system. Success in calibrating *ASM No.1* (a typical non-linear system) for N -removal in a full-scale carousel *WWTP* proved that the proposed procedure is successful and reliable. The loop-of-*CSTR*'s model proved to be an acceptable model for describing the behaviour of oxidation ditches under process conditions, with respect to influent and effluent quality. As under clean water conditions (Abusam et al., 2001), the aeration constant ($K_L a \cdot V_A$) can be estimated with a very high accuracy ($k = 276000 \pm 63.16 \text{ m}^3/\text{d}$), also under process conditions.

4.5 References

Abusam, A. and K.J. Keesman (1999), Effect of number of *CSTR*'s on the modeling of oxidation ditches: steady state and dynamic analysis, *Med. Fac. Landbouw. Univ. Gent*, 64/5a, pp 91-94.

Abusam, A., K.J. Keesman, K. Meinema and G. van Straten (2001), Oxygen transfer rate estimation in oxidation ditches for clean water measurements, *Wat. Res.* (in press)

Box, G.E.P. and N.R. Draper (1987), *Empirical model-building and response surfaces*, John Wiley and Sons.

DHV Water (1993), DHV Water BV, Dossier G8112-10-001, Amersfoort, The Netherlands.

Henze, M., C.P.L. Grady, jr, W. Gujer, G. van R. Marais and T. Matsuo (1987), *Activated sludge model no. 1*, IAWQ scientific and Technical Report no. 1, IAWQ, London, U.K.

Keesman, K.J., I. Hemmers and A. Witteborg (1996), Set-membership pre-processor in identification of complex dynamical models: a wastewater treatment example, *proc. World Congress '96, Montpellier, France, vol. 1, pp. 116-122.*

Lukasse, L.J.S., K.J. Keesman and G. van Straten (1996), Grey-box identification of dissolved oxygen dynamics in activated sludge processes, in *proc. 13th IFAC World Congress, vol. N, San Francisco, USA, pp 485-490.*

Lukasse, L.J.S., K.J. Keesman and G. van Straten (1997), Identification for model predictive control of biotechnological processes, case study: nitrogen removal in activated sludge process, in *proc. 11th IFAC Symp. on Sys. Ident., 3, Fukuoka, Japan, pp 1525-1530.*

Myers, R.H. and D.C. Montgomery (1995), *Response surface methodology: Process and product optimisation using designed experiments*, John Wiley and Sons.

Tackács, I., G.G. Patry and D. Nolasco (1991). A dynamic model of the clarification-thickening process, *wat res 25(10):1263-1271.*

Weijers, S.R., H.A. Preisig, J.J. Kok, A. Buunen and T.W.M. Wouda (1996), Parameter identifiability and estimation of the IAWQ activated sludge model no.1, *Med. Fac. Landbouw. Univ. Gent, 61/4a, pp 1809-1813.*

4.6 Appendix A: Operational pattern of the aerators

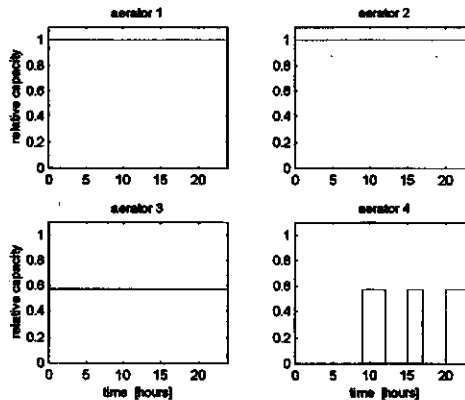


Fig. A1, Relative operational pattern of the aerators

4.7 Appendix B: Directions of dominant parameters

Given H (see Equation 2), eigenvalue decomposition of H gives:

$$M = \begin{bmatrix} 0.96 & 0.13 & -0.22 & -0.15 & -0.02 \\ 0.24 & -0.67 & 0.70 & -0.08 & -0.03 \\ -0.16 & -0.45 & -0.47 & -0.72 & -0.16 \\ 0.06 & -0.41 & -0.36 & 0.63 & -0.58 \\ 0.04 & -0.41 & -0.34 & 0.25 & 0.80 \end{bmatrix}$$

$$\Lambda = \text{diag}([403.17 \ 66.82 \ 21.40 \ -18.00 \ -14.33])$$

where M is the orthogonal matrix of eigenvectors, Λ is diagonal matrix with eigenvalues for V and "diag" defines diagonal matrix operations.

The rows of V correspond with the parameter sequence of table 1. Eigenvectors give directions of the principal axes of the ellipses, where lengths of these principal axes are inversely proportional to the square root of the absolute magnitude of corresponding eigenvalue. Hence, it can be concluded that the eigenvector $[0.96 \ 0.24 \ -0.16 \ 0.06 \ 0.04]^T$, which is roughly dominated by the first two elements, defines a dominant direction. Notice that this is also verified by Fig. 2 (plot $x_1 - x_2$), using the rough simulation data.

4.8 Appendix C: Evaluation of parameter uncertainties

$$\text{Cov}\hat{\theta}_N = 10^{-6} \cdot \begin{bmatrix} 0.1773 & -0.0354 & 0.0189 \\ -0.0354 & 0.0175 & -0.0068 \\ 0.0189 & -0.0068 & 0.0105 \end{bmatrix} \quad M = \begin{bmatrix} -0.9718 & 0.2332 & 0.0345 \\ 0.2075 & 0.7766 & 0.5949 \\ -0.1119 & -0.5853 & 0.8031 \end{bmatrix}$$

$$\Lambda = (\text{diag}(10^{-6} \cdot [0.1870 \ 0.0120 \ 0.0063]))$$

where "diag" defines diagonal matrix operations. The rows of M correspond to weights on m , η_g and η_b , respectively.

PART 2
MODEL ANALYSIS

5. Sensitivity analysis in oxidation ditch modeling: the effect of variations in stoichiometric, kinetic and operating parameters on the performance indices**

5.1 Abstract

This paper demonstrates the application of the factorial sensitivity analysis methodology in studying the influence of variations in stoichiometric, kinetic and operating parameters on the performance indices of an oxidation ditch simulation model (benchmark). Factorial sensitivity analysis investigates the sensitivities in a region rather than in a point. Hence, it has the advantage of giving more information about parameter interactions (non-linearity). Short-term results obtained have shown the following. The index *AE* is not significantly affected by variations in the value of parameters of the activated sludge model (*ASM*) No.1. The index *TSP* is greatly influence by heterotrophic yield (Y_H), heterotrophic decay (b_H) and specific hydrolysis (k_h) and the index *EQ* is dominated by Y_H , Monod coefficient (K_S), b_H , k_h , anoxic condition correction factors (η_p , η_h), hydrolysis half-saturation coefficient (K_X), autotrophs maximum specific growth rate (μ_A) and ammonia half-saturation coefficient (K_{NH}). Furthermore, the index *EQ* has shown to be very sensitive to parameter interactions, at certain regions.

Keywords: sensitivity analysis; oxidation ditch; control strategies; benchmark; wastewater.

Nomenclature:

β : weighting factor that converts different types of pollution into pollution units (dimensionless).

μ_A : maximum specific growth rate for autotrophic biomass (d^{-1}).

η_p : correction factor for μ_H under anoxic conditions (dimensionless).

η_h : correction factor for hydrolysis under anoxic conditions (dimensionless).

μ_H : maximum specific growth rate for heterotrophic biomass (d^{-1}).

a : column vector consisting of the coefficients of the linear terms

a_0 : scalar term.

A : symmetrical matrix formed from the quadratic terms.

$AC_{h,i}$: average hourly aeration capacity relative to the aerator full capacity.

AE: aeration energy index (kWh/d).

ASM: activated sludge model.

b_A : decay coefficient for autotrophic biomass (d^{-1}).

b_H : decay coefficient for heterotrophic biomass (d^{-1}).

BOD: biological oxygen demand (g/m^3).

C_L : operating oxygen concentration (g/m^3).

COD: chemical oxygen demand (g/m^3).

** Published by A. Abusam, K.J. Keesman, G. van Straten, H. Spanjers and K. Meinema in J. Chem. Tech. Biotech. 76(4):430-438.

CSTR: completely stirred tank reactor.

C_s^* : oxygen saturation concentration at field temperature, (g/m^3).

e : effluent.

EQ : effluent quality index (g/d).

F : average daily aeration capacity relative to the aerator full capacity ($F_i = \frac{1}{24} \sum_{j=0}^{24} AC_b$).

f_p : fraction of biomass leading to particulate products (dimensionless).

i : number of the aerated compartment, 1... 4.

i_{NB} : mass of nitrogen per mass of COD in biomass ($g N / (g COD^d)$).

i_{NP} : mass of nitrogen per mass of COD in products from biomass ($g N / (g COD^d)$ in endogenous mass).

j : daily time, in hours (0:1:24).

k : aeration constant, $K_L a \cdot V_A$, ($m^3 d^{-1}$).

k_a : ammonification rate ($m^3 COD / (g \cdot day)^{-1}$).

k_h : maximum specific hydrolysis rate (g slowly biodegradable COD (g cell COD.day) $^{-1}$).

$K_L a$: overall oxygen transfer rate (d^{-1}). Note that here $k_L a$ is calculated for the assumed aerated volume (compartment) and not for the whole ditch.

K_{NH} : ammonia half-saturation coefficient for autotrophic biomass ($g NH_4-N.m^{-3}$).

K_{NO} : nitrate half-saturation coefficient for denitrifying heterotrophic biomass ($g NO_3-N.m^{-3}$).

K_{O_A} : oxygen half-saturation coefficient for autotrophic biomass ($g O_2.m^{-3}$).

K_{O_H} : oxygen half-saturation coefficient for heterotrophic biomass ($g O_2.m^{-3}$).

K_S : half-saturation coefficient for heterotrophic biomass ($g COD.m^{-3}$).

K_X : half-saturation coefficient for hydrolysis of slowly biodegradable substrate (g slowly biodegradable COD (g cell COD) $^{-1}$).

M : sludge mass.

N : efficiency of the aerator at 22.4 °C (1.48 kg O_2/kWh).

n : number of aerators in the oxidation ditch ($n = 4$).

NH_4-N : ammonia nitrogen (g/m^3).

NO_3-N : nitrate nitrogen (g/m^3).

O_2 : oxygen.

PU : pollution unit (g/m^3).

Q : average daily flow (m^3/d).

S_i : soluble inert organic matter (g/m^3).

S_{ND} : soluble biodegradable organic nitrogen (g/m^3).

S_{NH} : $NH_4 + NH_3$ nitrogen (g/m^3).

S_{NO} : nitrate and nitrite nitrogen (g/m^3).

SRT : solid retention time.

S_S : readily biodegradable substrate (g/m^3).

T : evaluation period ($T = 7$ days)

t : time (day).

TKN : total kjeldahl nitrogen (g/m^3).

TSP : total sludge production index (g/d).

TSS : total suspended solids (g/m^3).

V_A : volume of the aerated compartment (m^3).

$V_{reactors}$: volume of the reactors (m^3).

$V_{settlers}$: volume of the settlers (m^3).

w : wasted sludge.

$WWTP$: wastewater treatment plant.

x : vector of parameters.

$X_{B,H}$: active autotrophic biomass (g/m^3).

$X_{B,H}$: active heterotrophic biomass (g/m^3).

X_i : particulate inert organic matter (g/m^3).

X_p : particulate products arising from biomass decay (g/m^3).

X_S : slowly biodegradable substrate (g/m^3).

Y_A : yield for autotrophic biomass (g cell COD formed ($g N$ oxidized) $^{-1}$).

Y_H : yield for heterotrophic biomass (g cell COD formed (g COD oxidized)⁻¹).

5.2 Introduction

Increasing pollution problems in receiving waters have contributed to an increased interest in minimising pollution loads coming from wastewater treatment plants (*WWTP*'s). In order to achieve this goal many control strategies have been proposed for improving the performance of *WWTP*'s. However, very few of these control strategies have been thoroughly evaluated, either in practical tests or in computer simulations. Furthermore, in practical tests the evaluation period is often too short to take into account all possible changes in the process (Alex *et al.*, 1999; Pons *et al.*, 1999).

In fact, due to time and money limitations, evaluation of all the proposed control strategies by carrying out practical tests is obviously impossible. Thus computer simulations offer a useful approach to solve this problem. In this direction, Working Group 2 of the European Concerted Action Programme (*COST*) 624 has proposed benchmarking of the performance of activated sludge *WWTP*'s (Pons *et al.*, 1999). Here a benchmark is defined as a standard simulation procedure that can be used in evaluating and comparing various control strategies. It consists of a description of the plant layout, a simulation model and definitions of (controller) performance criteria.

Sensitivity analysis is a very important stage in the benchmarking process. It is the stage at which the reliability and applicability of the developed simulation model will be accessed. It is often carried out in order to give insight as to the component of the model (parameters and/or inputs) that requires special attention. Different sensitivity analysis methods are available (Keesman, 1989): using (i) analytical or numerically approximated sensitivity functions, (ii) Taylor series expansion of the criterion function related to a parameter estimation problem or (iii) Monte Carlo simulations. Janssen (1994) classified sensitivity analysis methods as either direct or approximate. Whereas with former method, the model is directly evaluated for individual parameter perturbations, in the later approach the relationship between model output and model components is approximated by so-called meta-models. An example of the approximate method is the factorial sensitivity analysis method, which is based on a factorial design of the numerical experiments. Factorial sensitivity analysis method has two main advantages over the direct method: it is straightforward and it gives more information about the interaction (non-linearity) effect of variables (Janssen, 1994; Lee and Jones, 1996; Hu and Islam, 1997).

Towards benchmarking a very specific full-scale oxidation ditch *WWTP*, we have developed the simulation model (see Abusam *et al.*, 2000). The main objective of this paper is to demonstrate the use of the factorial sensitivity method in identifying and accessing the stoichiometric and kinetic parameters that have dominant influence on the *performance indices* of the oxidation ditch benchmark under development. In this paper a methodology is presented to perform a sensitivity study. The methodology can easily be translated to other studies where parameters sensitivity with respect to performance indices, or other criteria, is relevant.

5.3 Performance indices

Performance indices that are used in this particular oxidation ditch benchmark are more or less similar to those developed for benchmarking other activated sludge systems by *COST 624 Working-Group* (Pons *et al.*, 1999) and *LAWQ Task-Group* on respirometry (Copp, 2000). For two reasons the energy equations, proposed by these working groups, were slightly modified in order to make them applicable to oxidation ditch systems. First, oxidation ditches usually use mechanical aerators, which are different than air diffusers adopted by the previously mentioned working groups. Secondly, in an oxidation ditch there is no special pump for internal recirculation, since this is also carried out by the mechanical aerators.

Performance indices studied were the effluent quality index (*EQ*), total sludge production index (*TSP*) and aeration energy index (*AE*). In this study these indices were evaluated for a full-scale wastewater treatment plant, using real input data. Because the available real data was for 10 days, the actual evaluations were carried out from the beginning of the 3rd day to the end of 9th day, in order to avoid uncertainties in the initial conditions.

The effluent quality index (*EQ*), in units of *g/d*, is defined as:

$$EQ := \frac{1}{T} \int_{t_0}^{t_0+T} [PU_{TSS}(t) + PU_{COD}(t) + PU_{BOD}(t) + PU_{TKN}(t) + PU_{NO}(t)] Q_e(t) dt \quad (1)$$

where:

$$PU_{TSS}(t) = \beta_{TSS} TSS_e(t), \beta_{TSS} = 2$$

$$PU_{COD}(t) = \beta_{COD} COD_e(t), \beta_{COD} = 1$$

$$PU_{BOD}(t) = \beta_{BOD} BOD_e(t), \beta_{BOD} = 2$$

$$PU_{TKN}(t) = \beta_{TKN} TKN_e(t), \beta_{TKN} = 20$$

$$PU_{NO}(t) = \beta_{NO} NO_{3,e}(t), \beta_{NO} = 20$$

$$TSS_e = 0.75 (X_{S,e} + X_{BH,e} + X_{BA,e} + X_{P,e} + X_{I,e})$$

$$COD_e = S_{S,e} + S_{I,e} + X_{S,e} + X_{BH,e} + X_{BA,e} + X_{P,e} + X_{I,e}$$

$$BOD_e = 0.25 (S_{S,e} + X_{S,e} + (1 - f_P) (X_{BH,e} + X_{BA,e}))$$

$$TKN_e = S_{NH,e} + S_{ND,e} + X_{ND,e} + i_{XB} (X_{BH,e} + X_{BA,e}) + i_{XP} (X_{P,e} + X_{I,e})$$

$$NO_{3,e} = S_{NO,e}$$

As it can be seen from (1), the *EQ* index represents the weighted sum of the effluent load multiplied by the flow. Values given for the weighting factors (β 's) are for a denitrifying system (<http://www.ensic.u-nancy.fr/COSTWWTP/Benchmark/Benchmark1.htm>). More information about these weighting factors is given by Vanrolleghem *et al.* (1996).

The total sludge production (*TSP*) index, in units of *g/d*, is defined as:

$$TSP := [\Delta M(TSS_{system}) + M(TSS_w) + M(TSS_e)] / T \quad (2)$$

where:

$$\Delta M(TSS_{system}) = \Delta M(TSS_{reactors}) + \Delta M(TSS_{settlers}).$$

$$\Delta M(TSS_{reactors}) = (TSS_{reactors}(t_0+T) - TSS_{reactors}(t_0)) V_{reactors}$$

$$\Delta M(TSS_{settlers}) = (TSS_{settlers}(t_0+T) - TSS_{settlers}(t_0)) V_{settlers}$$

$$M(TSS_w) = 0.75 \int_{t_0}^{t_0+T} [X_{S,w}(t) + X_{I,w}(t) + X_{BH,w}(t) + X_{BA,w}(t) + X_{P,w}(t)] Q_w(t) dt$$

$$M(TSS_e) = 0.75 \int_{t_0}^{t_0+T} [X_{S,e}(t) + X_{I,e}(t) + X_{BH,e}(t) + X_{BA,e}(t) + X_{P,e}(t)] Q_e(t) dt$$

Here Eqn. (2) considers the total sludge production as the sum of the sludge in the reactors, in the settlers, in the waste stream, and in the effluent stream.

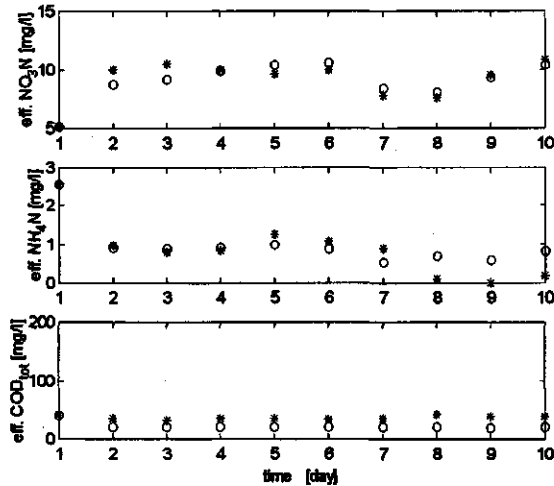
Finally, the aeration energy (*AE*), in units of *kWh/d*, is defined as:

$$AE := \frac{1}{T \cdot N} \int_{t_0}^{t_0+T} \sum_{i=1}^n F_i \cdot k_i \cdot (C_s^* - C_{L,i}) dt \quad (3)$$

In Eqn. (3), the *AE* index gives the electrical energy consumption, in *kWh/d*, as a function of the average oxygen input, which is in turn a function of the average oxygen deficit.

5.4 Method

Sensitivity analysis was carried out using a previously calibrated model for an oxidation ditch *WWTP* located in Rotterdam, The Netherlands (see Abusam et al., 2000). The model consisted of a reactor (carrousel) and a secondary settler. In this model, reactor hydraulics were approximated by a loop of 10 equal *CSTR*'s, biochemical processes were modelled by the *ASM No.1* (Henze et al., 1987), whereas the secondary settler was modelled as a 10-layers non-reactive settler, according to Takács et al., (1991). Fig. 1 shows that the model satisfactorily describes carbon and nitrogen



removals taking place in that plant.

Fig. 1, Model predictions versus experimental data for C and N removals (see Abusam et al., 2000).

Due to computational time problems, influent data used in the study were the same 10-days calibration data. Hence, our focus is on the short-term sensitivities in the *C/N* removal process.

Table 1 shows nominal parameter values, ranges, and levels to be used in this study. Parameter ranges were chosen in a way that include the values reported in literature (Henze *et al.*, 1987; Weijers and Vanrolleghem, 1997; Abasaheed, 1997; Abasaheed, 1999). Some of the nominal values were found after calibration (Abusam *et al.*, 2000) (presented in bold), and the rest were taken from literature. As it can be seen from Table 1, four levels have been chosen for studying the effect of possible changes in each parameter.

Table 1, Parameter nominal values, ranges and levels:

| Parameter | Nominal value | Range | Level |
|-----------|---------------|-------------|------------------------|
| Y_A | 0.24 | 0.1 – 0.3 | 0.10, 0.17, 0.23, 0.30 |
| Y_H | 0.62 | 0.45 – 0.7 | 0.45, 0.53, 0.61, 0.70 |
| f_P | 0.08 | 0.08 – 0.2 | 0.08, 0.12, 0.16, 0.2 |
| i_{XB} | 0.08 | 0.06 – 0.1 | 0.06, 0.07, 0.09, 0.10 |
| i_{XP} | 0.06 | 0.04 – 0.08 | 0.04, 0.05, 0.07, 0.08 |
| μ_H | 4.59 | 3.0 – 13.2 | 3.0, 6.4, 9.8, 13.2 |
| K_S | 20.0 | 10 – 180 | 10, 66, 123, 180 |
| $K_{O,H}$ | 0.33 | 0.1 – 1.0 | 0.1, 0.4, 0.7, 1.0 |
| K_{NO} | 0.5 | 0.1 – 0.5 | 0.10, 0.23, 0.37, 0.50 |
| b_H | 0.635 | 0.05 – 1.6 | 0.05, 0.57, 1.08, 1.60 |
| η_R | 1.0 | 0.6 – 1.0 | 0.6, 0.7, 0.9, 1.0 |
| η_h | 0.32 | 0.3 – 0.9 | 0.3, 0.5, 0.7, 0.9 |
| k_h | 1.72 | 1.0 – 4.0 | 1.0, 2.0, 3.0, 4.0 |
| K_X | 0.02 | 0.01 – 0.15 | 0.01, 0.06, 0.10, 0.15 |
| μ_A | 0.657 | 0.2 – 1.2 | 0.2, 0.5, 0.9, 1.2 |
| K_{NH} | 1.0 | 0.8 – 10.0 | 0.8, 3.9, 6.9, 10.0 |
| b_A | 0.098 | 0.05 – 0.15 | 0.05, 0.08, 0.12, 0.15 |
| $K_{O,A}$ | 0.4 | 0.01 – 1.0 | 0.01, 0.34, 0.67, 1.0 |
| k_a | 0.092 | 0.02 – 0.8 | 0.02, 0.28, 0.54, 0.80 |

Nominal values found after calibration are presented in bold.

In addition to the parameters, the effect of the operating condition in terms of solid retention time (*SRT*) has also been analysed. By trial and error, *SRT*'s equal to 8.6 and 22.6 days were found to be corresponding to waste sludge flow (Q_w) of 795 and 298 m^3/d , respectively.

The sensitivity analysis was conducted in two stages. In the first stage, one-at-a-time sensitivity analysis was performed in order to detect the parameters main effects. That is, all the parameters were varied in turn around their nominal value, while the others remained fixed. Results of this stage will show that the index *EQ* is significantly sensitive to only nine parameters out of the 19 parameters in *ASM No. 1*. In the second stage, the nine most sensitive parameters were then used to carry out a factorial sensitivity analysis (main plus interaction effects) for the same index *EQ*. This regional sensitivity analysis should give more information on the *EQ* index surface as a function of the nine parameters. In this stage, (see Table 2) a *normalised* second-order composite design (which contains cube, star and centre portions) around the reference parameter vector, as

recommended by Box and Draper (1987) was used. This design results in 531 (i.e. $2^9 + 9 \cdot 2 + 1$) simulation runs, for each of both *SRT* values. The results were analysed by modeling them by a second-order regression model (meta-model) of the form:

$$EQ = a_0 + a_1x_1 + a_2x_2 + \dots + a_9x_9 + a_{11}x_1^2 + a_{22}x_2^2 + \dots + a_{99}x_9^2 + a_{12}x_1x_2 + \dots + a_{89}x_8x_9 \quad (4)$$

where the equation coefficients (a_i and a_{ij}) represent the sensitivities. Furthermore, x_1, \dots, x_9 are defined in the last column of Table 2.

In matrix notations, Eqn. 4 can be rewritten as:

$$EQ = a_0 + a \cdot x + x^T \cdot A \cdot x \quad (5)$$

in which especially the system matrix *A* will be further analysed for interaction effects.

Table 2, Coded level of the most sensitive variables resulting from the first stage

| Variables | Coded levels, x_i | | | | | x_i in terms of the variables |
|-----------|---------------------|----------|---------|----------|----------|---------------------------------|
| | $x = -3$ | $x = -1$ | $x = 0$ | $x = +1$ | $x = +3$ | |
| Y_H | 0.45 | 0.54 | 0.58 | 0.62 | 0.7 | $x_1 := (Y_H - 0.58)/0.04$ |
| K_S | 10 | 66.67 | 95 | 123.33 | 180 | $x_2 := (K_S - 95)/28.33$ |
| b_H | 0.05 | 0.57 | 0.83 | 1.09 | 1.6 | $x_3 := (b_H - 0.83)/0.26$ |
| η_R | 0.6 | 0.73 | 0.8 | 0.87 | 1.0 | $x_4 := (\eta_R - 0.8)/0.07$ |
| η_h | 0.3 | 0.5 | 0.6 | 0.7 | 0.9 | $x_5 := (\eta_h - 0.6)/0.1$ |
| k_h | 1.0 | 2.0 | 2.5 | 3.0 | 4.0 | $x_6 := (k_h - 2.5)/0.5$ |
| K_X | 0.01 | 0.057 | 0.08 | 0.10 | 0.15 | $x_7 := (K_X - 0.08)/0.02$ |
| μ_A | 0.2 | 0.53 | 0.7 | 0.89 | 1.2 | $x_8 := (\mu_A - 0.7)/0.19$ |
| K_{NH} | 0.8 | 3.87 | 5.4 | 6.93 | 10 | $x_9 := (K_{NH} - 5.4)/1.53$ |

5.5 Results and discussion

Note that results reported here are highly dependent on the weighting factors used in the performance indices (see section 2). For more about these weighting factors see Vanrolleghem *et al.* (1996).

5.5.1 First stage: parameters main effect

Results of the first stage (parameters main effect) are given in Table 3. In this table parameter sensitivity factors are reported as sensitivities relative to the nominal values. Values less than one implies negative sensitivity, while values greater than one means positive sensitivity. The following can be concluded from Table 3.

First, as mentioned before, the index *EQ* is significantly sensitive to only nine parameters: Y_H , K_S , b_H , η_R , η_h , k_h , K_X , μ_A and K_{NH} . These parameters have one or more bold numbers in the corresponding rows (see Table 3). Here it is interesting to note that μ_H is not among these parameters, despite what is known about the significant effect it

has on COD removal. Insensitivity of the index EQ to μ_H is probably caused by the weighting factors adopted in the EQ -equation (see 1). As can be seen from Eqn. 1, TSS is weighted twice as much as COD . Note that this is a mathematical explanation rather a physical explanation. Furthermore, the same set of sensitive parameters is obtained for both SRT 's.

Secondly, the index AE is not significantly sensitive to changes in parameter values. As it can be seen, the maximum change in the index AE is about 11.5%, which is related to approximately 150% increase in b_H (see Table 1). This results might seem to contradict what is known about the role of b_H in determining the amount of biomass and consequently the oxygen requirements. However, this result can be explained by Eqn. 3, which shows that AE is directly proportional to the oxygen deficit ($C_s^* - C_L$). Expressing the index AE in terms of oxygen deficit results in a dampened effect of parameter variability, because the effect of parameter changes in C_L (usually between 1-2 mg/l) are insignificant as compared to the value of C_s^* .

Finally, as expected, the index TSP is significantly sensitive to Y_H , b_H and k_h . That is, the amount of sludge produced is directly related to the net growth of the heterotrophic biomass and to the rate of hydrolysis of particulate substances. An important thing to note here, as mentioned above, is that sludge growth is not significantly sensitive to changes in μ_H .

5.5.2 Second stage: factorial sensitivity analysis

In the second stage, factorial sensitivity analysis was carried only for the index EQ , because in the first stage, the other indices had shown to be either insensitive at all or sensitive to a very small number of parameters (see Table 3). Table 4 presents the results of the second stage, where all parameters have been normalised (see Table 2). However, for readability only the original parameter symbols have been maintained. As can be seen from this table, the index EQ is not only dominated by the nine previously given parameters but also by the products $Y_H b_H$, $K_S b_H$, $b_H \eta_h$, $b_H k_h$, $\eta_h k_h$, b_H^2 and k_h^2 . These second-order terms show the non-linearity effects.

Fig. 2 presents contour plots for some of the dominant parameter interactions (non-linear terms) that affect the index EQ (given in kg/d). It should be mentioned here that these contour plots have been drawn using data generated from extra simulations. Similar, but not exactly the same plots, can also be obtained using the meta-models (Eqn. 4) with corresponding parameters given in Table 4. Fig. 2 clearly shows that the sensitivity of some parameters depends on the actual value of other parameters. For example, at $b_H < 0.6$, EQ is influenced by the values of both b_H and k_h , whereas at $b_H > 0.6$, EQ is affected only by the value of k_h , for $k_h < 2.5$. Thus in this last case, where k_h is small, there is only a need to accurately identify the value of k_h .

Table 3, Parameter sensitivities (main effects) relative to indices nominal values

| Parameters. | SRT = 8.6 days | | | SRT = 22.6 days | | |
|-------------|----------------|--------|--------|-----------------|--------|--------|
| | BQ | AE | TSP | BQ | AE | TSP |
| | Y_A | 0.9724 | 1.0180 | 0.9277 | 0.9684 | 1.0154 |
| | 0.9839 | 1.0284 | 0.9542 | 0.9830 | 1.0073 | 0.9580 |
| | 0.9974 | 1.0011 | 0.9950 | 0.9974 | 1.0010 | 0.9941 |
| | 1.0179 | 0.9936 | 1.0293 | 1.0181 | 0.9943 | 1.0348 |
| Y_H | 0.8289 | 1.0047 | 0.4283 | 0.8364 | 1.0027 | 0.1953 |
| | 0.8407 | 1.0044 | 0.6613 | 0.8367 | 1.0029 | 0.6297 |
| | 0.9692 | 1.0009 | 0.9510 | 0.9672 | 1.0007 | 0.9338 |
| | 1.3996 | 0.9858 | 1.2975 | 1.4000 | 0.9886 | 1.3604 |
| f_p | 0.9421 | 1.0005 | 0.9224 | 0.9319 | 1.0002 | 0.8905 |
| | 0.9630 | 1.0003 | 0.9519 | 0.9562 | 1.0001 | 0.9319 |
| | 1.0067 | 0.9999 | 1.0083 | 1.0081 | 1.0000 | 1.0117 |
| | 1.0296 | 0.9996 | 1.0354 | 1.0360 | 0.9996 | 1.0301 |
| i_{ND} | 0.9895 | 0.9999 | 1.0227 | 0.9722 | 0.9994 | 1.0062 |
| | 0.9947 | 0.9999 | 1.0013 | 0.9861 | 0.9997 | 1.0031 |
| | 1.0025 | 1.0000 | 0.9988 | 1.0139 | 1.0003 | 0.9971 |
| | 1.0112 | 1.0000 | 0.9974 | 1.0278 | 1.0006 | 0.9942 |
| i_{RT} | 0.9777 | 0.9983 | 1.0023 | 0.9657 | 0.9983 | 1.0040 |
| | 0.9702 | 0.9977 | 1.0028 | 0.9540 | 0.9979 | 1.0032 |
| | 0.9357 | 0.9964 | 1.0035 | 0.9314 | 0.9967 | 1.0072 |
| | 0.9488 | 0.9957 | 1.0036 | 0.9206 | 0.9961 | 1.0081 |
| | 1.0191 | 0.9979 | 1.0148 | 1.0148 | 0.9981 | 1.0172 |
| μ_H | 1.0062 | 1.0016 | 0.9927 | 1.0126 | 1.0015 | 0.9917 |
| | 1.0263 | 1.0037 | 0.9864 | 1.0421 | 1.0033 | 0.9849 |
| | 1.0429 | 1.0049 | 0.9828 | 1.0651 | 1.0044 | 0.9814 |
| K_E | 1.0142 | 1.0028 | 0.9880 | 1.0256 | 1.0026 | 0.9868 |
| | 1.1256 | 0.9960 | 1.0505 | 1.1360 | 0.9962 | 1.0597 |
| | 1.3387 | 0.9941 | 1.1152 | 1.3890 | 0.9944 | 1.1330 |
| | 1.8882 | 0.9928 | 1.1800 | 1.6563 | 0.9931 | 1.2841 |
| K_{QH} | 1.1759 | 1.0214 | 0.9943 | 1.1876 | 1.0215 | 1.0103 |
| | 0.9734 | 0.9954 | 0.9970 | 0.9757 | 0.9953 | 0.9938 |
| | 0.9100 | 0.9792 | 0.9796 | 0.9136 | 0.9797 | 0.9695 |
| | 0.8732 | 0.9659 | 0.9597 | 0.8798 | 0.9671 | 0.9480 |
| K_{ND} | 0.9513 | 0.9995 | 1.0035 | 0.8928 | 0.9999 | 1.0178 |
| | 0.9676 | 0.9997 | 1.0026 | 0.9315 | 0.9999 | 1.0109 |
| | 0.9846 | 0.9998 | 1.0014 | 0.9686 | 1.0000 | 1.0049 |
| | 1.0000 | 1.0000 | 1.0000 | 1.0000 | 1.0000 | 1.0000 |
| b_H | 2.2959 | 0.8883 | 2.4881 | 2.2456 | 0.8847 | 2.3319 |
| | 0.9534 | 0.8991 | 1.0673 | 0.9524 | 1.0006 | 1.0937 |
| | 1.9419 | 0.8606 | 0.4656 | 2.3684 | 0.9599 | 0.4723 |
| | 2.8018 | 0.8916 | 0.3307 | 3.5985 | 0.8921 | 0.3856 |
| η_k | 1.2611 | 1.0094 | 0.9699 | 1.4797 | 1.0083 | 0.9722 |
| | 1.2452 | 1.0067 | 0.9816 | 1.3255 | 1.0058 | 0.9837 |
| | 1.0585 | 1.0020 | 0.9561 | 1.0801 | 1.0018 | 0.9569 |
| | 1.0000 | 1.0000 | 1.0000 | 1.0000 | 1.0000 | 1.0000 |
| η_b | 1.0356 | 0.9991 | 0.9937 | 1.0562 | 0.9989 | 0.9914 |
| | 0.8563 | 1.0016 | 0.9887 | 0.7520 | 1.0039 | 1.0027 |
| | 0.8424 | 1.0005 | 0.9668 | 0.7222 | 1.0031 | 0.9797 |
| | 0.9017 | 1.0017 | 1.0054 | 0.8368 | 1.0030 | 1.0136 |
| k_a | 2.1381 | 0.9464 | 0.6033 | 2.4620 | 0.9491 | 0.6166 |
| | 0.8514 | 1.0029 | 0.9977 | 0.7648 | 1.0050 | 1.0118 |
| | 0.8233 | 1.0012 | 0.9589 | 0.7052 | 1.0038 | 0.9444 |
| | 0.8332 | 1.0016 | 0.9335 | 0.7207 | 1.0037 | 0.9352 |
| K_X | 0.9077 | 1.0026 | 1.0133 | 0.8861 | 1.0027 | 1.0100 |
| | 1.2237 | 0.9930 | 0.9567 | 1.2913 | 0.9933 | 0.9722 |
| | 1.3659 | 0.9882 | 0.9276 | 1.4833 | 0.9887 | 0.9509 |
| | 1.4959 | 0.9833 | 0.8991 | 1.6620 | 0.9843 | 0.9283 |
| μ_a | 1.4970 | 0.9316 | 0.6034 | 1.6215 | 0.9322 | 0.6626 |
| | 1.0117 | 0.9923 | 0.9986 | 1.0177 | 0.9935 | 0.9981 |
| | 0.9960 | 1.0069 | 1.0013 | 0.9892 | 1.0059 | 1.0024 |
| | 0.9973 | 1.0113 | 1.0021 | 0.9847 | 1.0096 | 1.0047 |
| K_{XZ} | 1.0000 | 1.0000 | 1.0000 | 1.0000 | 1.0000 | 1.0000 |
| | 1.0790 | 0.9833 | 0.9970 | 1.0992 | 0.9835 | 0.9958 |
| | 1.1542 | 0.9763 | 0.9918 | 1.1939 | 0.9796 | 0.9938 |
| | 1.2272 | 0.9705 | 0.9873 | 1.2833 | 0.9749 | 0.9903 |
| b_A | 1.0196 | 1.0018 | 1.0337 | 1.0193 | 1.0017 | 1.0334 |
| | 1.0066 | 1.0007 | 1.0126 | 1.0063 | 1.0007 | 1.0187 |
| | 0.9934 | 0.9990 | 0.9866 | 0.9940 | 0.9991 | 0.9804 |
| | 0.9860 | 0.9975 | 0.9705 | 0.9873 | 0.9977 | 0.9772 |
| K_{QA} | 0.9729 | 1.0031 | 0.9892 | 0.9669 | 1.0024 | 0.9889 |
| | 0.9966 | 1.0009 | 0.9988 | 0.9943 | 1.0008 | 0.9986 |
| | 1.0188 | 0.9959 | 1.0016 | 1.0233 | 0.9963 | 1.0026 |
| | 1.0326 | 0.9924 | 1.0004 | 1.0653 | 0.9932 | 1.0018 |
| k_a | 1.1399 | 0.9960 | 0.9969 | 1.1641 | 0.9981 | 1.0018 |
| | 0.9761 | 0.9996 | 0.9984 | 0.9724 | 0.9997 | 0.9982 |
| | 0.9705 | 0.9999 | 0.9977 | 0.9659 | 0.9997 | 0.9976 |
| | 0.9687 | 1.0000 | 0.9977 | 0.9636 | 0.9998 | 0.9973 |

numbers in bold represent deviation by 20%, or more, from the nominal indices.

Table 4, Sensitivities in effluent quality (EQ) normalised meta-models

| Parameters | SRT = 8.6 days | | SRT = 22.6 days | |
|-------------------|------------------|--------------------|------------------|--------------------|
| | Coefficient in 4 | Standard deviation | Coefficient in 4 | Standard deviation |
| | 6644.0 | 277.6 | 5309.9 | 355.2 |
| Y_H | 678.0 | 12.1 | 578.8 | 15.5 |
| K_S | 776.3 | 12.1 | 728.3 | 15.5 |
| b_H | 797.8 | 12.1 | 929.6 | 15.5 |
| η_h | -399.8 | 12.1 | -383.2 | 15.5 |
| η_h^2 | -234.3 | 12.1 | -255.6 | 15.5 |
| k_h | -756.2 | 12.1 | -723.8 | 15.5 |
| K_X | 138.9 | 12.1 | 119.6 | 15.5 |
| μ_A | -418.6 | 12.1 | -410.3 | 15.5 |
| K_{NH} | 247.1 | 12.1 | 247.8 | 15.5 |
| Y_H^2 | 90.2 | 37.1 | 111.3 | 47.5 |
| K_S^2 | -8.9 | 37.1 | -14.4 | 47.5 |
| b_H^2 | 671.6 | 37.1 | 766.6 | 47.5 |
| η_h^2 | 12.7 | 37.1 | -3.5 | 47.5 |
| η_h^3 | 35.2 | 37.1 | 17.8 | 47.5 |
| k_h^2 | 374.8 | 37.1 | 421.9 | 47.5 |
| K_X^2 | 2.8 | 37.1 | -0.0108 | 47.5 |
| μ_A^2 | 199.3 | 37.1 | 184.5 | 47.5 |
| K_{NH}^2 | -34.2 | 37.1 | -54.4 | 47.5 |
| $Y_H K_S$ | 40.0 | 12.3 | 69.7 | 15.7 |
| $Y_H b_H$ | -287.8 | 12.3 | -351.1 | 15.7 |
| $Y_H \eta_h$ | -6.9 | 12.3 | -26.7 | 15.7 |
| $Y_H \eta_h^2$ | -1.1 | 12.3 | -12.7 | 15.7 |
| $Y_H k_h$ | 44.1 | 12.3 | -6.4 | 15.7 |
| $Y_H K_X$ | 20.2 | 12.3 | 31.8 | 15.7 |
| $Y_H \mu_A$ | 50.9 | 12.3 | 55.2 | 15.7 |
| $Y_H K_{NH}$ | -20.2 | 12.3 | -22.5 | 15.7 |
| $K_S b_H$ | 232.8 | 12.3 | 214.9 | 15.7 |
| $K_S \eta_h$ | -41.3 | 12.3 | -52.1 | 15.7 |
| $K_S \eta_h^2$ | 9.1 | 12.3 | 2.2 | 15.7 |
| $K_S k_h$ | 4.5 | 12.3 | -34.0 | 15.7 |
| $K_S K_X$ | 1.7 | 12.3 | 8.0 | 15.7 |
| $K_S \mu_A$ | 22.7 | 12.3 | 22.7 | 15.7 |
| $K_S K_{NH}$ | -10.7 | 12.3 | -11.1 | 15.7 |
| $b_H \eta_h$ | -57.8 | 12.3 | -55.9 | 15.7 |
| $b_H \eta_h^2$ | -307.3 | 12.3 | -234.4 | 15.7 |
| $b_H k_h$ | -687.7 | 12.3 | -593.4 | 15.7 |
| $b_H K_X$ | 34.7 | 12.3 | 30.1 | 15.7 |
| $b_H \mu_A$ | 20.0 | 12.3 | 23.9 | 15.7 |
| $b_H K_{NH}$ | -24.3 | 12.3 | -25.0 | 15.7 |
| $\eta_h^2 \eta_h$ | -0.1 | 12.3 | 4.3 | 15.7 |
| $\eta_h^2 k_h$ | 1.5 | 12.3 | 27.1 | 15.7 |
| $\eta_h^2 K_X$ | 3.2 | 12.3 | 1.0 | 15.7 |
| $\eta_h^2 \mu_A$ | 4.7 | 12.3 | 5.2 | 15.7 |
| $\eta_h^2 K_{NH}$ | -3.7 | 12.3 | -6.2 | 15.7 |
| $\eta_h^3 k_h$ | 228.9 | 12.3 | 282.6 | 15.7 |
| $\eta_h^3 K_X$ | -12.7 | 12.3 | -14.6 | 15.7 |
| $\eta_h^3 \mu_A$ | -38.2 | 12.3 | -40.0 | 15.7 |
| $\eta_h^3 K_{NH}$ | 14.4 | 12.3 | 14.3 | 15.7 |
| $k_h K_X$ | -74.8 | 12.3 | -93.9 | 15.7 |
| $k_h \mu_A$ | -93.6 | 12.3 | -91.0 | 15.7 |
| $k_h K_{NH}$ | 46.4 | 12.3 | 49.7 | 15.7 |
| $K_X \mu_A$ | 19.3 | 12.3 | 19.5 | 15.7 |
| $K_X K_{NH}$ | -2.4 | 12.3 | -1.1 | 15.7 |
| $\mu_A K_{NH}$ | -55.4 | 12.3 | -58.3 | 15.7 |

Significant numbers are printed in bold.

For contour plots such as those given in Fig. 2, important points, like maximum, minimum or saddle points, can be obtained from a surface analysis (Box and Draper,

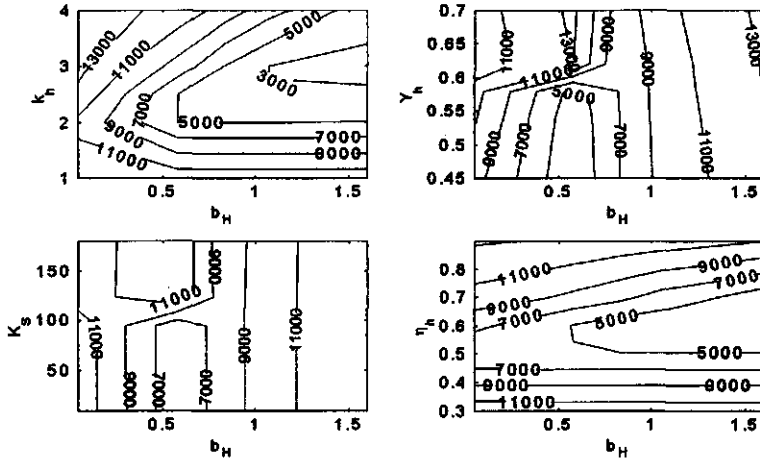


Fig. 2, Effect of parameter interactions on the effluent quality (EQ) in kg/d, at SRT = 8.6 days

1987). In fact, depending on the eigenvalues of the symmetrical matrix A given in Eqn. 5, four basic contour forms (in this case ellipses with minimum or maximum, minmax, parallel straight lines and circles) can be obtained. For the full understanding of the contour plots in Fig. 2, Fig. 3 illustrates how the contour shape depends on the eigenvalues of the two-dimensional symmetrical matrix A, for the following simple quadratic equation:

$$y = b_0 + b_1x_1 + b_2x_2 + b_{11}x_1^2 + b_{22}x_2^2 + b_{12}x_1x_2 \quad (6)$$

so that (see Eqn. 5)

$$A = \begin{bmatrix} b_{11} & b_{12}/2 \\ b_{21}/2 & b_{22} \end{bmatrix} \quad (7)$$

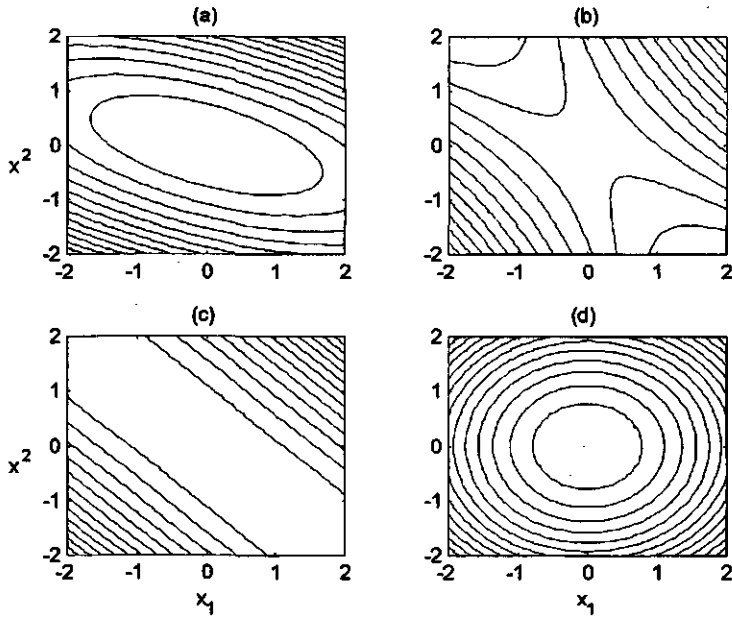


Fig. 3, Basic forms of the quadratic equation $y = b_0 + b_1x_1 + b_2x_2 + b_{11}x_1^2 + b_{22}x_2^2 + b_{12}x_1x_2$:

(a) eigenvalues same sign (b) eigenvalues different signs (c) one of the eigenvalues is zero (d) equal eigenvalues

Finally, it should be noted that results obtained in this study represent only the short-term effects of parameters variability on the performance indices, since the evaluation is carried for a period of seven days, using actual input data. In the long-term, different results might be obtained, due to the relatively slow process of biomass growth. However, the same procedure can be applied for studying the long-term effects. Further, the same procedure can also be used for other types of activated sludge systems.

5.6 Conclusions

This study has demonstrated the use of the factorial sensitivity analysis methodology in identifying and accessing the stoichiometric and kinetic parameters that have dominant influence on the performance indices of an oxidation ditch benchmark. The main advantage of this methodology is that more information about the interaction (non-linearity) can be obtained, in a region rather than in a point. In this study only the short-term effects of parameter variability on the performance indices were studied. For oxidation ditch or other activated sludge systems, however, the same procedure can also be used for studying the long-term effects.

Short-term results obtained have indicated the following. First, the aeration energy index (*AE*) is not significantly affected by variation in the values of the parameters of *ASM No. 1*. Secondly, the total sludge production index (*TSP*) is sensitive to Y_H , b_H and k_h . Finally, the effluent quality index (*EQ*) is dominated by Y_H , K_S , b_H , k_h , η_B , η_h , K_X , μ_A and K_{NH} , the interactions $Y_H \cdot b_H$, $K_S \cdot b_H$, $b_H \cdot \eta_h$ and $b_H \cdot \eta_h$ (for $b_H < 0.8 \text{ d}^{-1}$) $\eta_h \cdot k_h$, and the quadratic terms b_H^2 , and k_h^2 . Thus the parameters that need special attention are: Y_H , K_S , b_H , k_h , η_B , η_h , K_X , μ_A and K_{NH} .

5.7 References

- Abasaheed, E.A. (1997), Sensitivity analysis on a sequencing batch reactor model I: effect of kinetic parameters, *J. Chem. Tech. Biotechnol.* 70:379-383.
- Abasaheed, E.A. (1999), Sensitivity analysis on a sequencing batch reactor model II: effect of stoichiometric and operating parameters, *J. Chem. Tech. Biotechnol.* 74:451-455.
- Abusam, A., K.J. Keesman, G. van Straten, H. Spanjers and K. Meinema (2000), Parameter estimation procedure for complex non-linear systems: calibration of *ASM No.1* for N-removal in a full-scale oxidation ditch, in proc. of the *Watermatex2000*, Gent, Belgium.
- Alex, J., J.F. Beteau, J.B. Copp, C. Hellinga, U. Jeppsson, S. Marsilli-Libelli, M.N. Pons, H. Spanjers and H. Vanhooren (1999), Benchmark for evaluating control strategies in wastewater treatment plants, *ECC'99* (European control conference), Karlsruhe August 31 – September 3.
- Box, G.E.P. and N.R. Draper (1987), *Empirical model-building and response surfaces*, John Wiley and Sons (1987).
- Copp, J.B. (2000), Defining a simulation benchmark for control strategies, *Water21*, 1(2):44-49.
- Henze M, C.P.L. Grady jr, W. Guier, G. van R. Marias and T. Matsuo (1987), A general Model for single-sludge WWT systems, *Wat Res* 21(5):505-15.
- Hu, Z. and S. Islam (1997), Evaluation of sensitivity of land surface hydrology representations with and without land-atmosphere feedback, *Hydrological Processes* 11(11):1557-72.
- Janssen, P.H.M. (1994), *Assessing sensitivities and uncertainties in models: a critical evaluation, in predictability and nonlinear modeling in natural sciences and economics*, ed by J. Grasman and G. van Straten, pp 344-361, Kluwer Academic Publishers.
- Keesman, K. (1989), On the dominance of parameters in structural models of ill-defined systems, *Appl. Math. and Comp.* 30: 133-147.

Lee, A.H.W., and J.W. Jones (1996), Modeling of an ice-on-coil thermal storage system, *Energy Convers. Mgmt.* 37(10): 1493-1507.

Pons, M.N., H. Spanjers and U. Jeppsson (1989), Towards a benchmark for evaluating Control strategies in wastewater treatment plants by simulations, *Escape 9* (European symposium on computer aided process engineering-9), Budapest.

Takács I, G.G. Patry and D. Nolasco (1991), A dynamic model of the clarification-thickening process, *Wat. Res.* 25(10):1263-71.

Vanrolleghem, P.A., U. Jeppsson, J. Carstensen, B. Carlsson and G. Olsson (1996). Integration of WWTP design and operation – a systematic approach using cost functions, *Wat. Sci. Tech.* 34(3-4), 159-171.

Weijers, S.R. and P.A. Vanrolleghem (1997), A procedure for selecting best identifiable parameters in calibrating activated sludge model No. 1 to full-scale plant data, *Wat. Sci. Tech.* 36(5):69-79.

6. Uncertainty analysis

6.1 Estimation of uncertainties in the performance indices of an oxidation ditch benchmark^{††}

6.1.1 Abstract

Estimation of the influence of different sources of uncertainty is very important in obtaining a thorough evaluation or a fair comparison of the various control strategies proposed for wastewater treatment plants. This paper illustrates, using real data obtained from a full-scale oxidation ditch wastewater treatment plant, how the effect of the various uncertainty sources can be quantified. Monte Carlo simulation analysis method was preferred over first-order variance analysis method because it is more reliable and it provides the complete probability distribution. For various sources of uncertainty, except for the additive modeling error, samples were selected using the efficient Latin Hypercube Sampling technique. Large deviations in the benchmark performance indices from the nominal values, due to uncertainty in influent loads and parameter values, were especially found for effluent quality and total sludge production indices. However, relatively smaller deviations are found due to uncertainty in the states initial conditions. Effect of the model structural uncertainty on the performance indices was found to be negligible.

Keywords: wastewater; activated sludge; oxidation ditch; modeling; benchmark; uncertainty analysis.

Nomenclature:

θ : external parameter vector.

β : weighting factor that converts different types of pollution into pollution units (dimensionless).

θ : parameter vector.

ω : system noise.

$AC_{h,i}$: average hourly aeration capacity relative to the aerator full capacity (dimensionless).

C_L : operating oxygen concentration (g/m^3).

C_s^* : oxygen saturation concentration at field temperature, (g/m^3).

F_i : average daily aeration capacity relative to the aerator full capacity ($F_i = \frac{1}{24} \sum_{j=0}^{24} AC_{h,i}$), (dimensionless).

k : aeration constant, $K_L a V_A$ ($m^3 d^{-1}$).

$K_L a$: overall oxygen transfer rate (d^{-1}). Note that here $K_L a$ is calculated for the assumed aerated volume (compartment) and not for the whole ditch.

^{††} Submitted to J. Chem. Tech. Biotech. by A. Abusam, K.J. Keesman, H. Spanjers, G. van Straten and K. Meinema

N : efficiency of the aerator at 22.4 °C (1.48 kg O_2/kWh).
 n : number of aerators in the oxidation ditch ($n = 4$).
 S_I : soluble inert organic matter (g/m^3).
 S_{NB} : soluble biodegradable organic nitrogen (g/m^3).
 S_{NH} : $NH_4 + NH_3$ nitrogen (g/m^3).
 S_{NO} : nitrate and nitrite nitrogen (g/m^3).
 S_O : oxygen (g/m^3).
 S_S : readily biodegradable substrate (g/m^3).
 Q : average daily flow (m^3/d).
 T_{wat} : average daily water temperature (°C).
 t : time (day).
 u : input vector.
 V_A : volume of the aerated compartment (m^3).
 $X_{B,A}$: active autotrophic biomass (g/m^3).
 $X_{B,H}$: active heterotrophic biomass (g/m^3).
 X_I : particulate inert organic matter (g/m^3).
 X_P : particulate products arising from biomass decay (g/m^3).
 X_S : slowly biodegradable substrate (g/m^3).

indices:

e : effluent

i : number of the aerated compartment, 1...4.

j : daily time, in hours (0:1:24).

w : wasted sludge.

6.1.2 Introduction

In order to fulfil the stringent requirements that have been put on the effluents from wastewater treatment plants (*WWTP's*), many control strategies have been proposed. It is obvious, due to funds and time limitations, that a thorough evaluation of all these control strategies by carrying out practical tests is not possible. Thus computer simulations are an interesting approach for evaluating them. The standard simulation procedure that can be used in evaluating or comparing the various control strategies proposed for activated sludge *WWTP's* is called *benchmark* (see e.g. Pons *et al.*, 1999). This benchmark consists of a description of the plant layout, a simulation model and definitions of (controller) performance criteria.

Traditionally, water quality models are treated as deterministic systems. A deterministic approach usually ignores any expected variability, and consequently leads to inappropriate designs (Von Sperling, 1996) and, of course, to unreliable predictions. However, practice has proved that water quality models are neither exact nor perfect (Høybye, 1998). Large and complex models (like an oxidation ditch plant model) are especially capable of generating highly uncertain predictions (Beck, 1987). Therefore, a thorough evaluation of complex water systems, such as activated sludge systems, should carefully assess all possible sources of uncertainty.

Basic methods used for the quantitative estimation of uncertainties are first-order variance analysis and Monte Carlo simulations analysis (see e.g. Beck, 1987; Van Straten and Keesman, 1991). The Monte Carlo method is usually preferred because it provides

the complete probability distribution (Burgess and Lettenmaier, 1975), it is a simple numerical method (Beck, 1987) and it uses the full model, and usually leads to reliable results (Van Straten and Keesman, 1991). In contrast, the first-order variance analysis method requires much less computational time, but it is less accurate due to the inherent approximation in the linearization.

The aim of this paper is to illustrate, using full-scale plant data, how the propagation of uncertainties from the various sources to the performance indices of this particular oxidation ditch benchmark, or similar systems, can be analysed quantitatively. The intention is not to provide exact estimates of the uncertainties, but to demonstrate the methodology of uncertainty modeling and analysis. Uncertainty sources studied here are the following: (i) uncertainty in influent loads and parameter values, (ii) uncertainty in the initial states, (iii) uncertainty in the model structure, and (iv) uncertainty due to seasonal changes in water temperature.

This paper is organised as follows. In section 2, a theoretical background of uncertainty modeling and analysis is provided. In section 3, performance indices used in the study are described. In section 4, methods for quantifying the effect of the various sources of uncertainties are provided, and results are discussed. Finally, in section 5, the conclusions are formulated.

6.1.3 Theory

Let the dynamic system under study be described by the model:

$$x(t) = f[x(t), u(t), d(t); \theta] + w(t), \quad x(0) = x_0 \quad (1)$$

$$y(t) = g[x(t), u(t), d(t); \theta] + v(t) \quad (2)$$

where $x \in \mathfrak{R}^n$ is the state vector, $u \in \mathfrak{R}^m$ the control input vector, $d \in \mathfrak{R}^q$ disturbance vector, and $\theta \in \Theta \subset \mathfrak{R}^p$ a vector of model parameters. Elements of vector $y \in \mathfrak{R}^s$ are the observed outputs, and w and v are stochastic signals representing the system noise or modeling uncertainty and the measurement errors, respectively.

Typically, in an activated sludge plant, the states x are the concentrations of S_o , COD , S_{NH} , S_{NO} , and so forth, at various locations in the plant. The control input u contains variables like aeration intensity, recycle activated sludge (RAS) rate, waste activated sludge (WAS) rate and so forth, while the disturbances are mainly due to variations in the influent flow and composition. The outputs in y are the measurable variables in, for instance, the effluent.

Now define a set of integral criteria by which the performance is judged as:

$$J = \frac{1}{T} \int_{t_0}^{t_0+T} h[x(\tau), u(\tau), d(\tau); \mathcal{G}] d\tau \quad (3)$$

where h is a vector-valued function of states, control inputs, disturbances as well as the extended parameter vector \mathcal{G} , which contains, in addition to the model parameters,

parameters related to performance indices. In what follows, the uncertainty in these additional parameters is not taken into account. So J is a *vector* of performance indices, where T denotes the integration interval.

Let us now specify how the uncertainty analysis, given uncertainties in θ , d , x_0 , and w , is performed. Clearly the uncertainty in the output measurement errors, $v(t)$, will be neglected, given that we are generally not interested in the effect of measurement error in prediction. First, the effect of uncertainty in the parameters is evaluated. A set, which specifies a hypercube in the parameter space, is defined: $\Theta := \{\theta \in \mathfrak{R}^p; \theta_{\min} \leq \theta \leq \theta_{\max}\}$. Next, θ is assumed to be uniformly distributed over the range θ_{\min} to θ_{\max} . Then,

samples are drawn from this subspace in \mathfrak{R}^p , and the effect on the uncertainty J is evaluated. In this approach, it is assumed that the parameters are, in fact, time-invariant. That is, the selected values are randomly chosen, and kept constant in time. Second, different scenario's $d_1(t) \dots d_q(t)$ are defined, based on realistic observed patterns. Unobserved disturbances and model errors are thought to be included in $w(t)$. Third, the effect of uncertainty in the state initial conditions x_0 is evaluated, in the same way as the parameters uncertainty. Finally, the effect of system noise $w(t)$ is assessed. Treatment of system noise $w(t)$ is most difficult, as $w(t)$ is a stochastic signal. Thus, the system model contains stochastic differential equations, which are difficult to solve (see e.g. Bagchi, 1993). To simplify the issue, we only made the assumption that $w(t)$ is piece-wise constant band-limited white noise, where sampling time (band width) is chosen smaller than the smallest appropriate eigenvalue of the linearized system.

6.1.4 Performance indices

Performance indices that are used in this particular oxidation ditch benchmark are more or less similar to those developed for benchmarking other activated sludge processes (Pons *et al.*, 1999; Copp, 2000). For two reasons the energy equations, proposed by these working groups, were slightly modified in order to make them applicable to oxidation ditch systems. Firstly, oxidation ditches normally use mechanical aerators, which are different from air diffusers adopted by the previously mentioned researchers. Secondly, in an oxidation ditch there is no special pump for internal recirculation, since this is also carried out by the mechanical aerators.

Performance indices studied were the effluent quality index (EQ), aeration energy index (AE), total sludge production index (TSP) and disposed sludge (DS). In this study these indices were evaluated for a full-scale wastewater treatment plant, using real input data. Because the real data was for 10 days, the actual evaluations were carried out from the beginning of the 3rd day to the end of 9th day, in order to avoid undesired effects of the initial conditions.

The effluent quality index (EQ), in units of g/d , is defined as:

$$EQ := \frac{1}{T} \int_{t_0}^{t_0+T} [PU_{TSS}(t) + PU_{COD}(t) + PU_{BOD}(t) + PU_{TKN}(t) + PU_{NO}(t)] Q_e(t) dt \quad (4)$$

where:

$$\begin{aligned} PU_{TSS}(t) &= \beta_{TSS} TSS_e(t), \beta_{TSS} = 2 \\ PU_{COD}(t) &= \beta_{COD} COD_e(t), \beta_{COD} = 1 \\ PU_{BOD}(t) &= \beta_{BOD} BOD_e(t), \beta_{BOD} = 2 \\ PU_{TKN}(t) &= \beta_{TKN} TKN_e(t), \beta_{TKN} = 20 \\ PU_{NO}(t) &= \beta_{NO} NO_{3,e}(t), \beta_{NO} = 20 \end{aligned}$$

The composite variables are expressed in terms of *ASM No. 1* variables:

$$\begin{aligned} TSS_e &= 0.75 (X_{S,e} + X_{BH,e} + X_{BA,e} + X_{P,e} + X_{I,e}) \\ COD_e &= S_{S,e} + S_{I,e} + X_{S,e} + X_{BH,e} + X_{BA,e} + X_{P,e} + X_{I,e} \\ BOD_e &= 0.25 (S_{S,e} + X_{S,e} + (1 - f_p) (X_{BH,e} + X_{BA,e})) \\ TKN_e &= S_{NH,e} + S_{ND,e} + X_{ND,e} + i_{XB} (X_{BH,e} + X_{BA,e}) + i_{XP} (X_{P,e} + X_{I,e}) \\ NO_{3,e} &= S_{NO,e} \end{aligned}$$

As it can be seen from (4), the *EQ* index represents the weighted sum of the effluent load multiplied by the flow. Values given for the weighting factors (β 's) are for a denitrifying system (Vanrolleghem *et al.* 1996).

The total sludge production (*TSP*) index, in units of *g/d*, is defined as:

$$TSP := [\Delta M(TSS_{system}) + M(TSS_w) + M(TSS_e)] / T \quad (5)$$

where:

$$\begin{aligned} \Delta M(TSS_{system}) &= \Delta M(TSS_{reactors}) + \Delta M(TSS_{settlers}) \\ \Delta M(TSS_{reactors}) &= (TSS_{reactors}(t_0+T) - TSS_{reactors}(t_0)) V_{reactors} \\ \Delta M(TSS_{settlers}) &= (TSS_{settlers}(t_0+T) - TSS_{settlers}(t_0)) V_{settlers} \\ M(TSS_w) &= 0.75 \int_{t_0}^{t_0+T} [X_{S,w}(t) + X_{I,w}(t) + X_{BH,w}(t) + X_{BA,w}(t) + X_{P,w}(t)] Q_w(t) dt \\ M(TSS_e) &= 0.75 \int_{t_0}^{t_0+T} [X_{S,e}(t) + X_{I,e}(t) + X_{BH,e}(t) + X_{BA,e}(t) + X_{P,e}(t)] Q_e(t) dt \end{aligned}$$

In what follows, the daily sludge production (*g/d*) in the waste stream, denoted by *DS* (daily sludge production), will also be evaluated.

Here Eqn. (5) considers the total sludge production as the sum of the sludge in the reactors, in the settlers, in the waste stream, and in the effluent stream.

Finally, the aeration energy (*AE*), in units of *kWh/d*, is defined as:

$$AE := \frac{1}{NT} \int_{t_0}^{t_0+T} \sum_{i=1}^n F_i k_i (C_s^* - C_{L,i}) dt \quad (6)$$

In Eqn. (6), the *AE* index gives the electrical energy consumption, in *kWh/d*, as a function of the average oxygen input, which is in turn a function of the average oxygen deficit.

6.1.5 Estimation of performance indices uncertainties

6.1.5.1 Parameter values and input loads uncertainties

6.1.5.1.1 Methods

As for the other sources of uncertainty, a calibrated model of an oxidation ditch *WWTP* located in Rotterdam, the Netherlands (Abusam *et al.*, 2000), was used for quantifying the effect of parameter and input load uncertainties. Four different influent scenarios were used in the estimation: the real data file for the plant plus the three influent patterns given by Spanjers *et al.* (1998), after being scaled to the plant loading conditions. The artificial influent scenarios represent possible influent loads of a typical European *WWTP*, under dry, storm and rainy weather conditions. In this study, we have chosen to work with various influent scenarios rather than with ranges for the organic and hydraulic loading conditions because the latter can result in unrealistic combinations. The steps followed in quantifying the uncertainties were the following. First, the artificial influent data were scaled to the hydraulic and organic loading conditions of the *WWTP*. Second, ranges for the parameters of the activated sludge model (*ASM*) *No.1* were selected (see Table 1) on the basis of values found from previous calibration step (Abusam *et al.*, 2000) and values reported in literature (Henze *et al.*, 1987; Weijers *et al.*, 1997 and Abasaeed, 1997 and 1999). The Monte Carlo simulations were carried out as follows. Using the Latin Hypercube Sampling (*LHS*) technique, 500 uniformly distributed samples (parameter combinations) were generated from the pre-selected parameter ranges (see Table 1). *LHS* technique enhances the sampling efficiency by allowing the number of samples to be equal or greater than five times the number of the parameters (Janssen, 1994). Finally, simulations were carried out, 500 times, for each influent scenario.

Table 1, Nominal values and possible ranges for the parameters of ASM No.1

| Parameter | Nominal values | Possible range |
|-------------------------------------------------------------------------------------------------------------------------------|----------------|----------------|
| Y_A : yield for autotrophic biomass (g cell COD formed (g COD oxidized) ⁻¹). | 0.24 | 0.1 – 0.3 |
| Y_H : yield for heterotrophic biomass (g cell COD formed (g COD oxidized) ⁻¹). | 0.62 | 0.45 – 0.7 |
| f_p : fraction of biomass leading to particulate products (dimensionless). | 0.08 | 0.08 – 0.2 |
| i_{XB} : mass of nitrogen per mass of COD in biomass (g N.(g COD ⁻¹)). | 0.08 | 0.06 – 0.1 |
| i_{XP} : mass of nitrogen per mass of COD in products from biomass (g N.(g COD ⁻¹)). | 0.06 | 0.04 – 0.08 |
| μ_H : maximum specific growth rate for heterotrophic biomass (d ⁻¹). | 4.59 | 3.0 – 13.2 |
| K_S : half-saturation coefficient for heterotrophic biomass (g COD m ⁻³). | 20.0 | 10 – 180 |
| $K_{O,H}$: oxygen half-saturation coefficient for heterotrophic biomass (g O ₂ m ⁻³). | 0.33 | 0.1 – 1.0 |
| K_{NO} : nitrate half-saturation coefficient for denitrifying heterotrophic biomass (gNO ₃ -N.m ⁻³). | 0.5 | 0.1 – 0.5 |
| b_H : decay coefficient for heterotrophic biomass (d ⁻¹). | 0.635 | 0.05 – 1.6 |
| η_g : correction factor for μ_H under anoxic conditions (dimensionless). | 1.0 | 0.6 – 1.0 |
| η_h : correction factor for hydrolysis under anoxic conditions (dimensionless). | 0.32 | 0.3 – 0.9 |
| k_h : maximum specific hydrolysis rate (g slowly biodegradable COD (g cell COD.day) ⁻¹). | 1.72 | 1.0 – 4.0 |
| K_X : half-saturation coefficient for hydrolysis of slowly biodegradable substrate (g COD (g cell COD.day) ⁻¹). | 0.02 | 0.01 – 0.15 |
| μ_A : maximum specific growth rate for autotrophic biomass (d ⁻¹). | 0.657 | 0.2 – 1.2 |
| K_{NH} : ammonia half-saturation coefficient for autotrophic biomass (g NH ₄ -N.m ⁻³). | 1.0 | 0.8 – 10.0 |
| b_A : decay coefficient for autotrophic biomass (d ⁻¹). | 0.098 | 0.05 – 0.15 |
| $K_{O,A}$: oxygen half-saturation coefficient for autotrophic biomass (g O ₂ m ⁻³). | 0.4 | 0.01 – 1.0 |
| k_a : ammonification rate (m ³ COD(g.day) ⁻¹). | 0.092 | 0.016 – 0.8 |

η_g, η_h (presented in bold) and the aeration constant ($k = 1.84 \times 150000 \text{ m}^3/\text{d}$) are calibration values.

6.1.5.1.2 Results and discussion

Fig. 1 presents the results of the scaled dry weather scenario, while Table 2 summarises the results obtained for the various influent scenarios. As it can be seen from Fig. 1, it is clear that the distribution of the index AE is highly skewed to the left, while distributions of the other indices are slightly skewed to the right. However, normal probability plots given in Fig. 2 reveal that, except for AE , all the distributions can reasonably be approximated by normal distributions. This would also be seen from Table 2, in which

the reported values for the mean, median, skewness and kurtosis are very close to that for a normal distribution, that is: mean \approx median \approx mode, skewness \approx 0 and Kurtosis \approx 3.

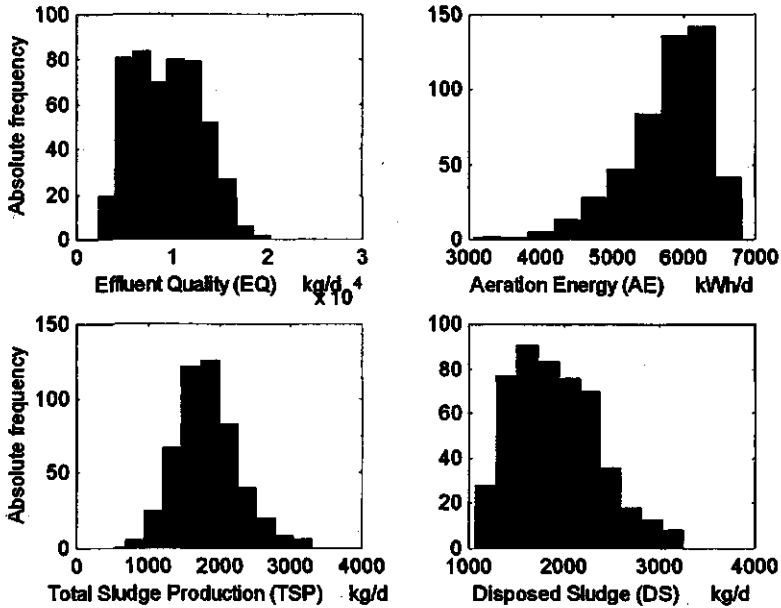


Fig. 1, Frequency distributions of the performance indices – dry weather scenario – for the full sample of parameter uncertainty.

From Table 2, one can also see that the effect of parameter uncertainty (horizontal direction) seems to be higher than the effect of influent load uncertainty (vertical direction). Further, it can be computed that the highest overall deviations from default values (due to uncertainties in both influent loads and parameter values) are +500%, -65%, +550% and +65% for indices *EQ*, *AE*, *TSP* and *DS*, respectively. Hence the most vulnerable for parameter uncertainties are the performance indices *EQ* and *TSP*.

Table 2, Statistics of the uncertainty in the performance indices

| Performance index | Flow type | Mean | Median | Mode | Std. dev. | Skewness | Kurto | CV(%) | Minimum | Maximum |
|-------------------|---------------|-------|--------|-------|-----------|----------|-------|-------|-------------|--------------|
| EQ (kg/d) | real data | 7819 | 7891 | 9321 | 3210 | 0.19 | 2.42 | 41 | 1839 | 18466 |
| | dry weather | 8934 | 8867 | 6796 | 3502 | 0.22 | 2.26 | 39 | 2318 | 20322 |
| | storm weather | 9594 | 9562 | 7222 | 3499 | 0.20 | 2.36 | 36 | 2671 | 20878 |
| | rainy weather | 10096 | 10332 | 13127 | 3485 | 0.21 | 2.48 | 35 | 3094 | 21335 |
| AE (kWh/d) | real data | 6842 | 6889 | 6971 | 398 | -0.63 | 3.29 | 6 | 5089 | 7598 |
| | dry weather | 5813 | 5942 | 6246 | 584 | -1.13 | 4.66 | 10 | 3070 | 6806 |
| | storm weather | 5805 | 5950 | 6217 | 610 | -1.20 | 4.80 | 11 | 2908 | 6801 |
| | rainy weather | 5699 | 5865 | 6123 | 660 | -1.22 | 4.75 | 12 | 2580 | 6749 |
| TSP (kg/d) | real data | 978 | 833 | 935 | 620 | 0.32 | 2.92 | 63 | -524 | 2717 |
| | dry weather | 2437 | 2194 | 1858 | 428 | 0.57 | 3.59 | 18 | 689 | 3287 |
| | storm weather | 2689 | 2456 | 2058 | 452 | 0.30 | 3.11 | 17 | 882 | 3495 |
| | rainy weather | 2333 | 2146 | 1782 | 439 | 0.15 | 2.75 | 19 | 767 | 3022 |
| DS (kg/d) | real data | 2650 | 2627 | 1896 | 404 | 0.19 | 2.03 | 15 | 1253 | 3178 |
| | dry weather | 2588 | 2499 | 1614 | 451 | 0.54 | 2.81 | 17 | 1070 | 3245 |
| | storm weather | 2993 | 2892 | 1870 | 510 | 0.50 | 2.73 | 17 | 1262 | 3694 |
| | rainy weather | 3099 | 3000 | 1973 | 545 | 0.44 | 2.62 | 18 | 1350 | 3840 |

- At nominal parameter values: EQ = 5149, AE = 7110, TSP = 1278 and DS = 1401
 - extreme values are presented in bold

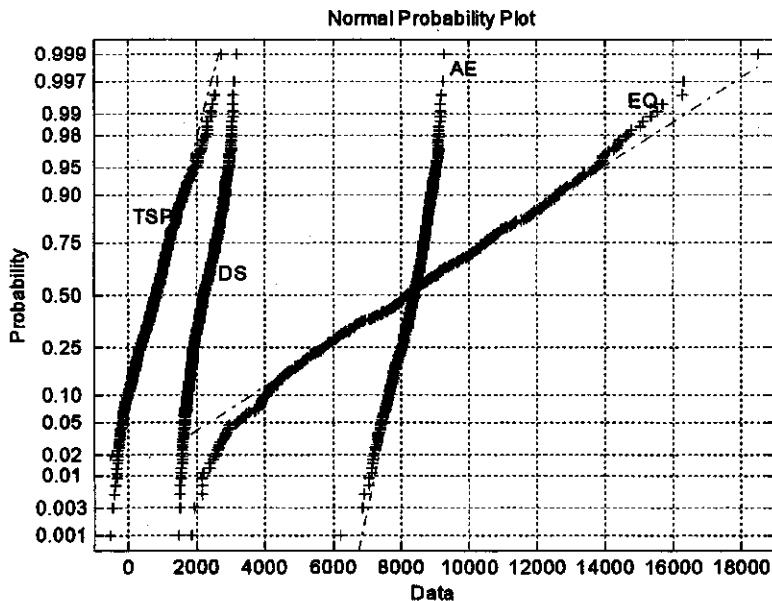


Fig. 2, Normal probability test of the results obtained by using the dry weather scenario.

6.1.5.2 Initial state uncertainties

6.1.5.2.1 Methods

For illustrating this part, certain assumptions were made. First, all the state variables of *ASM No.1* and *TSS* (total suspended solids) concentration at the bottom layer of the ten-layers secondary settler were assumed to vary within the range of $\pm 50\%$ of the steady state simulation values.

Further, *TSS* profile along the secondary settler was assumed to have initially the same shape as that obtained from the steady

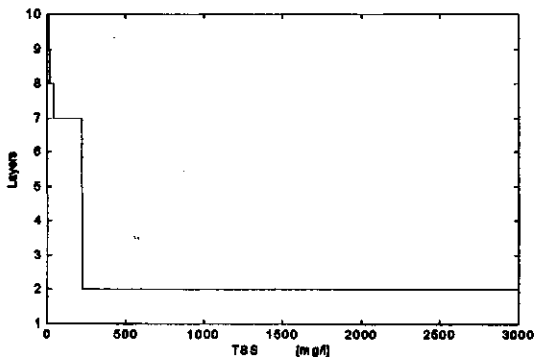


Fig. 3, Profile of the initial TSS concentrations along the secondary settler (layer 1 is the bottom layer).

state simulation, as shown in Fig. 3. After making these assumptions, 500 uniform samples (combination of initial state values) were selected, as before using the *LHS* technique, and Monte Carlo simulations were carried out by running the plant model 500 times, using the real data file.

6.1.5.2.2 Results and discussion

From the results presented in Fig. 4, it is clear that the shape of the distributions is more or less the same as that shown in Fig. 1. However, if the values obtained here will be compared with that obtained for the effect of influent load and parameter uncertainty (Fig. 1), it will be found that the effect of initial state uncertainties seems to cause relatively smaller variability in the predicted values for the performance indices. Nonetheless, this small effect has to be taken into account, if an exhaustive evaluation or a reliable comparison of the control strategies must be achieved.

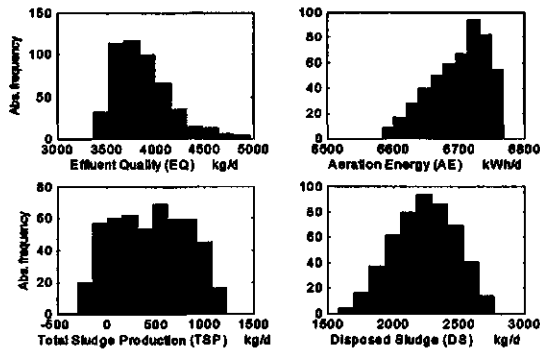


Fig. 4. The effect of uncertainties in the initial conditions of the reactor and the settler – real data scenario.

6.1.5.3 Model structure uncertainties

6.1.5.3.1 Methods

In order to avoid problems that may arise due to any of Monod terms being negative, the states were constrained to positive values only. The unobserved disturbances and model errors were thought to be included in $w(t)$. Then $w(t)$ was modelled as a piece-wise constant band-limited white noise (mean = 0 and standard deviation = 1). Subsequently, the noise signal was scaled using the steady state concentration for the various components. Next, the sampling time (0.1 day with the real influent file, and 0.001 day with the other influent files) was chosen smaller than the smallest appropriate eigenvalue of the linearized system.

For demonstration, the plant model was run 100 times, using the real influent data. In order to have an idea about the effect of the influent scenario, a single run of the model was also performed, using the other influent types.

6.1.5.3.2 Results and discussion

Results of the simulations with the real influent data are depicted in Fig. 5, whereas comparison of the influence of the model structural uncertainty under the various loading scenarios is presented in Table 5. As it can be seen from the range of values presented in Fig. 5, the effect of the model structural uncertainty on the performance indices seems to be negligible. This can also be seen from the small standard deviations, which were found to be 19.7, 1.9, 1.2 and 0.5 for *EQ*, *AE*, *TSP* and *DS*, respectively. The reason for the small values found due to the effect of the model structural uncertainty might be the filtering action of the performance indices, which seems to be true under the various influent scenarios (see Table 3).

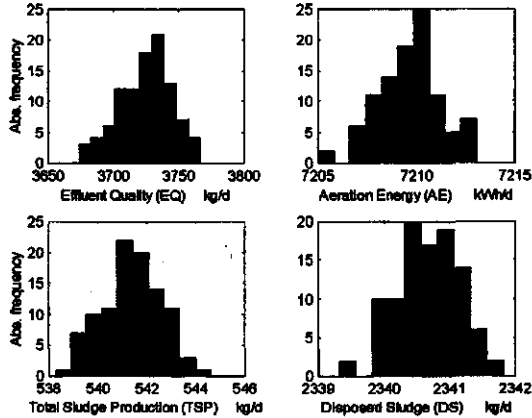


Fig. 5. The influence of model uncertainties on the performance indices – real data scenario.

Fig. 6 compares the distribution of the readily biodegradable substrate (S_S) on the third day to that on the ninth day. As expected, this figure clearly demonstrates that different shapes of probability distributions can exist at the different time instances of simulations.

Table 3. Mean values of the effect of modeling error on the performance indices

| | <i>EQ</i> | <i>AE</i> | <i>TSP</i> | <i>DS</i> |
|---------------|------------------|----------------|----------------|----------------|
| real data | 7798 (7819) | 6838 (6842) | 981 (978) | 2650 (2650) |
| dry weather | 9247 (8934) | 5759 (5813) | 2206 (2437) | 2394 (2588) |
| storm weather | 9559 (9594) | 5803 (5805) | 2698 (2689) | 2993 (2993) |
| rainy weather | 10347 (10096) | 5660 (5699) | 2239 (2333) | 2883 (3099) |

Values between parenthesis are obtained without introducing model structural disturbances.

A good example of model structural error is the error due to the seasonal variation in temperature, when this effect is not explicitly taken into account. Quantification of the effect of seasonal changes in temperature on the performance indices is illustrated in the next section.

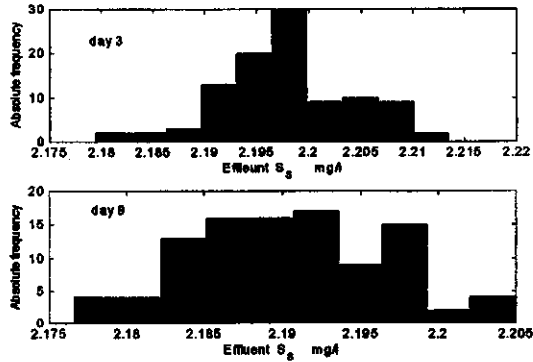


Fig. 6, Distribution of effluent S_5 at the third day compared to that at the ninth day, due to system noise

6.1.5.4 Uncertainty due to seasonal changes in water temperature

6.1.5.4.1 Methods

The measured average daily water temperature in the oxidation ditch in 1993 is represented in Fig. 7. This figure shows that the seasonal variations in water temperature can be adequately modelled by

$$T_{wat} = 17.4 - 4.97 \cdot \sin \frac{2\pi(t - 622)}{365} \quad (7)$$

Real performance measurements given in Fig. 8 show that TN (total nitrogen) removal efficiency follow approximately the same sinusoidal pattern for water temperature. However, COD removals seem to be not significantly affected by the seasonal changes in water temperature. Comparison of the average daily flow with the TN removal

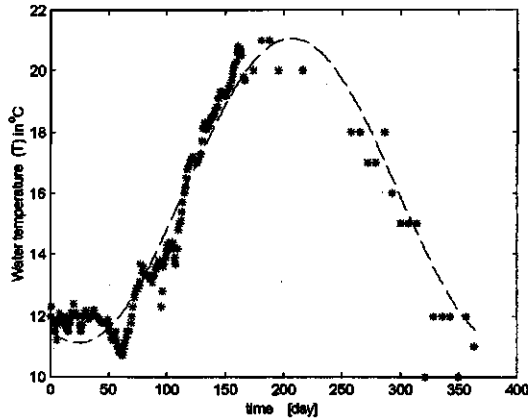


Fig. 7, Modeling the seasonal changes in the ditch water (day 1 is January first).

efficiency clearly indicates that the sinusoidal seasonal pattern of *TN* removal efficiency is not caused by changes in the daily influent flow. This was also confirmed from the cross correlation of *TN* removals and average daily flow (not shown here).

In order to see if the oxidation ditch model predicts the same real seasonal patterns for *COD* and *TN* removals, values of the kinetic parameters and the aeration constant (k) were allowed to change with temperature according to the Arrhenius relationship given by:

$$P_T = P_{20} \cdot \theta^{(T-20)} \quad (8)$$

As suggested by DHV (1993), temperature activity coefficients (θ 's) were given the following values: 1.07, for μ_H , b_H , k_b , b_A and k_A ; 1.12 for μ_A and 1.00 for k_X . However, the value 1.024 was assumed for the aeration constant (k), as recommended by Metcalf and Eddy (1991).

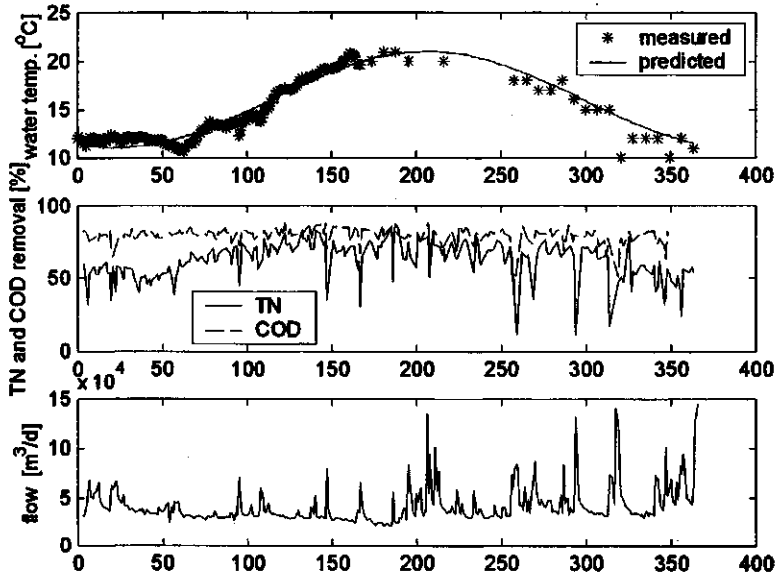


Fig. 8, Real effect of seasonal changes in water temperature on the performance of the oxidation ditch

Fig. 9 presents the results obtained from one simulation of the oxidation ditch, using nominal values (Table 1), Eqn. (7) and (8) and average daily influent data. From comparison with Fig. 8, this figure clearly demonstrates that the model is able to predict approximately the real seasonal patterns for *TN* and *COD* removals.

Thus it can be concluded that uncertainty due to seasonal changes in temperature can be quantified, in the same way as for the other uncertainty sources illustrated above, by Monte Carlo simulations.

For illustrating how uncertainty due to seasonal changes in temperature can be quantified, the following assumptions were first made:

(i) the change in water temperature is between 7 to 30 °C, and (ii) temperature activity coefficient (θ) varies between 1 to 1.08, for kinetic parameters, and between 1 to 1.047, for the aeration constant (k). Here it is worth to note the following. First, Fig. 7 shows that in 1993, temperature varied between about 10 to 22 °C, but here we are using temperature range of 7 to 30 °C to study the possible effect that may take place during a number of years. Second, here we are not investigating the temperature effects on a particular day, rather we are estimating the effects over a period of seven days, which can be in the summer or winter season, under constant temperature conditions. Then, as before, the LHS technique was used for generating 500 uniformly distributed samples from the assumed ranges. Finally, Monte Carlo simulations were carried out, using the real data scenario.

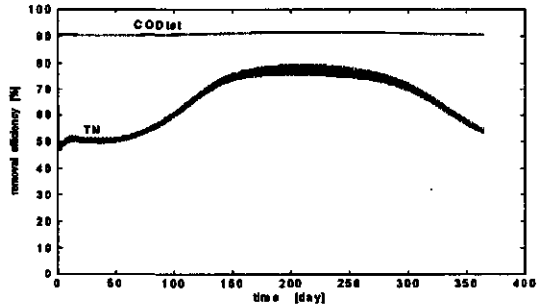


Fig. 9, Predicted effect of seasonal temperature changes on the performance of the oxidation ditch

6.1.5.4.2 Results and discussion

Results of simulations are presented in Fig. 10. As for the other uncertainty sources, the effect of uncertainty due to seasonal changes in water temperature is greater on the performance indices *EQ* and *TSP* than on the other indices (see e.g. C.V., coefficient of variation, given in Table 2). However, unlike other uncertainty sources, uncertainty in water seasonal temperature has induced the highest variation in the index *AE*. Of course, this is due to allowing the aeration

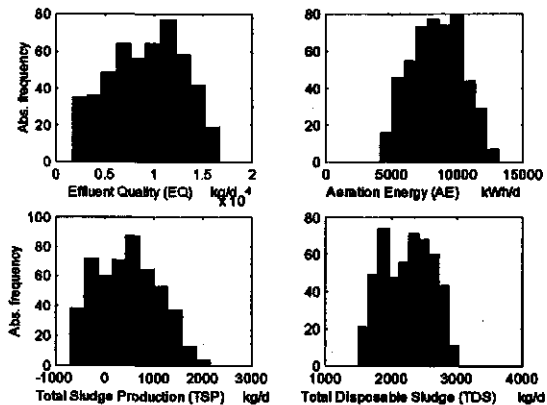


Fig. 10, Frequency distributions of the performance indices due to seasonal changes in water temperature between 7 to 30 °C, using the real data scenario.

constant (k) to vary with the changes in water temperature.

Given the possible ranges of water temperature and possible values of temperature activity coefficients (θ 's), propagation of seasonal temperature uncertainty can also be quantified together with parameter values and influent loads uncertainties given in section 4.1.

6.1.6 General discussion

It should be noted that results obtained in this study represent only the short-term effects of the various uncertainty sources on the performance indices, since the evaluation is carried out for a period of only seven days. Because of the relatively slow process of biomass growth, different results might be obtained for the long-term effects. However, the same procedures followed here can be applied for studying the long-term effects.

Note also in this paper, the effects of the different sources of uncertainty on the performance indices were individually quantified. In fact, this is done only for illustration purposes. However, in reality, the benchmark user needs to quantify the combined effect of the major sources. For achieving that, the user is advised to evaluate the effect of all these major sources at one time.

Estimation of the individual uncertainty contributions of the various sources is especially important when one of the sources become actually known. It is also equally important for designing experimental or monitoring programmes with the aim of reducing the uncertainty. In a previous work (Abusam *et al.*, 2001), we have shown that the effect of some of the parameters of the *ASM No. 1* on the performance indices depends on the value of some other parameters. Thus for computing the individual uncertainty contribution of the various sources, the benchmark user is advised to use a method that deals with correlation cases, e.g. the so-called '*partial uncertainty contribution method*' (Johansson and Janssen, 1994). For more about uncertainty reduction, the benchmark user is referred to e.g. Van Straten and Keesman (1991) who describe a full strategy for reducing uncertainty in forecasting.

For the benchmark user, practical implications of accurate estimation of uncertainty propagation are the following. First, selection can be made, under uncertainty, among various control strategies. Secondly, decision can be made about the usefulness of a certain control strategy, which is claimed to be useful under certain conditions.

6.1.7 Conclusions

This study has demonstrated how the effect of the various uncertainty sources can be quantified. Uncertainty sources considered are: (i) parameter values, (ii) influent loads, (iii) values of the initial states, (iv) model structure, and (v) seasonal changes in water

temperature. Although only the short-term effects were studied here, the same procedures can also be applied for studying the long-term effects.

Short-term results obtained have indicated the following. Due to uncertainty in influent loads and parameter values, large deviations, from the nominal values, in the benchmark performance indices will be found for effluent quality and total sludge production indices. However, relatively smaller deviations will be found due to uncertainty in the states initial conditions. Effect of the model structural uncertainty on the performance indices seems to be negligible.

6.1.8 References

Abasaheed, E. A. (1997), Sensitivity analysis on a sequencing batch reactor model I: effect of kinetic parameters, *J. Chem. Tech. Biotechnol.* 70:379-383.

Abasaheed, E. A. (1999), Sensitivity analysis on a sequencing batch reactor model II: effect of stoichiometric and operating parameters, *J. Chem. Tech. Biotechnol.* 74:451-455.

Abusam, A., K.J. Keesman, G. van Straten and K. Meinema (2000), Parameter estimation procedure for complex non-linear systems: calibration of ASM No.1 for N-removal in a full-scale oxidation ditch, in *Proc. of the Watermatex2000, Gent, Belgium.*

Abusam, A., K.J. Keesman, G. van Straten and K. Meinema (2001), Sensitivity analysis on oxidation ditches: the effect of variations in stoichiometric, kinetic and operating parameters on the performance indices, *J. Chem. Tech. Biotech.* 76(4):430-438.

Bagchi, A. (1993), *Optimal control of stochastic systems*, Prentice Hall.

Beck, M.B. (1987), Water quality modeling: a review of the analysis of uncertainty, *Water Resources. Research* 23(8):1393-1442.

Burges, S.J. and D.P. Lettenmaier (1975), Probabilistic methods in stream quality management, *Wat. Res. Bulletin* 11:115-130.

Copp, J.B. (2000), Defining a simulation benchmark for control strategies, *Water*21, 1(2):44-49.

DHV Water BV (1993), Dossier G8112-10-001, Amersfoort, The Netherlands.

Henze, M., C.P.L. Grady, jr, W. Gujer, G van R. Marais and T. Matsuo (1987), a general model for single-sludge WWT systems, *Wat Res* 21(5):505-15.

Høybye, J.A. (1998), Model error propagation and data collection design: an application in water quality modeling, *Water, Air and Soil pollution* 103:101-119.

Janssen P.H.M. (1994), Assessing sensitivities and uncertainties in models: a critical evaluation, in *predictability and non-linear modeling in natural sciences and economics*, Ed by Grasman J and van Straten G., pp 344-361, Kluwer Academic Publishers.

Johansson, M.P. and P.H.M. Janssen (1994), Uncertainty analysis on critical loads for forest soils in Finland, in *predictability and non-linear modeling in natural sciences and economics*, ed by Grasman J and van Straten G., pp 447-459, Kluwer Academic Publishers (1994).

Metcalf & Eddy (1991), *Wastewater engineering: treatment, disposal and reuse*, 3rd ed, McGraw-Hill.

Pons M. N., H. Spanjers and U. Jeppsson, Towards a benchmark for evaluating control strategies in wastewater treatment plants by simulations, *Escape 9* (European symposium on computer aided process engineering-9), Budapest (1999).

Spanjers, H., P. Vanrolleghem, K. Nguyen, H. Vanhooren and G.G. Patry (1998), Towards a simulation-benchmark for evaluating respirometry-based control strategies, *Wat. Sci. Tech.* 37(12): 219-226.

Vanrolleghem, P.A., U. Jeppsson, J. Carstensen, B. Carlsson and G. Olsson (1996), Integration of WWTP design and operation – a systematic approach using cost functions, *Wat. Sci. Tech.* 34(3-4), 159-171 (1996).

Van Straten, G. and K.J. Keesman (1991), Uncertainty propagation and speculation in projective forecasts of environmental change: a lake-eutrophication example, *J. of Forecasting* 10:163-190.

Von Sperling, M. (1996), Design of facultative ponds based on uncertainty analysis, *Wat. Sci. Tech.* 33(7):41-47.

Weijers, S. R. and P. A. Vanrolleghem (1997), A procedure for selecting best identifiable parameters in calibrating activated sludge model No. 1 to full-scale plant data, *Wat. Sci. Tech.* 36(5):69-79.

6.2 Forward and backward uncertainty propagation in mathematical models^{††}

6.2.1 Abstract

In the field of water technology, forward uncertainty propagation is frequently used, whereas backward uncertainty propagation is rarely used. In forward uncertainty analysis, one moves from a given (or assumed) parameter subspace towards the corresponding distribution of the output or objective function. However, in the backward uncertainty propagation, one moves in the reverse direction, from the distribution function towards the parameter subspace. Backward uncertainty propagation, which is a generalisation of parameter estimation error analysis, gives information essential for designing experimental or monitoring programmes, and for tighter bounding of parameter uncertainty intervals. The procedure of carrying out backward uncertainty propagation is illustrated in this technical note by a working example.

Keywords: wastewater; activated sludge; oxidation ditch; modeling; uncertainty analysis.

6.2.2 Introduction

Uncertainty analysis is a very important step in the model building process. It contributes directly to the reliability and applicability of the developed mathematical model. It is mainly concerned with the effect that various sources of uncertainty have on the model output. Model sources of uncertainty can be in: (i) model inputs, (ii) model parameter values, (iii) initial state conditions, and in (iv) model structure. The method illustrated in this paper is particularly applicable to types (i) to (iii) of sources of uncertainty.

In the field of water technology, uncertainty analysis or error propagation – if it is carried out at all – is usually executed in one direction: forward direction. That is, starting the uncertainty analysis from a given (or assumed) parameter subspace, defined in terms of ranges or distributions, and moving towards the corresponding distribution of the output or objective function. However, the backward uncertainty propagation is rarely performed. Clearly the backward uncertainty propagation is the reverse of the forward uncertainty propagation, and it can be seen as a generalisation of parameter estimation error quantification from given experimental data. It can be used for obtaining, in a systematic way, essential information about which part of the parameter space, or which parameter combinations, contributed mostly to some interesting part of the distribution function. For instance, which inputs, parameters or initial conditions lead to extreme or off-normal process conditions? Such information will be the important ingredients that help the plant manager in designing and carrying out a monitoring programme. Through a monitoring programme, the plant manager usually wants to find out accurate values for model parameters or initial conditions that are suspected of causing or contributing to a certain part of interest in the distribution function found from forward uncertainty propagation.

^{††} Submitted to Wat. Res. by A. Abusam, K.J. Keesman and G. van Straten

This can even further generalized by formulating extreme or off-normal process conditions, *a priori*.

6.2.3 Theory

Let the model of the dynamic system be defined as a set of equations in standard state-space form:

$$\frac{dx}{dt} = f[x, u, t; \theta] + w(t), \quad x(0) = x_0 \quad (1)$$

$$y(t) = g[x, u, t; \theta] + v(t) \quad (2)$$

where both f and g are vector-valued functions, x is n -dimension state vector with initial state vector x_0 , u is the m -dimension input vector, θ is the p -dimension parameter vector, y is the q -dimension output vector and v and w are stochastic signals representing the system noise and the measurement errors, respectively. Further, let there be an interest in the performance of the plant, expressed by some objective function defined as:

$$J = \phi(y, u, t; \theta) + \int_0^T L[y, u, t; \theta] dt \quad (3)$$

where ϕ defines the terminal cost, and L defines the running cost. Notice that according to (3) J is a real-valued scalar function. Extension to a vector-valued objective function is straightforward, as in Abusam (2000).

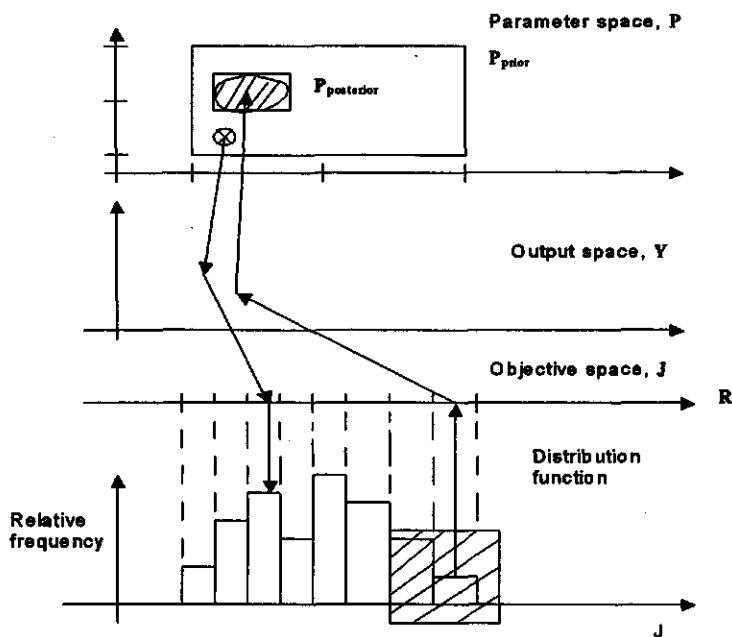


Fig. 1, Forward and backward uncertainty propagation

The forward approach of uncertainty propagation, as illustrated in Fig. 1 by downward arrows, moves from the given (or assumed) parameter subspace (P_{prior}) towards the corresponding distribution of the objective function (J). Statistical indicators, which are necessary for quantifying the error propagation (e.g. the mean, variance, range, and the shape of the distribution), can be obtained by analysing the distribution function.

In the backward error propagation, however, one starts from a given distribution function and moves backward towards finding out the set of parameter vectors that have resulted in a class or classes of interest in the given distribution function (J). This approach is depicted in Fig. 1 by upward arrows. In this approach, the interest is often in finding out the subset of parameters ($P_{\text{posterior}}$) that are responsible for extreme objective function values. The procedure of backward uncertainty propagation can be summarised in the following indirect procedure, which is essentially based on sampling the parameter space.

Step 1: Sample a subset in P , denoted by P_{prior} and calculate the resulting distribution function.

Step 2: Select a class or classes of interest.

Step 3: Collect the subset of parameter vectors in the parameter space (P), denoted by $P_{\text{posterior}}$, that have resulted in this class of interest, and find "statistical" indicators of this subset, such as mean, range, shape and orientation of the subset.

Step 4: Identify parameters of potential interest, by comparing parameter values in the subset $P_{\text{posterior}}$ and in its complement ($P_{\text{complement}}$) to parameter values in the prior parameter set, P_{prior} , where not a single parameter vector, as in search algorithms, is evaluated, but a complete set of parameter vectors. This approach is clearly related to the discrete method for solving set-membership estimation problems (Keesman, 1990).

6.2.4 Working Example

Let us illustrate the backward uncertainty propagation approach by *finding* those *ASM No. 1* (Henze et al., 1987) parameters or combinations that have resulted in a decline in total sludge production (negative *TSP*), as shown by the marked bars relative to negative *TSP* in the frequency distribution given in Fig. 2. Here, it is worth mentioning that the result presented in Fig. 2 is a part of a larger research work aimed at quantifying the effect of various uncertainty sources in a model of an oxidation ditch plant on the performance indices of a benchmark especially developed for that plant (Abusam, et al., 2000). As proposed by COST (2000) the following equation can be used for calculating the daily *TSP* over a certain period.

$$TSP = \frac{1}{T}(TSS_{reactor,T} - TSS_{reactor,0}) + \frac{1}{T}(TSS_{settler,T} - TSS_{settler,0}) + \frac{0.75}{T} \int_0^T TSS_{waste} \cdot Q_{waste} \cdot dt + \frac{0.75}{T} \int_0^T TSS_{effluent} \cdot Q_{effluent} \cdot dt \quad (6)$$

where TSS is the total suspended solids concentrations, Q is the flow and T is the evaluation period, which in this study is chosen to be 7 days. As can be seen from the first two terms in the right hand side of equation (6), the calculated TSP can be negative, if the initial TSS concentration is higher than at the end of the evaluation period (T).

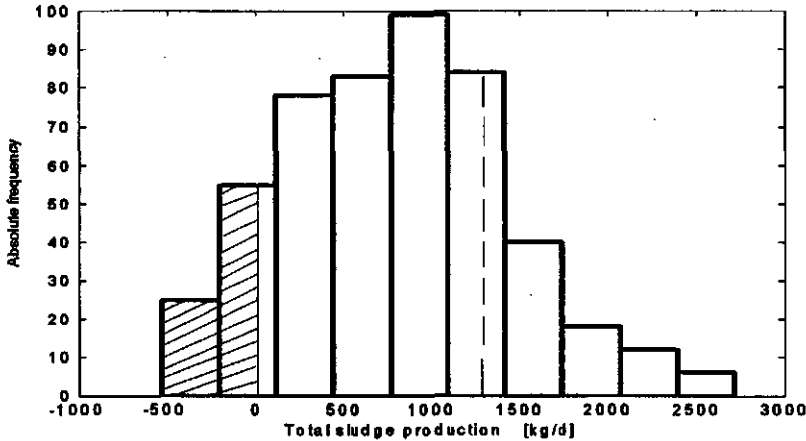


Fig. 2, Influence of *ASM No.1* parameters on the predicted total sludge production of an oxidation ditch WWTP model (Abusam *et al.*, 2000).

Let us now apply the backward uncertainty propagation procedure.

Step 1: Consider the case where the prior subset P_{prior} was sampled 500 times using a Latin Hypercube (LH) scheme (Abusam *et al.*, 2000). Ranges that define the subset P_{prior} are given in Table 1, together with mean and calibration values. The resulting distribution function for TSP is presented in Fig. 2. TSP related to the calibrated parameter vector (column 2 in Table 1) is shown in Fig. 2 by a dashed line.

Step 2: Let us assume that the classes of interest are that part in the distribution function having a total sludge production less than zero. Note that these classes were selected only for illustration purposes. These classes are shown in Fig. 2 by marked bars.

Step 3: Moving backwards from the distribution function, we found that 57 out of the 500 sampled *ASM No. 1* parameter vectors defining ($P_{posterior}$), have resulted in total sludge less than zero. This also means that the number of parameter combinations ($P_{complement}$) that have resulted in TSP greater than zero is 443. Mean and range of *ASM No. 1* parameters in

both $P_{\text{posterior}}$ and $P_{\text{complement}}$ are presented in Table 2. Significant change in the mean or range is presented by bold in Table 2. The shape and orientation of the subset ($P_{\text{posterior}}$) can be analysed via ellipsoidal analysis.

Table 1, Calibration values and possible ranges for parameters of ASM No. 1

| Parameters | Calibration values | Parameter subspace (P_{prior}) | |
|------------|--------------------|-------------------------------------------|-------------|
| | | mean | range |
| Y_A | 0.24 | 0.20 | 0.10-0.30 |
| Y_H | 0.62 | 0.58 | 0.45-0.70 |
| f_P | 0.08 | 0.14 | 0.08-0.2 |
| i_{XB} | 0.08 | 0.08 | 0.06-0.10 |
| i_{XP} | 0.06 | 0.06 | 0.04-0.08 |
| μ_H | 4.59 | 8.10 | 3.00-13.20 |
| K_S | 20.0 | 90.0 | 10.00-180.0 |
| K_{OH} | 0.33 | 0.55 | 0.10-1.00 |
| K_{NO} | 0.50 | 0.30 | 0.10-0.50 |
| b_H | 0.635 | 0.83 | 0.05-1.60 |
| η_B | 1.0 | 0.80 | 0.60-1.00 |
| η_h | 0.32 | 0.60 | 0.30-0.90 |
| k_h | 1.72 | 3.00 | 1.00-4.00 |
| K_X | 0.02 | 0.08 | 0.01-0.15 |
| μ_A | 0.657 | 0.70 | 0.20-1.20 |
| K_{NH} | 1.0 | 5.40 | 0.80-10.00 |
| b_A | 0.098 | 0.10 | 0.05-0.15 |
| $K_{O,A}$ | 0.4 | 0.51 | 0.01-1.00 |
| k_a | 0.092 | 0.41 | 0.02-0.8 |

Let $P_{\text{posterior}} = \{ \theta_1, \dots, \theta_M \}$, where θ is the parameter vector ($\theta \in \mathbb{R}^{19}$). In this case $M = 57$.

Define the matrix $P = [\theta_1, \dots, \theta_M]$. Then,

$$\xi = \{ \theta : (\theta - \theta_0)^T (PP^T)^{-1} (\theta - \theta_0) \leq \alpha \} \quad (4)$$

is an ellipsoid that approximates the region $P_{\text{posterior}}$ where θ_0 is the centre. Tight bounding can be obtained by evaluating the smallest upper bound of α for which (4) holds, given $\theta_1, \dots, \theta_M$. Eigenvalue decomposition of the $p \times p$ matrix (PP^T) gives

$$(PP^T)V = VA \quad (5)$$

where A is a diagonal matrix with eigenvalues, and V is an orthogonal matrix with the eigenvectors. The eigenvectors give directions of the principal axes of the ellipsoids, where lengths of these principal axes are proportional to the square root of the absolute magnitude of corresponding eigenvalue (see e.g. Bard, 1974; Hidalgo and Ayesa, 2001). Hence, in this way insight can be obtained in the shape and orientation of the subset, given in higher dimensional vector spaces.

Table 2 also presents the partial result of the ellipsoidal (shape and orientation) analysis of the subset $P_{\text{posterior}}$. The last column of Table 2 presents the eigenvector corresponding to the smallest eigenvalue. Values greater than 0.35 are shown in bold. As we will see later, ellipsoidal analysis gives information about parameters interaction effects.

Table 2, Analysis of ASM No. 1 parameters that have resulted in decline of total sludge production

| Parameters | First-order analysis | | | | Second-order analysis |
|------------|----------------------------------------------------|---------------------|----------------------------------------------------|---------------------|-------------------------------------------------------------------------------------------------|
| | Subspace of interest ($P_{\text{posterior}}$) | | Complement subspace ($P_{\text{complement}}$) | | Eigenvector corresponding to the smallest eigenvalue ($\lambda_{\text{min}} = 0.83$) |
| | mean | range | mean | range | |
| Y_A | 0.19 | 0.10-0.30 | 0.20 | 0.10-0.30 | 0.0329 |
| Y_H | 0.53 | 0.45-0.70 | 0.58 | 0.45-0.70 | 0.3516 |
| f_P | 0.12 | 0.08-0.19 | 0.14 | 0.08-0.20 | 0.3735 |
| i_{XB} | 0.08 | 0.06-0.10 | 0.08 | 0.06-0.10 | -0.1635 |
| i_{XP} | 0.06 | 0.04-0.08 | 0.06 | 0.04-0.08 | -0.0378 |
| μ_H | 8.99 | 4.16-13.15 | 7.99 | 3.01-13.19 | -0.0860 |
| K_S | 79.18 | 10.36-175.01 | 97.04 | 10.24-179.89 | 0.1234 |
| K_{OH} | 0.58 | 0.13-1.00 | 0.55 | 0.10-1.00 | 0.2459 |
| K_{NO} | 0.32 | 0.11-0.50 | 0.30 | 0.10-0.50 | -0.1412 |
| b_H | 1.20 | 0.66-1.58 | 0.78 | 0.05-1.60 | -0.0013 |
| η_g | 0.83 | 0.60-1.00 | 0.80 | 0.60-1.00 | -0.2139 |
| η_h | 0.55 | 0.33-0.87 | 0.61 | 0.30-0.90 | 0.0796 |
| k_h | 1.60 | 1.01-3.85 | 2.62 | 1.00-4.00 | 0.6804 |
| K_X | 0.08 | 0.01-0.15 | 0.08 | 0.01-0.15 | 0.0379 |
| μ_A | 0.75 | 0.25-1.18 | 0.70 | 0.20-1.20 | -0.0896 |
| K_{NH} | 5.55 | 0.98-9.42 | 5.38 | 0.82-10.00 | -0.0603 |
| b_A | 0.10 | 0.05-0.15 | 0.10 | 0.05-0.15 | -0.0127 |
| K_{OA} | 0.50 | 0.02-0.97 | 0.51 | 0.01-1.00 | 0.0907 |
| k_a | 0.36 | 0.02-0.74 | 0.41 | 0.02-0.80 | 0.2608 |

Significant values are presented in bold

Step 4: From a first-order analysis of the subspace $P_{\text{posterior}}$ and its complement $P_{\text{complement}}$ (Table 2) and looking at the shifts in means and ranges, it can be said that only four parameters (μ_H , K_S , b_H and k_h , given in bold) are responsible for the decline in total sludge production. Fig. 3 presents the effect of three combinations of these four parameters on the TSP.

While it is expected that increase in heterotrophic decay (b_H) or decrease in specific hydrolysis (k_h) can result in decline of TSP, it is unexpected that increase in heterotrophic maximum specific growth rate (μ_H) or decrease in Monod coefficient (K_S) can also cause

decline of TSP (Table 2). The most probable explanation, here, is that μ_H and K_S can cause decline in TSP , due to interactions with the other parameters. Results of simulations carried out where only μ_H and K_S were varied, while the rest of the parameters were kept constant at the calibration values (Table 1), have confirmed this explanation, as TSP , in this case, was always positive.

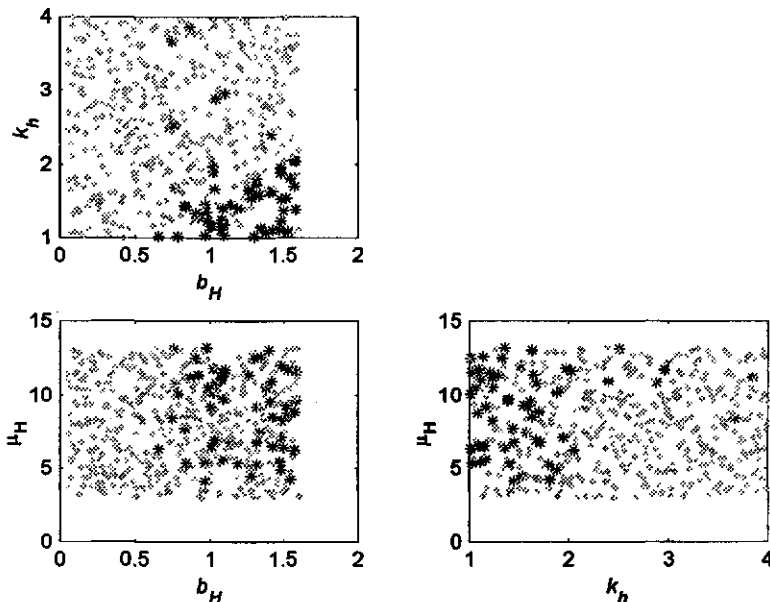


Fig. 3, Effect of projected values of μ_H , b_H and k_h on total sludge production (TSP): (*) negative TSP and (.) positive TSP .

As an illustration of these interaction effects, Fig. 4 below presents two cases of the effect of b_H and k_h on TSP : (i) when the interaction with the other parameters is neglected (Fig. 4A) i.e. when the other parameters are kept constant, and (ii) when the interaction is taken into account (Fig. 4B). Hence, this figure clearly illustrates the effect of parameter interaction on TSP . As can be seen, Fig. 4A shows a different pattern than Fig. 4B. In Fig. 4A, the sets are distinct. However, due to the interaction effects, the sets in Fig. 4B are no longer distinct.

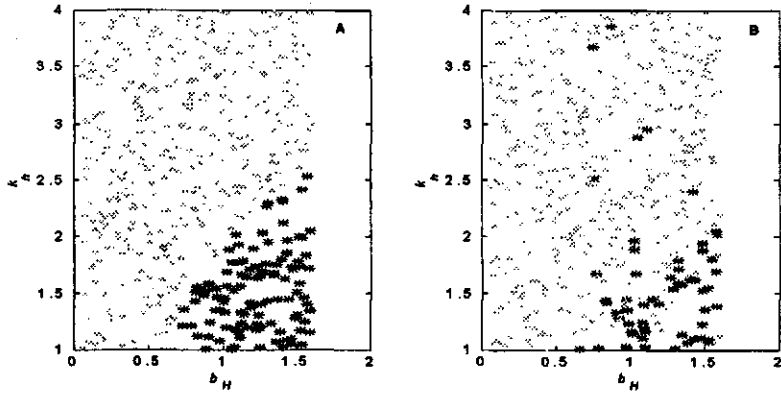


Fig. 4, Effect of parameter interaction on total sludge production (*TSP*). (A) When only b_H and k_h were varied. (B) When all parameters were varied: (*) negative *TSP* and (.) positive *TSP*

Another way of looking at such data presented in Fig. 4B is through cumulative frequency plots (see e.g. Hornberger and Spear (1981)), for each individual parameter. As an example, Fig. 5 presents the relative cumulative plots for b_H and k_h , when all parameters are varied (i.e. the same data used in plotting Fig. 4B). From Fig. 5, one can conclude the following: (i) there is a clear cut between b_H values, as well as k_h , that have caused

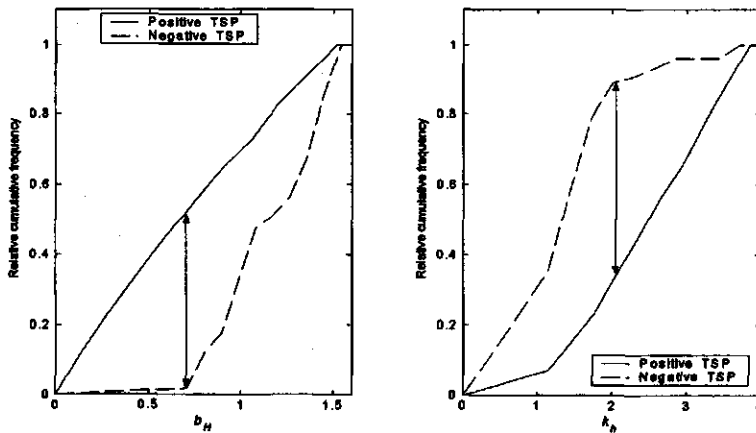


Fig. 5, Relative cumulative frequency of positive and negative total sludge production (*TSP*), using data from Fig. 4B

negative *TSP* and values that have caused positive *TSP*, and (ii) decline of *TSP* is caused by b_H being greater than 0.7 and k_h being less than, roughly, 2. Hence, these cumulative frequency plots give extra useful information as compared to the results obtained from

first-order analysis (see Table 2). However, complete parameter interactions have not been made visible, here.

Therefore, as described above, ellipsoidal (second-order) analysis was carried out for the subset $\mathbb{P}_{\text{posterior}}$. Results of this analysis are presented in the last column of Table 2. These results show that not only μ_H , K_S , b_H and k_h (as found from the first-order analysis) can cause decline in *TSP*, but also the combinations of yield for heterotrophic biomass (Y_H), fraction of particulate biomass (f_P), and maximum specific hydrolysis rate (k_h) can contribute to the negative *TSP*. In particular (see the last column of Table 2), the parameter combination $0.3516Y_H + 0.3735f_P + 0.6804k_h$ is sensitive for predicting negative *TSP*. Of course, contribution of the last group of parameters on negative *TSP* is not directly, but rather through interactions. Nonetheless all the six parameters should be considered in a monitoring programme aimed at determining accurate values of parameters that can cause or contribute to negative *TSP*. Effort to estimate these parameters more accurately would reduce the uncertainty on the distribution of interest. In fact, if, from prior knowledge, it is known that the distribution (resulting from the prior space) is too wide, backward uncertainty analysis then gives, through e.g. cutting off the distribution tails, information that the actual parameters are confined to a smaller parameter uncertainty region.

6.2.5 Conclusions

A generalised uncertainty propagation problem has been formulated and illustrated. A procedure for carrying out backward uncertainty propagation, which is a generalisation of parameter estimation error analysis, is illustrated with a working example. Results obtained from this example have demonstrated that information essential for further modelling, designing model-based experimental or monitoring programmes and tightening of parameter intervals can be obtained by carrying out backward uncertainty propagation analysis.

6.2.6 References

- Abusam, A., K.J. Keesman, G. van Straten and K. Meinema (2000), Estimation of uncertainties in the performance indices of an oxidation ditch, *J Chem. Tech. Biotech.* (submitted).
- Bard, Y. (1974), *Non-linear parameter estimation*, Academic Press.
- COST (2000), www.ensic.u-nancy.fr/COSTWWTP/Benchmark/Benchmark1.htm.
- Henze, M., C.P.L. Grady, jr, W. Gujer, G van R. Marais and T. Matsuo (1987), a general model for single-sludge WWT systems, *Wat. Res.* 21(5):505-515.

Hidalgo, M.E. and E. Ayesa (2001), Mathematical and graphical description of the information matrix in calibration experiments for state-space models, (to appear in *Wat. Res.*).

Hornberger, G.M. and Spear, R.C. (1981), An approach to the preliminary analysis of environmental systems, *J. of Env. Manag.* 12:7-18.

Keesman, K.J. (1990), Membership-set estimation using random scanning and principal component analysis, *Math. Comp. Simul.*, 32(5-6), 535-544.

PART 3
BENCHMARKING

7. The benchmarking procedure

7.1 Introduction

So far, the core of the benchmark has been developed. The basic simulation model (part 1) and sensor models (Appendix II) have been developed and analyzed (part 2). Also the evaluation criteria have been developed (Appendix III). The purpose of this chapter is to briefly describe the benchmarking procedure. Because it is meant to be used in evaluating the performance of any specific oxidation ditch plant, no reference to a generic plant is made in this procedure. It worth mentioning that in this benchmarking procedure the part related to model calibration and validation is more or less the same as that proposed by STOWA (2000) for activated sludge plants. It should be noted that although the procedure is developed in Matlab\Simulink environment, it could also be used on any other simulation platform like GPS-X and WEST.

7.2 Components of the benchmark

The main parts of the benchmark are the following: (i) a basic simulation model, (ii) performance criteria and (iii) the evaluation procedure (protocol). The basic simulation model is composed of the reactor, settler, sensors, and actuators such as aerators and pumps. Further, standardized influent data for three different weather conditions have been used. Details on the performance criteria are given in Appendix III together with the evaluation procedure.

7.3 Step-by-step benchmarking procedure

Fig. 1 presents the major steps of the benchmarking procedure, which can be carried out on any simulation platform. As mentioned above, the procedure is independent of the simulation platform. In the following more details are given about the steps of the benchmarking procedure.

Step 1: Collection of plant design and operational data

- Make a sketch of the plant layout.
- Collect the following plant design data:
 - * Volume and dimensions (length, width and depth) of the oxidation ditch and the secondary settler.
 - * Number of aerators, their design capacity, in kg O_2/h , and location.
 - * Design organic loads, in kg COD/d and kg N/d , and hydraulic loads, in m^3/d .

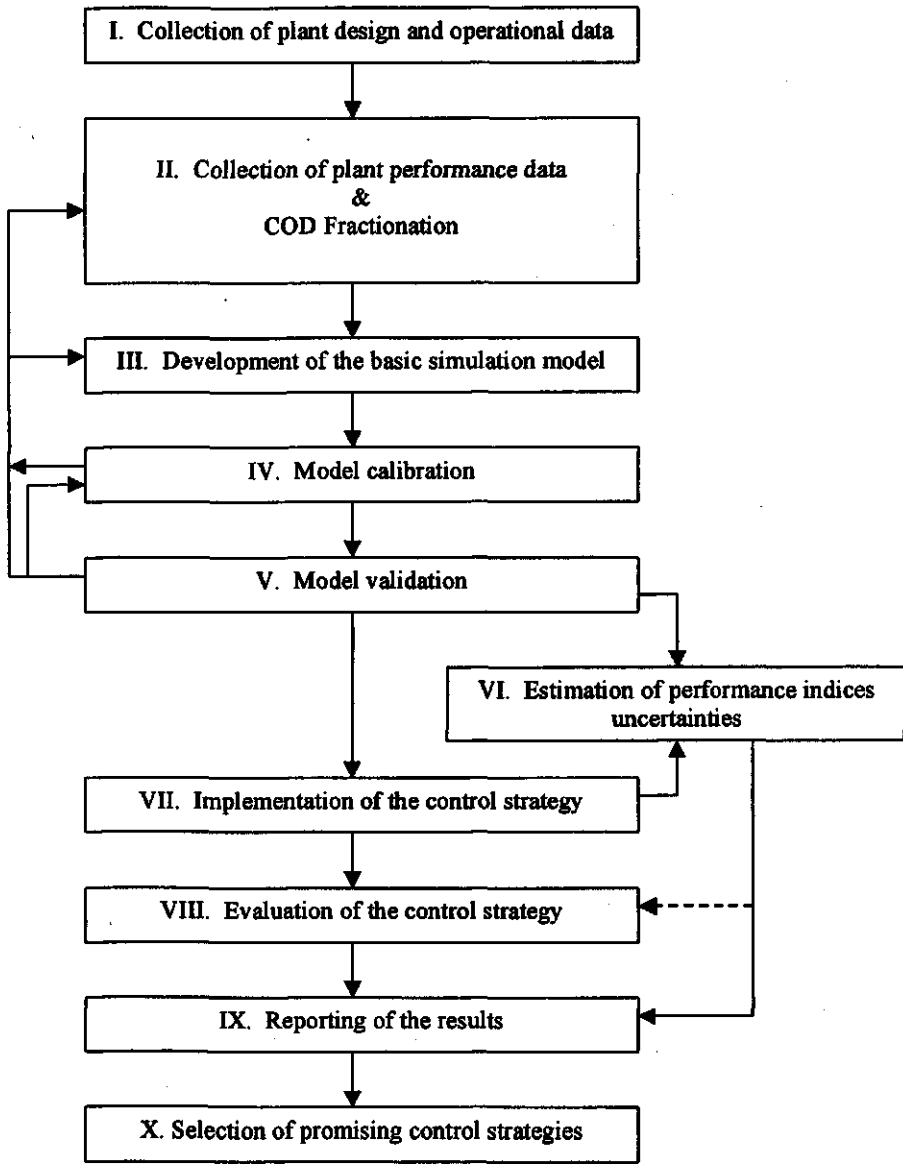


Fig. 1, Schematic of the benchmarking procedure

Step 2: Collection of plant performance data and wastewater characterization

- Carry out a daily measuring campaign for about two weeks, in order to collect the following averaged performance data:

* **Flow measurements** (m^3/d) for the following streams: (i) influent stream, (ii) effluent stream, (iii) wasted activated sludge (*WAS*) and (iv) recirculated activated sludge (*RAS*).

* **Velocity measurements**: average horizontal velocity, m/s.

* **Concentration measurements**, in mg/l: (i) *DO*, total *COD*, *TN*, *TKN*, *NH₄*, *NO₃*, and *TSS* concentrations in the influent and the effluent streams (composite samples), (ii) *TSS* concentrations in *WAS* and *RAS* streams (iii) *DO* concentrations, at a number of points along the reactor and especially at the in/outlet ports, and (iv) influent and effluent alkalinity, in moles/ m^3 .

* **Aeration energy** (*AE*), per aerator, in kWh/d.

* **Pumping energy** (*PE*), per pump, in kWh/d.

Reactor water temperature, in °C.

Aerators operational patterns, for each aerator over the day.

- Conduct an **intensive measuring campaign** (sample time is 2-4 hours) for 2 or 3 days, in order to determine the dynamics of the influent and effluent flow, *COD*, *NH₄* and *NO₃*.

- Break down the various concentrations measured in this step into the corresponding components of *ASM No. 1*, using previous knowledge about wastewater characteristics at the plant. If necessary, carry out some additional laboratory experiments (see for example Solfrank and Gujer, 1991; Henze, 1992; STOWA, 1996 and 2000).

Step 3: Development of the basic simulation model

- From the plant layout drawn in step 1, model only the reactor (oxidation ditch) and secondary settler. That is to say, neglect all other treatment units like the primary settlers and sludge treatment units. If the plant has more than one treatment line, model only the layout of one treatment line. Note that the simulation model can be developed on any platform, e.g. GPS-X, Matlab\Simulink, or its shell SIMBA.

- Model the oxidation ditch as a loop-of-*CSTR*'s, without back flows, using equal volume *CSTR*'s. Use aerated *CSTR*'s for modeling the aerated zones, and non-aerated *CSTR*'s for modeling the non-aerated zones. Depending on the number of aerators and the ditch layout, limit the number of *CSTR*'s needed for modeling a single oxidation ditch to 10 to 15 *CSTR*'s. For more information about the number of *CSTR*'s needed for modeling an oxidation ditch, see chapter 3.

- Use ASM No. 1 (Henze *et al.* 1987) for modeling biochemical processes that take place along the reactor.

** A sample template is provided in Appendix V.

- Use the double exponential settling velocity model (Takács *et al.* 1991) to model the secondary settlers.

Step 4: Model calibration

- Before starting the calibration process, think about the data needed to validate the model. If it is not planned to collect a new set of performance data at a different season of the year, leave half of the data collected in step 2 for model validation step (the next step).

- Use default or literature values for all parameters of *ASM No. 1*, except the following most sensitive ones: Y_H , b_H , K_S , k_h , K_{NH} , K_X , μ_A , η_p and η_h (see chapter 5). These parameters need special attention. Try to accurately determine, through experiments, the actual values of the parameters that are claimed to be measurable, such as: Y_H , b_H , and K_S (see for example Ekama *et al.*, 1986; Kappeler and Gujer, 1992).

- Estimate the values of 3 to 5 of the most sensitive parameters mentioned above. In addition, estimate the aeration constant ($k = K_L a \cdot V_A$, where V_A is the volume of the aerated *CSTR*), using the design data collected in step 1. Chapter 2 shows that it is not possible to individually identify $K_L a$ or V_A , due to the hyperbolic relationship between them. However, it also shows that their product (k) can be estimated very accurately. Note that for equal volume *CSTR*'s, it makes no difference whether k or $K_L a$ is estimated.

- In the parameter estimation step a conventional calibration procedure or the (novel) procedure proposed in this thesis (see chapter 4) may be followed. According to STORA (2000), where it is assumed that $K_L a$ is known in advance, one may calibrate first sludge production, then effluent ammonia concentration, and finally nitrate concentration. With the new calibration procedure, which is based on response surface analysis (*RSM*) to determine the most sensitive parameters and initial parameters estimates, the three above-mentioned functions can simultaneously be calibrated.

- Note that steps 2 and 3 may need to be repeated until a well-calibrated model is obtained (see Fig. 1).

Step 5: Model validation

- Validate the model, using data collected at a different season. If this is not possible, use the data left for this purpose in step 4.

- For obtaining appropriate results, the last step or even last three steps may need to be repeated (see Fig. 1).

Step 6: Estimation of performance indices uncertainties

- Study carefully the performance criteria provided in the Appendix III.
- Follow the procedures demonstrated in sections 6.1 and 6.2, to quantify the influence of the various sources of uncertainty on the performance indices, under the existing control strategy. Note that in sections 6.1 and 6.2 only the short-term effects were studied. However, the same procedures may be used to study the long-term effects (4-5 times the sludge age).
- Summarize the results obtained in this step in terms of standard deviations or ranges, for each performance index.

Step 7: Implementation of the control strategy

- Study thoroughly the control strategies that will be evaluated, in order to evaluate and identify the following: (i) control objective, (ii) measured, controlled and manipulated variables, and (iii) control configuration and algorithms.
- At the implementation stage, pay particular attention to the simulator special features, such as DO modeling. Experience has shown that these special features impact specially the closed-loop results. Therefore, closed-loop results may not be the same for different simulators (COST, 2000b).
- Tune the controllers, for example, using the Ziegler and Nichols method for PID controller tuning, or any other tuning familiar method.
- Implement models of DO and N sensors (given in Appendix II), where measurements will be taken. Locations where measurements will be taken are usually specified in the description of the control strategy. Note that delay time and dynamics need to be adjusted for these sensors.
- If necessary, setup and incorporate models of other sensors and actuators like pumps and aerators.

Step 8: Evaluation of the control strategy

- Download the various weather influent files (dry, stormy and rainy conditions) provided by COST 624 on their web site (COST, 2000a) and scale the flow in these files to the flow of the plant under study.

- Put the sensors OFF (open-loop) and carry out a 100-day steady state simulation, using the average concentrations of the dry weather influent file. Here, *RAS* and *WAS* should be kept constant at some typical values.
- Save the state values obtained at the end of the steady state simulation, because they will be used as initial values in the dynamic simulations.
- Put the sensors ON (closed-loop) and conduct dynamic simulations to evaluate the implemented control strategy, using each of the real and scaled weather files (dry, storm and rain weather files), separately.
- Evaluate the plant performance under the new-implemented control strategy, for each weather file separately, in terms of performance indices together with uncertainties and violation times of the effluent constraints, as shown in Appendix III.

Step 9: Reporting of the results

- Report in a table format, for each evaluated control strategy, the values of performance indices and time of violations obtained in the previous step.
- Report also the performance indices uncertainties obtained in step 6 and 8.

Step 10: Selection of promising control strategies

- Based on the reported performance indices and the information about uncertainties in these indices, make a decision about the most promising control strategies to your plant. Note that it is not an easy task to make such selection. For example, based only on performance indices, a certain control strategy may look very promising. When taking into account the uncertainties in the performance indices, however, it may be difficult to distinguish this control strategy from the other strategies. For more about the selection of the most promising control strategy or strategies see section (9.1).

7.4 References

Ekama, G.A., P.L. Gold and G.v.R. Marais (1986), Procedure for determining influent COD and the maximum specific growth rate of heterotrophs in activated sludge, *Wat. Sci. Tech.* 18(6):91-114.

COST (2000a), www.ensic.u-nancy.fr/COSTWWTP/Benchmark/Benchmark1.htm.

COST (2000b), The COST simulation benchmark: description and simulator manual, edited by John B. Copp, European Cooperation in the field of Scientific and Technical Research (COST), (draft of a book).

Henze, M. (1991), Characterization of wastewater for modeling of activated sludge processes, *Wat. Sci. Tech.* 25(6):1-15.

Henze, M., C.P.L. Grady, jr, W. Gujer, G. van R. Marais and T. Matsuo (1987), Activated sludge model no. 1, IAWQ scientific and Technical Report no. 1, IAWQ, London, U.K.

Kappeler, J. and W. Gujer (1992), Estimation of kinetic parameters of heterotrophic biomass under aerobic conditions and characterization of wastewater for activated sludge modeling, *Wat. Sci. Tech.* 25(6):125-139.

Sollfrank, U. and W. Gujer (1991), Characterization of domestic wastewater for mathematical modeling of activated sludge process, *Wat. Sci. Tech.* 23(4-6):1057-1066.

STOWA (1996), methoden voor influentkarakterisering – inventarisatie en richtlijnen, STOWA, 80-96 (in Dutch).

STOWA (2000), SIMBA-protocol, richtlijnen voor het dynamisch modelleren van actiefslibsystemen, STOWA, 2000-16 (in Dutch).

Takács, I., G.G. Patry and D. Nolasco (1991), A dynamic model of the clarification-thickening process, *Wat. Res.* 25(10):1263-71.

8. Illustration of the use of the benchmark

8.1 Introduction

The aim of this chapter is to demonstrate the use of the developed benchmark. In section 8.2, the benchmark will be used to study the effect of the horizontal velocity, which is considered as a control variable with respect to *TN* removal efficiency, on the performance of oxidation ditches. In oxidation ditches, mechanical aerators have dual function: (i) to introduce oxygen into the ditch and (ii) to create sufficient horizontal velocity to prevent organic solids from depositing on the channel bottom surface. A change in the aerators operating conditions (immersion depth or rotational speed) will, therefore, affect both the amount of oxygen input and the horizontal velocity. In turn, a change in the horizontal velocity influences the amount oxygen and nitrate recirculated from the aerated zones to the anoxic zones. Thus, the whole nitrogen removal process will be affected by a change in the aerators operating conditions.

In section 8.3, the benchmark is used to evaluate some basic control strategies and an advanced control strategy. Basic control strategies evaluated are: (i) splitting of the influent flow between the aerated compartments, (ii) rate of activated sludge recirculation (*RAS*) and (iii) rate of activated sludge wasted (*WAS*). The main idea behind an advanced control strategy aimed at saving in the sludge disposal costs, and probably in the aeration energy costs by optimising the amount of biomass (*MLSS*) needed in the reactor during the different seasons of the year, will be evaluated here.

8.2 Effect of oxidation ditch horizontal velocity on the nitrogen removal process^{§§}

8.2.1 Abstract

Simulations of oxidation ditch plants are frequently carried out while variations in the horizontal velocity are neglected. However, taking the variations in the horizontal velocity into consideration, it is found that, at non-limiting oxygen concentration, especially the denitrification process is drastically affected by a small change in the horizontal velocity. The study was carried out for a model of an oxidation ditch plant, which has the same volumes and dimensions as a real typical plant. Results of the study were further assessed, using real measurements. The study concluded that to counteract the negative impacts of the horizontal velocity on the nitrogen removal processes, either of the followings can be done: (i) to consider the horizontal velocity as a control variable, from *TN* removal efficiency point of view, or (ii) to decouple the aeration and propulsion functions, for maintaining robust operation of the plant and saving energy, by using air diffusers and flow recirculating pumps (boosters) instead of mechanical aerators.

Keywords: horizontal velocity, oxidation ditch, carousel, modeling, benchmark, control strategies.

Nomenclature

ASM: activated sludge model.
BOD: biological oxygen demand.
COD: chemical oxygen demand.
CSTR: completely stirred tank reactor.
DO: dissolved oxygen, mg/l.
K_La: overall oxygen transfer rate (h⁻¹).
NH₄-N: ammonia nitrogen, mg/l.
NO₃-N: nitrate nitrogen, mg/l.
TKN: total Kjeldahl nitrogen, mg/l.
TN: total nitrogen, mg/l.
TSS: total suspended solids, mg/l.

8.2.2 Introduction

In oxidation ditches, horizontal velocity can vary between 0.25 to 0.60 m/s, with typically values between 0.25 to 0.35 m/s (Metcalf & Eddy, 1991). A minimum velocity of 0.25 m/s is usually required to prevent the organic particles from settling on the channel surface (Fair and Geyer, 1958), whereas the velocity is restricted to a maximum of 0.60 m/s to avoid excessive erosion, hydraulic jump, or other undesirable non-uniform flow phenomena (Babbitt and Baumann, 1958).

^{§§} Submitted to *Wat. Res.* by A. Abusam, K.J. Keesman, H. Spanjers, G. van Straten and K. Meinema

Horizontal velocity in oxidation ditches is principally created by the operation of mechanical aerators. Oxygen input into the ditch depends on (i) number of aerators in operation, (ii) aerator design (diameter and shape of the rotor) and (iii) aerator operational pattern (immersion depth and the rotational speed). For oxidation ditches that are equipped with brush rotors, Stalzer and von der Emde (1972) found that the mean horizontal velocity increases with an increase in the specific energy input (W/m^3), irrespective to the different combinations of rotors to be chosen. Further, variations in the influent flow also affect the horizontal velocity. In simulations, however, this effect is neglected so that the horizontal velocity is frequently assumed to be constant.

Variation of the horizontal velocity in the range of 0.25 to 0.60 m/s (which corresponds to internal recirculation ratios equal to 60 - 120, depending on the reactor dimensions), however, can significantly affect the performance of the ditch. Due to the high internal recirculation rate, significant amounts of nitrate and dissolved oxygen are recirculated from the last compartment to the first compartment. These amounts will obviously affect the *DO* profile along the ditch, and consequently the ditch performance. For reducing the impacts of internal recirculation of nitrate and dissolved oxygen on nitrogen removal processes, Olsson and Newell (1999) suggest that the effluent *DO* should be kept as small as possible.

In the following simulation example, which is based on realistic conditions, we illustrate the effect of both the horizontal velocity and the aeration intensity ($K_L a$) on oxidation ditch nitrogen removal processes. In this study, we have chosen to evaluate the effect by simulation, because evaluation by carrying out practical tests is obviously too expensive or even impossible, due to natural variations in the influent flow. Thus, computer simulations offer a useful approach to solve this problem. In order to help the reader in realizing the real effects of the horizontal velocity, data from real measurements of horizontal velocity variations were also incorporated in assessing the results.

8.2.3 Simulation example

The simulations were carried out for a typical (10^5 p.e.) oxidation ditch plant. Values and sizes were taken from a real plant with the same capacity. Volume of the reactor is 6000 m^3 ($187.5\text{m} \times 8\text{m} \times 4\text{m}$), and volume of the secondary settler is 6000 m^3 . Further, the oxidation ditch has two aerators: one at the inlet port (1st *CSTR*), and the other at the mid-point (6th *CSTR*).

The reactor was modelled as a loop of 10 equal-volume (600 m^3) *CSTR*'s, as suggested by Abusam and Keesman (1999), whereas the non-reactive ten-layer settler model (Takács *et al.*, 1991) was used for modeling the secondary settler. *ASM No. 1* (Henze *et al.*, 1987) was used for modeling the biochemical processes taking place in the reactor.

First, 100-day steady state simulations were carried out. Then, two sets of simulations, in which the horizontal velocity was manipulated using the internal recirculation rate, were

carried out. The influent flow and concentrations used in these simulations were assumed to be constant, i.e. an influent flow of 18446 m³/d with an average biodegradable COD concentration of 300 mg/l and NH₄-N concentration of 30 mg/l. Further information about the composition of the influent and parameter values for ASM No. 1 are given by the European Concerted Action Programme COST 624 on its web site (COST, 2000).

In the first set of simulations, the effect of horizontal velocities: 0.2, 0.3, 0.4, 0.5 and 0.6 m/s on the nitrogen removal processes was investigated at constant K_{La} value in compartment 1 and 6. Thus ignoring the interdependence between horizontal velocity and K_{La} that can be expected when the aerators act both for aeration and propulsion. By trial and error, K_{La} was adjusted to give about 2 mg DO/l in the aerated compartments; at the nominal velocity of 0.3 m/s. Results of this simulation are shown in Fig. 1 and 2. In the second set of simulations, the effect of varying simultaneously the horizontal velocity and K_{La} on TN removal was studied (see Fig. 3 and 4).

As can be seen from Fig. 1, a change in the horizontal velocity, while keeping K_{La} constant, significantly affects the DO profile. With high speed, the DO profile becomes more flat. It is important to note that DO concentration in the effluent increases with the increase in the horizontal velocity. Consequently, both the nitrification and denitrification processes will be affected (see Fig. 2). Nitrification and denitrification simultaneously take place in the alternating zones of aerobic and anoxic conditions that exist along the ditch. Fig. 2 also shows that the impact on the denitrification process, in terms of mg N converted, is higher than that on the nitrification process. It is apparent that at high horizontal velocities, the rate of nitrate removal is lower than the rate of ammonia removal. Thus leading to high TN concentration in the effluent, at high horizontal velocity.

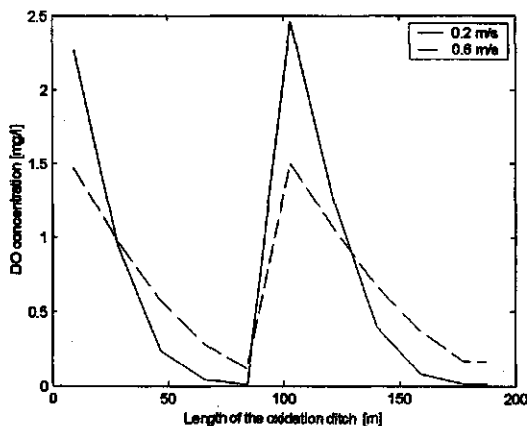


Fig. 1, Effect of horizontal velocity on DO profile: K_{La} in the aerated compartment is 28.3 h⁻¹, effluent port is 187.5 m away from the inlet port (first aerator).

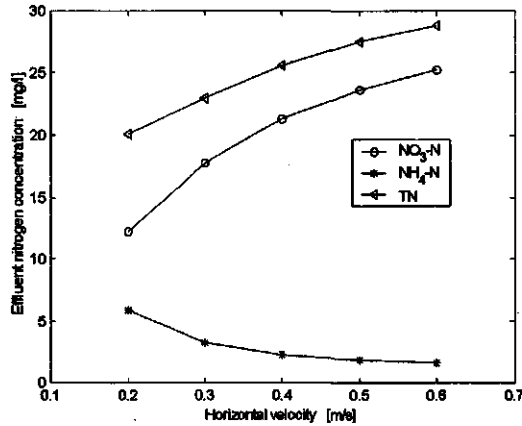


Fig. 2, Effect of horizontal velocity on the nitrogen removal processes: nominal velocity is 0.3 m/s.

Fig. 3 depicts the contour plot of the effect of both aeration intensity ($K_L a$) in *CSTR* 1 and 6 and the horizontal velocity on the *TN* removal efficiency (%). As it can be seen from this figure, at high aeration, the horizontal velocity has significant effect on the *TN* removal. When the oxygen input into the system is not enough, it is well known that *N* removal will be very poor. Thus, as expected, Fig. 3 shows no effect for the horizontal velocity when the aeration intensity ($K_L a$) is inadequate.

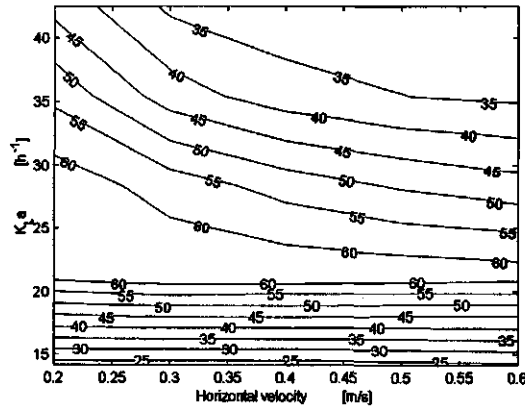


Fig. 3, Effect of $K_L a$ and horizontal velocity on *TN* removal efficiency (%).

Fig. 4 shows that the effect of the horizontal velocity on the effluent quality fines is the same as the effect on *TN* removal. As can be seen from this figure, at excess aeration, the horizontal velocity has a substantial effect on the effluent quality fines to be paid.

Effluent fines are based on the effluent quality index (EQ), which is the weighted sum of the effluent components (COD , BOD , NO_3-N , TKN and TSS) that have major influence on the receiving water. For more information about the effluent quality index and effluent quality fines see *COST* (2000). Note that 30 Euro per kg/d effluent load is used in computing effluent fines presented in Fig. 4.

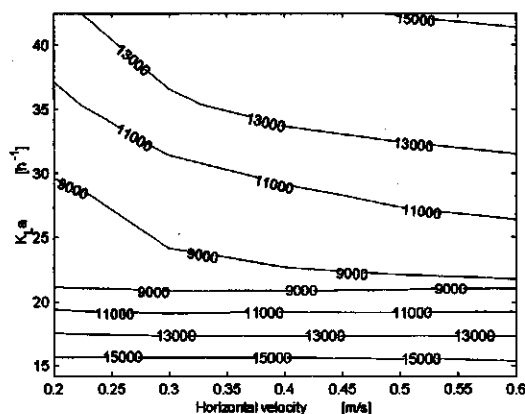


Fig. 4. Effect of K_{La} and horizontal velocity on effluent quality fines (Euro/d), calculated at 30 Euro per kg/d of pollution load.

8.2.4 Practical assessment

In order to help the reader visualize the effect of the horizontal velocity, in conjunction with concurrent changes in K_{La} , we have used some real measurements for the horizontal velocity (DHV Water, 1986a) in this study. These measurements were obtained from a full-scale oxidation ditch that has almost the same capacity, dimensions (210m x 8m x 4m deep) and position of the aerators, as the hypothetical oxidation ditch. Furthermore, it is equipped with two Landy-F type mechanical aerators. The rotor diameter of these aerators is 3.15 m. Horizontal velocity measurements were carried out at various combinations of rotor speed (33.5, 25.1 or 0.0 rpm) and immersion depths (-20.8, -10.0, 0.0, +10.0, +13.0 and 15.0 cm). Electrical energy consumption (kW) was also measured. Data of horizontal velocity and the electrical energy consumption are obtained at various operating conditions for the aerators. From the energy consumption, we have calculated K_{La} using the reported average aeration efficiency of 2.2 kg O_2 /kWh (DHV Water, 1986b). Fig. 5 presents the calculated K_{La} versus the measured horizontal velocity plotted on top of Fig. 3 (the contour plot of TN removal efficiency). The dashed lines roughly indicate the working area for these aerators in terms of horizontal velocity and K_{La} . Fig. 5 clearly shows that only few combinations of horizontal velocity and K_{La} allows the oxidation ditch to work at high TN removal efficiency. In agreement with the findings of Gillot *et al.* (2000), Fig. 5 also shows that oxygen input increases as horizontal velocity increases.

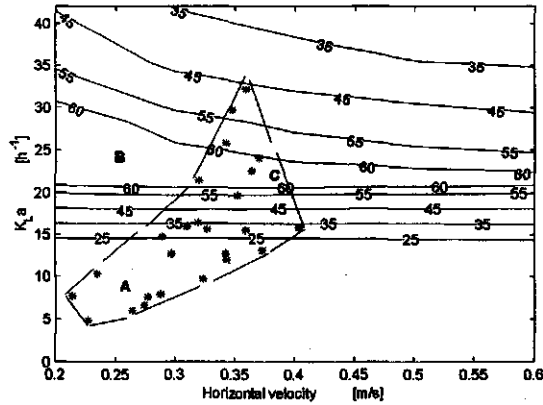


Fig. 5, Real velocity measurements plotted on top the contour of TN removal efficiency (%)

Thus, it is clear that the relationship between the oxygen input and the horizontal velocity should be taken into consideration when optimising the performance of an oxidation ditch for achieving a maximum *TN* removal efficiency. As a matter of fact, this requires that the relationship between oxygen input and horizontal velocity, on the one hand, and aerator operating conditions (speed and immersion depth), on the other hand, should be found first.

Impacts of horizontal velocity variations on nitrogen removal processes can be taken care of either by (i) considering the horizontal velocity as a control variable, from *TN* removal efficiency point of view, or by (ii) decoupling the effects of horizontal velocity and oxygen input, in order to maintain a robust operation of the plant and to save some energy. From Fig. 5, it can be seen that the plant is more robust to K_{La} variations at low horizontal velocity (point B) than at high horizontal velocity (point C). In fact, by decoupling, it would be possible to operate the plant in this robust region (moving from point A to point B). In contrast, high removal efficiency can also be achieved by increasing the aerator speed to e.g. point C, but, in this case, the plant would be working in less robust region.

Decoupling of the horizontal velocity and the oxygen input (K_{La}) can be achieved by using air diffusers and flow recirculating pumps (boosters) instead of the mechanical aerators, as in the conventional activated sludge systems. With such arrangements, the horizontal velocity can be kept at a value that prevents settling of organic particles and minimizes the negative effects of the recirculated nitrate and *DO*, based on *TN* removal efficiency, while the oxygen input can independently be varied according to the system needs. However, practical studies are needed to investigate the feasibility of this proposed solution.

8.2.5 Conclusions

Because of the significant impact on the nitrogen removal processes, changes in oxidation ditch horizontal velocity should be taken into account when maximizing the TN removal efficiency. To maintain robust operation of the plant and save energy, a solution will be to decouple the effects of horizontal velocity and oxygen input, by using air diffusers and flow recirculating pumps (boosters) instead of the mechanical aerators. However, feasibility of this solution needs further investigations.

8.2.6 References

Abusam, A. and K.J. Keesman (1999), Effect of number of CSTR's on the modeling of oxidation ditches: steady state and dynamic analysis, *Med. Fac. Landbouw. Univ. Gent*, 64/5a, pp 91-94.

Babbitt, H.E. and E.R. Baumann (1958), *Sewerage and sewage treatment*, 8th ed, John Wiley & Sons, Inc.

COST (2000), www.ensic.u-nancy.fr/COSTWWTP/Benchmark/Benchmark1.htm.

DHV Water (1986a), Flow velocity measurements in the carousel of the sewage treatment plant Al Hasa (Saudi Arabia).

DHV Water (1986b), Measurements of oxygen transfer capacity of the aeration system of the sewage treatment plant Al Hasa (Saudi Arabia).

Fair, G.M. and J.C. Geyer, (1958), *Elements of water supply and wastewater disposal*, 5th ed, John Wiley & Sons, Inc.

Henze, M., C.P.L. Grady, jr, W. Gujer, G. van R. Marais and T. Matsuo (1987), *Activated sludge model no. 1*, IAWQ scientific and Technical Report no. 1, IAWQ, London, U.K.

Gillot, S., S. Capela and A. Heduit (2000), Effect of horizontal flow on oxygen transfer in clean water and in clean water with surfactants, *Wat. Res.* 34(2):678-683.

Metcalf & Eddy (1991), *Wastewater engineering: treatment, disposal and reuse*, 3rd ed, McGraw-Hill.

Olsson, G. and B. Newell (1999), *Wastewater treatment systems: modeling, control and diagnosis*, IWA Publishing.

Stalzer, W. and W. von der Emde (1972), Tanks with turbulent flow generated by mammoth rotors, *Wat. Res.* 6:417-421.

Takács, I., G.G. Patry and D. Nolasco (1991), A dynamic model of the clarification-thickening process, *Wat. Res.* 25(10):1263-1271.

8.3 Evaluation of control strategies using an oxidation ditch benchmark^{***}

8.3.1 Abstract

This paper presents validation and implementation results of a benchmark developed for a specific full-scale oxidation ditch wastewater treatment plant. A benchmark is a standard simulation procedure that can be used as a tool in evaluating various control strategies proposed for wastewater treatment plants. It is based on model and performance criteria development. Testing of this benchmark, by comparing benchmark predictions to real measurements of the electrical energy consumptions and amounts of disposed sludge for a specific oxidation ditch WWTP, has shown that it can (reasonably) be used for evaluating the performance of this WWTP. Subsequently, the validated benchmark was then used in evaluating some basic and advanced control strategies. Some of the interesting results obtained are the following: (i) influent flow splitting ratio, between the first and the fourth aerated compartments of the ditch, has no significant effect on the TN concentrations in the effluent, and (ii) for evaluation of long-term control strategies, future benchmarks need to be able to assess settlers' performance.

Keywords: oxidation ditch, carousel, modeling, benchmark, control strategies.

8.3.2 Introduction

In the last few decades, the public has become more aware about the causes of the increasing pollution problems in receiving waters. This has led to enforcements of very strict standards for the effluents of wastewater treatment plants (*WWTP*) (EC, 1999; UNEP, 1999). For achieving these strict standards, at minimum costs, numerous control strategies have been proposed for use in controlling the performance of *WWTP*'s (Lindberg, 1997; Lukasse, 1999; Singman, 1999; Weijers, 2000). However, a thorough evaluation of these control strategies by carrying out experimental works is obviously not possible. Wastewater treatment processes are very complex processes that are subject to large disturbances in influent load and composition. Furthermore, it is practically not possible to prevent the effect of the rapidly changing environmental conditions surrounding these processes. Therefore, computer simulations offer a useful approach to solve this problem.

Recently, Keesman *et al.*, (1997) and Spanjers *et al.*, (1997) have pointed out the need for a rigorous methodology (benchmarking) for evaluating and comparing the numerous control strategies proposed for *WWTP*'s. The idea to produce a standardised simulation benchmark, as a tool for evaluating the performance of activated sludge *WWTP*'s, was

^{***}Will be presented at the 1st IWA Conf. on IAC and Sensors, Malmö, Sweden, 3-7 June 2001, by A. Abusam, K.J. Keesman, H. Spanjers, G. van Straten and K.Meinema.

then developed further by the IWA Task Group on Respirometry together with the European Co-operation in the field of Scientific and Technical Research (COST) 682/624 (Copp, 2000). The COST Group defines the benchmark as "A protocol to obtain a measure of performance of control strategies for activated sludge plants based on numerical, realistic simulations of the controlled plant". According to this definition, the benchmark will be consisting of a description of the plant layout, a simulation model and definitions of (controller) performance criteria.

The purpose of this paper is to validate and demonstrate the implementation of a benchmark developed for a full-scale oxidation ditch WWTP located in Rotterdam, The Netherlands. The paper layout is as follows. In the next section, a brief description of the various components of the benchmark will be given. Then the benchmark will be validated using real data. In section 3, implementation of the benchmark will be demonstrated by evaluating three basic and one advanced control strategies. Finally, conclusions will be presented in section 4.

8.3.3 Benchmarking a specific WWTP

8.3.3.1 Plant layout

The WWTP studied here is a 300 000 p.e. carousel located in Rotterdam, The Netherlands. This plant consists of two main parallel treatment lines. Each line has two primary settlers, one selector, one carousel (406.25m x 8m x 4m deep), and three circular secondary settlers (each has a diameter = 52.9 m and side wall depth = 2 m). Each carousel has four surface aerators. About 67% of the combined effluent flow of the two primary settlers is directed to the first aerated compartment and the rest to the fourth aerated compartment.

8.3.3.2 Model development and validation

A single treatment line was modeled as a reactor (carousel) plus a secondary settler. Reactor hydraulics were approximated by a loop-of-equal CSTR's, biochemical processes were modeled by the activated sludge model (ASM) No.1 (Henze *et al.*, 1987), whereas the secondary settler was modeled as a 10-layers non-reactive settler, according to Takács *et al.* (1991). As suggested by Abusam and Keesman (1999), 10 CSTR's were used in modeling the reactor.

This model was previously calibrated for data obtained at constant water temperature of 22 °C, in July-August 1992 (see Abusam *et al.*, 2000a). In the calibration, values of the following three parameters were optimized: the aeration constant ($k = K_L a \cdot V_A$), η_S and η_b . To validate this previously calibrated model with data obtained at a different season of the year (January-February 1993), however, recalibration of the parameters for the effect of temperature was needed. In the recalibration stage, kinetic parameters and

oxygen transfer rate were made dependent on water temperature, using the Arrhenius relationship (Eqn. 1).

$$r_T = r_{20} \theta^{(T-20)} \quad (1)$$

where θ is the temperature-activity coefficient to be calibrated, and r_T is reaction rate at T °C. Following Weijers (2000), only some kinetic parameters were optimized for the effect of temperature, whereas the rest of the kinetic parameters were assigned the default value of $\theta = 1.04$ suggested by Metcalf & Eddy (1991). Kinetic parameters, which were optimized, were divided into the following three groups: (i) μ_H , b_H , k_H , K_X and k_A (ii) μ_A and b_A and (iii) K_{NH} . Each group was assigned the same temperature coefficient. Rate of oxygen transfer (here $k = K_L a \cdot V_A$) was also made temperature dependent. Thus, values of four temperature coefficients were optimized, using the data obtained for January 1993, during which water temperature ranged from 11.4 to 12.1 °C (Schieland, 1994). Optimum temperature coefficients (θ) obtained for the three groups of kinetic parameters and the oxygen transfer rate were found to be: 1.0, 1.08, 1.08 and 1.0179, respectively. Using parameter values obtained in the recalibration stage, the model was then verified by the data collected in February 1993 (Schieland, 1994).

Fig. 1 shows the recalibration results, whereas Fig. 2 presents the validation results. From these figures, it is clear that the recalibrated model describes reasonably the system behavior. However, it is also apparent that system dynamics are not very well predicted, especially in the first half of the test period. Furthermore, the residues are not randomly distributed; hence the model may not have the content needed to describe the finer details. Nonetheless, the model predictions are acceptable enough to be used for evaluating integrated performance indices as described in the next section.

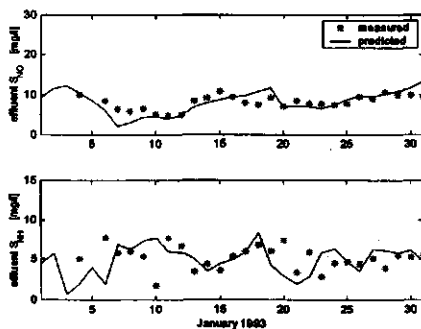


Fig. 1, Results of model recalibration for temperature effects

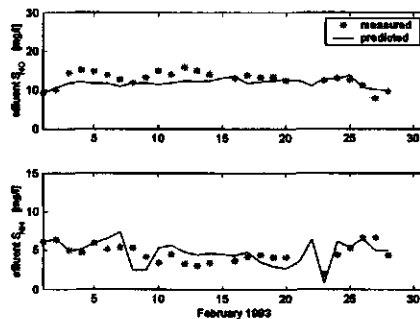


Fig. 2, Results of model validation

8.3.3.3 Performance criteria

The performance criteria developed for this oxidation ditch benchmark are more or less the same as those proposed by *COST* and *IWA* Working Groups (see *COST*, 2000). Exceptions are the necessary modifications made in the energy equations. Oxidation ditches often use mechanical aerators, which are different from air diffusers used in conventional activated sludge systems. Furthermore, in oxidation ditches there are no special pumps used for internal recirculation, as the mechanical aerators themselves perform this task. Therefore, the equations for *AE* (aeration energy index, kWh/d) and *PE* (pumping energy index, kWh/d) were modified. For more about the modification made in the performance indices see *Abusam et al.*, (2001).

8.3.3.4 Testing of the benchmark

In validating the benchmark, real measurements of *AE* and *DS* (disposed sludge index, kg/d) were compared with the benchmark predictions (Fig. 3). Note that values reported in this figure are for the whole treatment plant (i.e. the two treatment lines). As can be seen, the benchmark prediction of both *AE* and *DS*, is generally acceptable. Deviation of benchmark predictions from the real measurements is, on average, less than 10 per cent. The relatively poor fit obtained during the first 10 days can be attributed to low initial biomass concentrations. Except in these 10 days, changes in the performance indices seem to be predicted fairly well by the benchmark. It should be noted, however, that the natural variations in the observed data is too limited to allow for a more thorough validation.

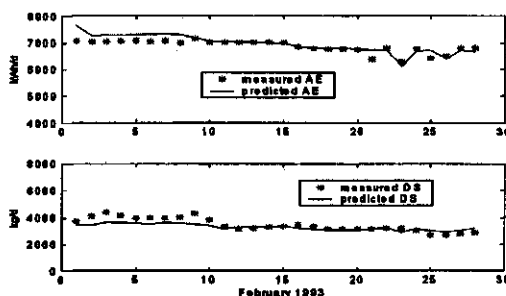


Fig. 3, Results of the benchmark validation.

8.3.4 Implementation of the benchmark

The procedure for evaluating the short-term control strategies was the following. First, a 100-day steady-state simulation was conducted to determine the initial conditions. Secondly, dynamic simulations were performed using three scaled weather files (dry, rain and storm weather). That is, weather files proposed by *COST* were scaled up to suit this particular plant. Thirdly, the outputs of the last seven days were used to assess: (i) violation of effluent constraints and (ii) effluent quality costs, which is expressed in terms of performance indices. Finally, the performance indices were expressed in monetary terms (Euros). Because the long-term control strategy was evaluated over the whole year,

the steps two (use of weather files) and three (evaluation over seven days) of the procedure described above were skipped in the long-term evaluation.

8.3.4.1 Evaluation of the short-term control strategies

8.3.4.1.1 Control strategy No. 1: Splitting of the influent flow

In each treatment line of the *WWTP*, effluent flows of the two primary settlers are usually combined in one stream, which is then divided between the first and the fourth aerated compartments of the oxidation ditch. Usually about 67% of the ditch influent is directed towards the first aerated compartment, while about 33% is taken to the fourth aerated compartment. In order to find the optimum splitting ratio that maximizes *TN* removal, simulations were carried out at splitting ratio ranging from zero to one (Table 1). As this table shows, concentration of *TN* in the effluent is not significantly affected by the change in the splitting ratio. In fact, this is expected, because the whole influent flow represents only a small fraction of the flow that recirculates around the ditch. In oxidation ditches, recirculation flow is usually about 60 – 120 times of the influent flow, depending on the dimensions of the ditch. Thus, regarding the concentration of the effluent *TN*, the ratio of splitting the influent flow between the first and the fourth aerated compartments makes no difference. However, by not joining the effluent flows of the two primary settlers, some saving in the design and operational costs can be made, as effluent of primary settlers will no longer be combined in one stream. Thus, the control strategy No. 1 is to operate the *WWTP* at a splitting ratio equal 0.5. That is, effluent of one primary settler is directed to the first aerated compartment, whereas effluent of the other settler is taken to the fourth aerated compartment. Assessment results of this control strategy are reported in Table 2.

Table 1, Effect of splitting the influent flow (Q_s) between the first aerator (Q_1) and the fourth aerator (Q_4)

| Q_s / Q_{in} | 0.0 | 0.1 | 0.2 | 0.3 | 0.4 | 0.5 | 0.6 | 0.7 | 0.8 | 0.9 | 1.0 |
|-------------------|-------|-------|-------|-------|-------|-------|-------|-------|-------|-------|-------|
| Average | 10.84 | 10.82 | 10.78 | 10.75 | 10.73 | 10.70 | 10.67 | 10.64 | 10.62 | 10.59 | 10.57 |
| TN_{eff} (mg/l) | | | | | | | | | | | |

8.3.4.1.2 Control strategy No. 2: RAS

Control strategy No. 2 is intended to optimise the recirculated activated sludge (*RAS*) with respect to *EQ* and the other performance indices. *RAS* is a ratio of the recirculated amount of sludge to the influent flow. To find the optimum value of *RAS*, the plant was simulated for different values of *RAS* (0:0.1:1.0). Fig. 4 shows the effect of *RAS* on the performance indices, which are reported in Euro. From this figure it can be seen that the costs of the pumping energy

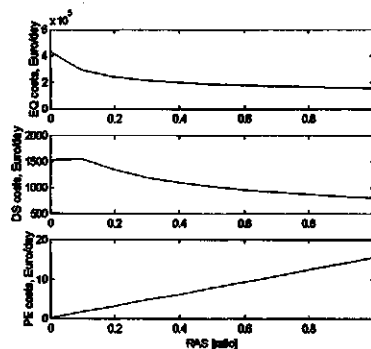


Fig. 4, Effect of *RAS* on the performance indices expressed in Euros/d.

(PE) steadily increases with the increase in the RAS ratio, whereas EQ and TSP (total sludge production index, kg/d) decrease, especially beyond RAS equals 0.6, relatively slowly. However Fig. 4 also shows that PE cost is negligible, compared to the costs of EQ or TSP. Thus, it is clear that some operational costs, in terms of EQ and TSP costs, can be saved, when the plant is operated at RAS equal 1. This control strategy was then implemented as the control strategy No. 2. As before, evaluation results are reported in Table 2.

8.3.4.1.3 Control strategy No. 3: Aeration pattern

Fig. 5 depicts the fixed OFF-ON aeration patterns during the calibration period, July-August 1992 (DHV Water, 1993). From a first glance at this figure, it may seem that complete shutdown of the aerator No. 4 is possible.

Fig. 5 shows that the first and the second aerators work at full capacity all the day, whereas the third and fourth aerators work at low capacity all the day. In fact, the fourth aerator works only few hours a day. Therefore, it was decided to shutdown completely the aerator No. 4, and to find a new operational pattern for the aerator No. 3 that is equivalent to both the operational pattern of the third and fourth aerators, with respect to amount of oxygen needed for maximum TN removal. To develop the operational pattern of the aerator No. 3, it was assumed that ammonia concentrations in the effluent should be between optimum bounds that maximize TN removal (see also Lukasse *et al.*, 1999). Optimum ammonia bounds were found to be equal to 1.2 and 2.25, which were used in finding out the operating pattern of the aerator No. 3. Then, the control strategy No. 3 was implemented. As before, assessment results are reported in Table 2.

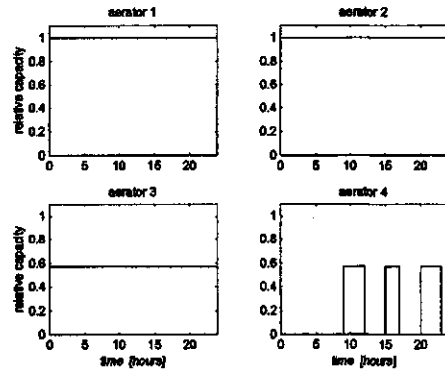


Fig. 5, Operational patterns for the four aerators in July-August 1992 (DHV Water 1993)

Table 2 summarizes the results obtained from implementing the three short-term control strategies, and compared that to the real performance of the treatment plant (reference performance). As can be seen, in general, all the performance indices and percent time of violations for the implemented control strategies are almost the same as that for the reference performance of the plant. An exception is the saving in the cost of AE (about 100 Euro/d) that can be made, when implementing the control strategy No. 3. However, it is highly uncertain that this saving in AE costs can really be made. This because that in a previous study (Abusam *et al.*, 2000b) we have found that due to uncertainty in the parameter values, deviation of the performance from the nominal values can reach +473%, -64%, +544% and +64% for indices EQ, AE, TSP and DS, respectively.

However, here should be clear that our intention was not to develop new control strategies, but rather to demonstrate the use of the benchmark.

8.3.4.2 Evaluation of a long-term control strategy

As an example of the applicability of the benchmark methodology to evaluate a long-term control strategy, the control scheme proposed by Lukasse (1999), for yearly average *TN* control (see Fig. 6) was partly implemented. The main idea behind this proposed control strategy is that saving can be made in the costs of the *DS* and probably in the costs of *AE*, by optimising the amount of biomass (*MLSS*) needed during the different seasons of the year. It is well known that biomass activity depends on the seasonal change in water temperature. In order to meet the yearly *TN* standard for the effluent, at minimum costs, Lukasse (1999) suggests to manipulate *MLSS* according to the seasonal needs.

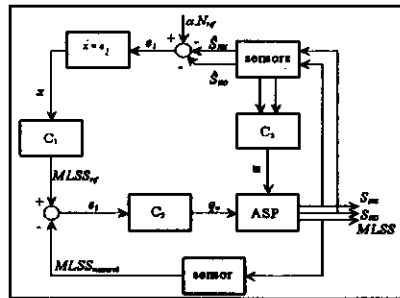


Fig. 6, Feedback control loop for yearly-averaged *TN* control (Lukasse, 1999)

Lukasse's control strategy was implemented without the controller C_3 , because the interest was in the long-term effects only. In stead, the fixed ON-OFF patterns of the aerators (Fig. 5), was used. The Ziegler and Nichols method was used in designing the controller C_1 , as P controller, and the controller C_2 , as PI controller. For comparison, performance data with the existing strategy were obtained from the same full-scale oxidation ditch plant for the whole year of 1993 (Schieland, 1994). Because there was no information about the actual aeration, it was assumed that the fixed OFF-ON pattern for the calibration period in 1992 (see Fig. 5) was also applied in 1993.

Fig. 7 presents effluent *TN* concentrations, over the whole year, whereas Fig. 8 presents both *MLSS* concentrations and *WAS* rates that are needed for achieving about 9 mg/l yearly average *TN*. Table 5 compares the results obtained from implementing the control strategy proposed by Lukasse (1999) to the real performance. Note that here all sensors were assumed to be perfect (i.e. sensor dynamics and time delays were neglected).

Table 2, Short-term assessment of three basic control strategies.

| Index | Reference: Splitting = 0.67; RAS=1 Aeration (Fig. 5) | Strategy No. 1: Splitting ratio = 0.50; RAS=1 | | | Strategy No. 2: Splitting ratio = 0.67; RAS=1 | | | Strategy No. 3: Splitting ratio = 0.67; RAS=1 | | |
|----------------------|---------------------------------------------------------------|--------------------------------------------------|---------------|----------------|--------------------------------------------------|---------------|----------------|--------------------------------------------------|---------------|----------------|
| | | Dry weather | Rainy weather | Stormy weather | Dry weather | Rainy weather | Stormy weather | Dry weather | Rainy weather | Stormy weather |
| EQ [kg/d] | 5149 | 4331 | 5805 | 4865 | 4364 | 5832 | 4896 | 4444 | 5757 | 4998 |
| AE [kWb/d] | 7110 | 8001 | 8011 | 8026 | 8013 | 8021 | 8037 | 6582 | 6629 | 6608 |
| PE [kWb/d] | 251 | 250 | 341 | 291 | 250 | 341 | 291 | 250 | 341 | 291 |
| DS [kg/d] | 1401 | 2284 | 2717 | 2691 | 2294 | 2727 | 2702 | 2534 | 3024 | 2969 |
| EQ costs [Euro/d] | 154470 | 129930 | 174160 | 145950 | 130930 | 174960 | 146880 | 140740 | 176840 | 156430 |
| AE costs [Euro/d] | 512 | 580 | 580 | 580 | 580 | 580 | 580 | 480 | 480 | 480 |
| PE costs [Euro/d] | 18 | 18 | 25 | 21 | 18 | 24.6 | 21 | 18 | 24.6 | 21 |
| DS costs [Euro/d] | 813 | 1325 | 1576 | 1561 | 1331 | 1582 | 1567 | 1555 | 1842 | 1817 |
| % Time of violations | S_{NH} | 18.0 | 24.3 | 19.6 | 18.0 | 23.7 | 19.2 | 17.3 | 22.3 | 18.6 |
| | TN | 0 | 0 | 0 | 0 | 0 | 0 | 0 | 0 | 0 |
| | BOD ₅ | 0 | 0 | 0 | 0 | 0 | 0 | 0 | 0 | 0 |
| | COD | 0 | 0 | 0 | 0 | 0 | 0 | 0 | 0 | 0 |
| | TSS | 0 | 0 | 0 | 0 | 0 | 0 | 0 | 0 | 0 |

Effluent constraints are 4, 18, 25, 125 and 30 for NH_4-N , TN, BOD₅, COD and TSS, respectively.
 Indicative unit price: for EQ is 30 Euro/kg; for AE and PE is 0.072 Euro/kWh; and for DS is 0.58 Euro/kg.
 Aeration pattern for control strategies 1 and 2 is presented in Fig. 5, whereas for strategy 3 bounds of 1.2-2.25 for effluent ammonia were used.

As can be seen from Fig. 7, the yearly average $S_{NH^+}S_{NO}$ of 9 mg/l was met. However, Fig. 8 shows this was met by keeping MLSS at high values (> 6000 mg/l), all through the first half of the year. With high MLSS concentrations for such a long time, however, outside the validity range of the model, the settler might not function properly. However, evaluation of the settler performance is beyond the scope of this benchmark.

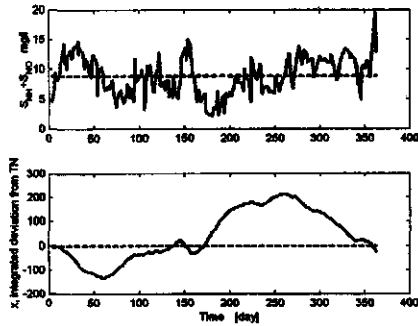


Fig. 7, Profile of effluent TN obtained by Lukasse (1999) scheme, with $\alpha N_{Tq} = 9$ mg/l.

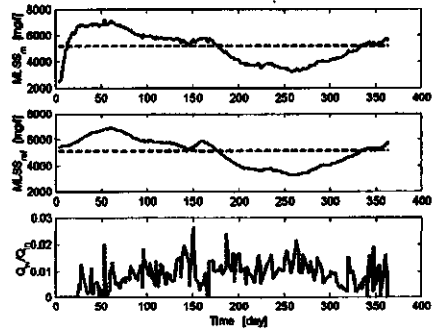


Fig. 8, Profile of effluent MLSS and WAS as obtained for the control strategy proposed by Lukasse (1999).

From the comparison presented in Table 5, it is clear that a substantial reduction in the costs of DS (about 2500 Euro/day) can be achieved using Lukasse's control strategy. However, the same table shows that no savings can be made in the costs of AE . But this is expected since the controller C_3 was not implemented. Also the relatively long time of violation of the NH_4-N constraints (see Table 5) can be attributed to the fact C_3 was not implemented. However, Table 5 also shows that Lukasse's control strategy reduces TN violation time. In short, Lukasse's control strategy seems to be very promising.

Table 5, Results of implementing a simplified version of Lukasse (1999) control scheme in comparison to the existing control scheme

| Control strategy | | Existing strategy | Lukasse's strategy (simplified) |
|---------------------|----------|-------------------|---------------------------------|
| EQ [kg/d] | | 26254 | 20832 |
| AE [kWh/d] | | 13672 | 14332 |
| DS [kg/d] | | 7530 | 4680 |
| EQ costs [Euro/d] | | 787620 | 624960 |
| AE costs [Euro/d] | | 984 | 1032 |
| DS costs [Euro/d] | | 4367 | 2714 |
| Violation time (%) | NH_4-N | 50.9 | 89.2 |
| | TN | 8.6 | 0.5 |

8.3.4 Conclusions

A benchmark was developed for a specific full-scale oxidation ditch WWTP. Testing showed that the benchmark could reasonably be used for evaluating the performance of this WWTP. Implementation of the benchmark was demonstrated through evaluation of some short- and long-term control strategies. Some of the interesting results obtained from this evaluation are the following: (i) influent flow splitting ratio, between the first and the fourth aerators of the ditch, had no significant effect on the TN concentrations in the effluent, (ii) RAS needed to be kept at maximum, (i.e. $RAS = 1$), and (iii) for the evaluation of the long-term control strategies, future benchmarks need to be able to assess settlers' performance.

8.3.5 References

Abusam, A. and K.J. Keesman (1999), Effect of number of CSTR's on the modelling of oxidation ditches: steady state and dynamic analysis, Med. Fac. Landbouw. Univ. Gent, 64/5a, pp 91-94.

Abusam A., K.J. Keesman, G. van Straten, H. Spanjers and K. Meinema (2000a), Parameter estimation procedure for complex non-linear systems: calibration of ASM No.1 for N-removal in a full-scale oxidation ditch, in Proc. of the Watermatex2000, Gent, Belgium (2000).

Abusam, A., K.J. Keesman, G. van Straten and K. Meinema (2001), Sensitivity analysis on oxidation ditches: the effect of variations in stoichiometric, kinetic and operating parameters on the performance indices, J. Chem. Tech. Biotech 76(4):430-438.

Abusam, A., K.J. Keesman, G. van Straten and K. Meinema (2000b), Estimation of uncertainties in the performance indices of an oxidation ditch benchmark, J. Chem. Tech. Biotech (submitted).

Copp, J.B., (2000), Defining a simulation benchmark for control strategies, Water21, 1(1):44-49.

COST (2000), www.ensic.u-nancy.fr/COSTWWTP/Benchmark/Benchmark1.htm.

DHV Water (1993), DHV Water bv, Dossier G8112-10-001, Amersfoort, The Netherlands, (in Dutch).

EC (1999), Implementation of Council Directive 91/271/EEC of 21 May 1991 concerning urban waste water treatment, as amended by Commission Directive 98/15/EC of 27 February 1998: summary of the measures implemented by the member states and assessment of the information received pursuant to article 17 and 13 of the Directive,

European Commission, Office for Official Publications of the European Communities, Luxembourg.

Henze, M., C.P.L. Grady, jr, W. Gujer, G. van R. Marais and T. Matsuo (1987), Activated sludge model no. 1, IAWQ scientific and Technical Report no. 1, IAWQ, London, U.K.

Keesman, K.J., H. Spanjers, P. Vanrolleghem, and J. Alex (1997), Benchmarks for control strategies in activated sludge plants, TMR Research Proposal No. ERB4061PL970020, Wageningen, The Netherlands.

Lindberg, C-F. (1997), Control and estimation strategies applied to the activated sludge process, Ph.D. thesis, Uppsala University, Sweden.

Lukasse (1999), Control and identification in activated sludge processes, Ph.D. thesis, Wageningen University, The Netherlands.

Lukasse, L.J.S. K.J. Keesman, A. Klapwijk and G. van straten (1999), A comparison of NH_4/NO_3 control strategies for alternating activated sludge processes, *Wat. Sci. Tech* 39(4):93-102

Metcalf & Eddy (1991), Wastewater engineering: treatment, disposal and reuse, 3rd ed, McGraw-Hill.

Schieland (1994), Hoogheemraadschap van Schieland , Procestecnologische gegevens: water en sliblijn, G25.2-32537, Rotterdam, The Netherlands, (in Dutch).

Spanjers, H., Vanrolleghem, P.A. Nguyen, K., Vanhooren, H., and Patry, G.G. (1997). Towards a simulation-benchmark for evaluating respirometry-based control strategies, *Wat. Sci. Tech.*, 37(12):219-226.

Singman, J. (1999), Efficient control of wastewater treatment plants – a benchmark study, M.Sc. thesis, Uppsala University, Sweden.

Takács, I., G.G. Patry and D. Nolasco (1991). A dynamic model of the clarification - thickening process, *Wat. Res.* 25(10):1263-71.

UNEP (1999), Global environment outlook 2000, United Nations Environment Programme, Earthscan Publication Ltd, London.

Weijers, S. (2000), Modelling, identification and control of activated sludge plants for nitrogen removal, Ph.D. Thesis, Eindhoven University of Technology, The Netherlands.

9. General discussion and conclusions

9.1 Discussion

The aim of this thesis is to propose a benchmarking methodology that can be used in evaluating and comparing the various control strategies proposed for oxidation ditch WWTP's. Each chapter in the thesis is individually discussed and evaluated. So here we discuss the whole work with focus on the practical applicability of the proposed methodology.

The benchmarking methodology proposed here (chapter 7) can be used to assess the performance of individual oxidation ditch WWTP's, based on real design and operational data. In contrast, the benchmark proposed by both COST 624 and the IWA Respirometry Task Group is for a typical WWTP, which is assumed to have typical design values and to be subject to typical influent flows. The approach taken in this thesis does not yield a specific or just one generic oxidation ditch model. Instead, the benchmarking procedure consists of a set of well-defined steps that lead in a systematic way to a simulation tool and standardized performance measures that can be used to judge the performance of the proposed scheme of operation and control.

With respect to individual WWTP's, the benchmarking procedure proposed here is more realistic, because it takes into account the very specific design and operational characteristics of the plant that will be benchmarked. An additional advantage over the "one-typical-plant" approach is that the procedure can be applied to various WWTP designs in order to compare their performance.

The proposed benchmarking methodology is developed in the Matlab/Simulink environment. The main reasons for choosing Matlab/Simulink were: (i) flexibility of Matlab/Simulink for future developments, which means possibility of addition of more details without changing the main structure, (ii) Matlab is easy to program and to understand, and (iii) Matlab is an extensive calculation tool. However, the benchmarking methodology proposed here does not rely on any simulation tool, and therefore can be applied using other simulation platforms such as Simba, GPS-X, WEST, STOAT, or FORTRAN code.

Among the various models used for oxidation ditches, we have decided to base the benchmarking methodology on the loop-of-CSTR's model, without back-flows. The reasons for that are the following: (i) it is simple, (ii) it can adequately describe the input-output behavior of the oxidation ditch, (iii) it can easily be used in controller design, and (iv) available simulation packages are based on models with a finite number of states. For other types of models, e.g. the 3D advection-dispersion model, a whole new methodology would have to be developed. However, the procedure, as outlined in section 7.3, would remain the same.

The CSTR model is developed under the assumption that C-oxidation and nitrification take place in the aerated zones, whereas denitrification occurs in the anoxic zones. For

the aerated and anoxic zones, *ASM No. 1* is used to describe biochemical processes that take place in these zones. This approach of modeling the nitrification and denitrification processes in oxidation ditch is based on the assumption that nitrification occurs in the aerated zones whereas denitrification occurs in the anoxic zones. However, due to the short travel time (few minutes) bacteria rapidly shift from aerobic to anoxic zones. For this reason, some researchers argue that nitrification and denitrification simultaneously occur in the aerobic and anoxic microzones within the biological floc, respectively (chapter 1). Although this is absent from *ASM No. 1*, it could well explain some of the discrepancies between model and data.

In chapter 4 (model calibration), the response surface methodology (*RSM*) is used, prior to iterative non-linear least-square estimation. *RSM* has the following advantages: (i) it is a straightforward approximate calibration method, and (ii) it can be used for problems with a multi-objective criterion function. In chapter 4, it is used successfully for simultaneous calibration of effluent ammonia and nitrate. Especially here, it also proved to be useful in providing good initial parameter values for the formal least-square estimation step, and in selecting the best identifiable parameters. In fact, in chapter 4, *RSM* is used for selecting the best identifiable parameters among a small number of selected parameters. Future works need to investigate the identifiability of the full *ASM No. 1*, using the *RSM*. However, if the full factorial design is used, the computational time will be the real problem that needs to be solved. Computational time increases exponentially with the increase of number of parameters. Thus, for investigating the identifiability of the full *ASM No.1*, using *RSM*, it is suggested to use the so-called *fractional factorial design* instead of the full factorial design.

In this research work, it is assumed that the actuators work perfectly. That is, dynamics and time delays for these actuators are neglected. *Appendix II* provides only the dynamic models of *DO* and *N* sensors. Furthermore, it can be noted that the effect of possible sensor failures on plant performance was not investigated, although this would be perfectly possible with the model resulting from the benchmarking procedure. In fact, it was not possible to come up with realistic scenarios of failure, as there is no adequate information available in the literature. Thus, to enhance the benchmark, future research needs to address the issues of modeling the actuators and developing standardized and realistic scenarios of failures for both sensors and actuators.

Performance criteria developed here (see *Appendix III*) are more or less the same as those proposed by COST 624 and IWA Respirometry Task Group, except the modifications made in the energy equations (*AE* and *PE*). After the 100-day steady state simulation, the above-mentioned groups have proposed the use of influent files that have a length of 14 days. Due to high sludge age (10-30 days) in oxidation ditches, we think that these 14-days influent files would not be adequate for assessing the performance of oxidation ditches. Hence, we advice potential users of this benchmark to make sure that the length of the influent file they are going to use has a length of 4-5 times the plant sludge age.

The *AE* equation developed here is for a very specific type of aerators, normally Landy-F type of aerators. For other types of aerators, the benchmark user needs to make necessary

adjustments in the *AE* equation (see *Appendix III*), based on manufacturer specifications and real measurements of energy consumption (kWh/d). Of course, field temperatures should be taken into account as well.

In part 2, methodologies suggested for carrying out sensitivity and uncertainty analysis were demonstrated by performing short-term analysis. In fact, for long-term evaluations, these analyses need to be carried out for at least 4-5 times the stabilization period of biomass. However, still the same suggested methodologies could be used in the long-term analysis.

The last step of the benchmarking procedure (chapter 7) is about the selection of the most promising control strategies. In fact, this is not a trivial task and is beyond the scope of this thesis. However, how such selection can be made will briefly be discussed here. A rational approach to be followed in such case is to formulate multi-objective criteria. Obviously, economy (minimum cost) and effluent quality (satisfying the standards) will be part of the criteria. Reliability of the operation and robustness against model uncertainty should also be elements of the criteria. Reliability addresses issues such as how to maintain the plant running and how to avoid process upsets. Examples of process upset are sludge washout, loss of biological activity, too high *MLSS* concentrations and sludge bulking. Of course, there may be some other plant specific objectives that need to be included in such criteria. The plant manager has to decide that. Also the plant manager has to decide how the trade-offs between the various objectives can be carried out.

In section 8.2.5, it is concluded that a change in oxidation ditch horizontal velocity significantly affects the nitrogen removal process. Therefore, a change in oxidation ditch horizontal velocity should be taken into account. However, for the plant benchmarked here, it can be noted that the horizontal velocity is assumed to be constant. The reason for that is the lack of information about the real horizontal velocity. Nonetheless, the benchmark user needs to take the effect of the horizontal velocity into account, by considering the coupling between oxygen input and the horizontal velocity when evaluating any control strategy.

As done in section 8.3.4.2, the benchmark can be used for evaluating long-term control strategies. The benchmark can easily be modified to suit any evaluation period. This can be achieved by adjusting the evaluation period (*T*) to the desired one, and by using appropriate influent files. As suggested above, influent files obtained from the COST website need to be scaled and to be repeated a number of times, according to the sludge age used in the plant, before being used in the simulations.

9.2 General conclusions

In contrast to other benchmarks proposed in literature (e.g. COST 624), the benchmark proposed here uses real data obtained from a specific full-scale WWTP that will be benchmarked. The methodology was developed using available process data obtained from a full-scale WWTP located in Rotterdam, The Netherlands. However, it should be

clear that this plant is not meant to be the reference plant. That is, without referring to this plant, the developed methodology can be used for evaluating the performance of any other specific oxidation ditch plant, using real design, operational and performance characteristics. The step-by-step benchmarking procedure is described in this thesis.

A realistic new simple method that can be used in the estimation of the standard oxygen transfer rate (*SOTR*) is developed. The new method uses the loop-of-*CSTR*'s model, which can easily be incorporated in control algorithms, for modeling the oxidation ditches. It is based on the estimation of the aeration constant k ($= K_L a \cdot V_A$, where V_A is the volume of aerated *CSTR*). Under both clean water measurements and process conditions, the developed method for estimation the *SOTR* proved to be very accurate (specific objective I).

Performance evaluation criteria (specific objective II) have been developed for oxidation ditches. To develop the criteria, necessary changes have been made in the criteria proposed for benchmarking other activated sludge systems by both the COST 624 and IWA Respirometry Task-Group. The main changes made are in the energy equations (aeration energy, *AE*, and pumping energy, *PE*). Furthermore, long-term evaluation criteria have also been developed.

Sensitivity analysis (specific objective III) was conducted for specifying *ASM No. 1* parameters that need special attention from the benchmark user. Short-term results obtained have shown that *ASM No. 1* parameters that need to be accurately estimated are: Y_H , K_S , b_H , k_h , η_p , η_h , K_X , μ_A and K_{NH} . Long-term effects can also be studied using the same procedure used in studying the short-term effects.

Study of the effect of the various sources of uncertainties on the performance indices (specific objective IV) has shown the following short-term effects: (i) the performance indices effluent quality (*EQ*) and total sludge production (*TSP*) have shown to be significantly affected by variations in influent loads and *ASM* parameter values, (ii) effect of model uncertainty on the performance indices seems to be negligible. Similar to the sensitivity analysis, long-term effects can also be studied using the same procedures used in studying the short-term effects.

Real performance measurements of the aeration energy consumed (*AE*) and the disposed amount of sludge (*DS*) were used to test the benchmark (specific objective V). Results of these tests have shown that the benchmark can reasonably used for evaluating the performance of the full-scale WWTP benchmarked here.

Implementation of the benchmark (specific objective VI) is illustrated by using it in the evaluation of some basic and advanced control strategies. The implementation has indicated clearly that, for evaluation of long-term control strategies (section 8.3.4.2), future benchmarks should be able to assess settlers' performance

Finally, the following achievements and novelties characterize the contribution of this thesis:

- In contrast to the benchmarks developed elsewhere, the procedure developed here is directed towards benchmarking oxidation ditch WWTP's.
- The introduction of the benchmarking procedure, without trying to define a generic reference plant, allows benchmarking of any specific oxidation ditch WWTP.
- In comparison to the existing standard methods, a realistic and simple method that can be used in the estimation of the standard oxygen transfer rate (*SOTR*) in oxidation ditches is developed.
- Short-term, as well as long-term, evaluation criteria for the performance of oxidation ditch WWTP's, are developed.
- Development of systematic procedures for parameter estimation and uncertainty assessment.

Appendix I: Activated sludge model (ASM) No. 1

| Component | i | 1 | 2 | 3 | 4 | 5 | 6 | 7 | 8 | 9 | 10 | 11 | 12 | 13 | Process rate, ρ_j |
|------------------------------|------------------------------|-------|------------------|-------|-----------|----------|----------|-------|---------------------------|-----------------|---------------------------|----------|-----------------------|---------------------------------------|------------------------------------------------------------------------------------------------------------------------------------------------------------------------------------------------|
| j | Process | S_j | S_S | X_T | X_S | X_{BH} | X_{BA} | X_P | S_O | S_{NO} | S_{NH} | S_{ND} | X_{ND} | S_{ALK} | |
| 1 | Aerobic growth heterotrophs | | $-\frac{1}{Y_H}$ | | | 1 | | | $-\frac{1-Y_H}{Y_H}$ | | $-i_{XB}$ | | | $-\frac{i_{XB}}{14}$ | $\hat{\mu}_H \left(\frac{S_S}{K_S + S_S} \right) \left(\frac{S_O}{K_{OH} + S_O} \right) X_{BH}$ |
| 2 | Anoxic growth heterotrophs | | $-\frac{1}{Y_H}$ | | | 1 | | | $-\frac{1-Y_H}{2.86Y_H}$ | | $-i_{XB}$ | | | $-\frac{i_{XB}}{14}$ | $\hat{\mu}_H \left(\frac{S_S}{K_S + S_S} \right) \left(\frac{K_{OH}}{K_{OH} + S_O} \right) \times \left(\frac{S_{NO}}{K_{NO} + S_{NO}} \right) \eta_e X_{BH}$ |
| 3 | Aerobic growth autotrophs | | | | | | 1 | | $-\frac{4.57 - Y_A}{Y_A}$ | $\frac{1}{Y_A}$ | $-i_{XB} - \frac{1}{Y_A}$ | | | $-\frac{i_{XB}}{14} - \frac{1}{7Y_A}$ | $\hat{\mu}_A \left(\frac{S_{NH}}{K_{NH} + S_{NH}} \right) \left(\frac{S_O}{K_{OA} + S_O} \right) X_{BA}$ |
| 4 | Decay heterotrophs | | | | $1 - f_P$ | -1 | | f_P | | | | | $i_{XB} - f_P i_{XP}$ | | $b_H X_{BH}$ |
| 5 | Decay autotrophs | | | | $1 - f_P$ | -1 | | f_P | | | | | $i_{XB} - f_P i_{XP}$ | | $b_A X_{BA}$ |
| 6 | Ammonification | | | | | | | | | | 1 | -1 | | $\frac{1}{14}$ | $k_a S_{NO} X_{BH}$ |
| 7 | Hydrolysis organic compounds | | 1 | | -1 | | | | | | | | | | $k_k \frac{X_S / X_{BH}}{K_X + X_S / X_{BH}} \left(\frac{S_O}{K_{OH} + S_O} \right) + \eta_h \left(\frac{K_{OH}}{K_{OH} + S_O} \right) \left(\frac{S_{NO}}{K_{NO} + S_{NO}} \right) X_{BH}$ |
| 8 | Hydrolysis organic N | | | | | | | | | | | 1 | -1 | | $\rho_N \left(\frac{X_{ND}}{X_S} \right)$ |
| $r_j = \sum_i v_{ij} \rho_i$ | | | | | | | | | | | | | | | |
| Conversion rate. | | | | | | | | | | | | | | | |

Appendix II: Modeling of DO and N sensors

1.0 Introduction

Because the main aim of this thesis is to evaluate the performance of nitrogen removing processes in oxidation ditch plants, we have concentrated in modeling only dissolved oxygen (*DO*) and nitrogen (*N*) sensors. Future work needs to address the issue of modeling other types of sensors commonly used in wastewater treatment plants.

1.1 Types and measuring principles:

According to (Gernaey 1997), sensors used for nitrogen removal processes can be divided into three main groups: (i) direct probe (e.g. *DO* probe), which are physical or chemical sensors that have direct contact with the wastewater, (ii) indirect probes (e.g. $NH_4^+ - N$ or $NO_3^- - N$ analysers), which operate close to the measuring point, but the sample is transported to them and (iii) biosensors which have an active biology directly involved in the measurements. Table 1 summaries the techniques used in N-analysers, which are commonly used in WWTP's

Table 1, Working principles and techniques used in the commercially available sensors for use in wastewater treatment processes (source: Thomsen and Kisbye (1996))

| parameter | principle | method |
|-----------|-------------------|--------------------------------------------------------------------------------------------------------------------------------------------------------------------------------------------------------|
| NH_4-N | gas electrode | - ammonia-selective electrode: conversion of NH_4-N to NH_3-N under alkaline conditions. - ammonia-selective electrode: using known addition |
| | colorimetry | - phenate: formation of blue indophenol - nesslerization: conversion of NH_4-N to NH_3-N , formation of a yellow compound |
| NO_3-N | electrode | - Nitrate electrode - ammonia selective electrode: after reduction from nitrate to ammonia |
| | direct photometry | - ultraviolet-spectrophotometric: UV-absorption, no use of reagents |
| | colorimetry | - cadmium reduction: reduction of NO_3-N to NO_2-N with cadmium, formation of a red azo dye - hydrazine reduction: reduction of NO_3-N to NO_2-N with hydrazine, formation of a red azo dye |

1.2 Design characteristics:

Design characteristics of the commercially available sensors differ from one trademark to another. As it can be seen from Table 2 and Table 3, each sensor has different design characteristics. This simply implies that each sensor is unique.

Table 2, Some of the technical specifications given by the supplier for NH_4-N analysers (source: Wacheux *et al.* (1996))

| Manufacturer | Measuring range (mg/l) | Detection limit (mg/l) | Accuracy (%) | Response time (min.) |
|-----------------|------------------------|------------------------|--------------|----------------------|
| ABB Kent Taylor | 0.05-5000 | 0.05 | 3 | 5 |
| Applikon | 0-20000 | 0.10 | 1 | 5 |
| Contronic | 0.01-1000 | 0.01 | 2 | 5 |
| Hydro Environ. | 0-2000 | 0.10 | 2 | 5 |
| STIP | 0-2000 | 0.10 | 2 | 5 |
| Danfoss | 0-5 | --- | 5 | 2 |
| Data Link | 0.05-100 | 0.10 | 5 | 2 |
| Meerestechnik | 0.02-100 | 0.005 | 2 | 15 |
| Skalar | 0.2-10 | 0.025 | 2 | 10 |

Table 3, Some of the technical specifications given by the supplier for NO_3-N analysers (source: Wacheux *et al.* (1993))

| Manufacturer | Measuring range (mg/l) | Detection limit (mg/l) | Accuracy (%) | Response time (min.) |
|----------------|------------------------|------------------------|--------------|----------------------|
| ABB Kent | 0-1100 | 1 | 5 | 4-5 |
| BRAN ET LUBBE | 0-1000 | 0.05 | 3 | 7 |
| Hydro Environ. | 0-200 | 0.1 | 5 | 10 |
| PHOX | 0-100 | 0.05 | 3 | <4 |
| POLY METRON | 0-100 | --- | 4 | 5 |
| PROC. STYRNING | 2-40 | 0.1 | 5 | 15 |
| SERES | 0-22 | 0.1 | 2 | 10 |
| TACUSSEL | 10-1000 | 1 | 5 | 3 |
| SKALAR | 5-100 | 0.01 | 4 | 7 |
| Meerestechnik | 0-100 | 0.1 | 2 | 10 |
| DATA LINK | 0-22.6 | 0.1 | -- | immediate |
| DR LANGE | 0-22.6 | 0.1 | 4 | immediate |

1.3 Operational characteristics:

Few studies have been conducted for evaluating the performance of sensors used in wastewater treatment processes. Among these studies, Kulin *et al.* (1983) have estimated, for 13 DO-meters, the instrumental error as 0.12 mg/l, calibration error as 0.12 mg/l and the drift as 0.10 mg/l. Wacheux *et al.* (1993 and 1996) have found that actual characteristics of sensors are different from that specified by the manufacturers. Using a step response method, De Jager (1996) approximated the dynamics of ammonia-analyser type, by a first order transfer function with dead time. He estimated the time constant as 3 min., gain as 1 and dead-time as 15 min. Thomsen and Kisbye (1996) have suggested that, for mainly domestic wastewater, the accuracy of nutrient sensors can be taken as ± 0.3 mg/l, for ammonia-analysers, and as ± 0.5 mg/l, for nitrate-analysers.

2. Mathematical modeling of sensors

In general, the sensor output signal can be approximated by the following linear dynamic model:

$$y(t) = \begin{cases} G(s).u(t) + \varepsilon_1(t) + \varepsilon_2(t), & y > 0.1 \\ 0.1, & y \leq 0.1 \end{cases}$$

where

$y(t)$: sensor output signal (mg/l).

ε_1 : systematic error, which will be defined by the user (it is about 5%).

ε_2 : random error, which has a mean equal to zero and variance equal to 0.1.

s : derivative operator ($s = \frac{d}{dt}$).

The corresponding transfer function of the sensor $G(s)$ will be:

$$G(s) = \frac{K_p \cdot e^{-\tau_d s}}{\tau_p \cdot s + 1}, \text{ if the sensor is modelled as a first-order system, or}$$

$$G(s) = \frac{K_p \cdot e^{-\tau_d s}}{\tau_p^2 s^2 + 2\xi \tau_p s + 1}, \text{ if the sensor is modelled as a second-order system,}$$

where:

$u(t)$: sensor input signal (mg/l).

K_p : gain of the process ($K_p = 1$).

τ_p : time constant of the process.

τ_d : sensor pure time delay in minutes

ξ : damping factor.

When sensor dynamics can be neglected, that is at $\tau_p = 0$, the transfer function simply becomes:

$$G(s) = K_p \cdot e^{-t_d s}$$

3. Matlab/Simulink models of sensors

In Matlab/Simulink, two types of models are built for both DO sensors (Fig.1 and 2) and N-analysers (Fig. 3 and 4). In the first type sensor dynamics is taken into account, whereas in the second type sensor dynamics are neglected. As can be seen from these figures, the first type of sensors consists of: (i) a transport-delay block, (ii) transfer function block (first or second order transfer function) to represents the dynamics of the sensor (process time constant and process gain), (iii) random-error block, (iv) systematic-error block and (v) lower detection limit block. The second type of the models has been built similar to the first type, except that it has no transfer function block. Transfer function block has been removed because it has been assumed that sensor dynamics can be neglected and sensor response can be modelled by pure dead time after which sensor response will immediately reach the maximum. This type of models will be useful especially in long-term simulations because transfer functions with small time constants will probably slow down the simulation speed.

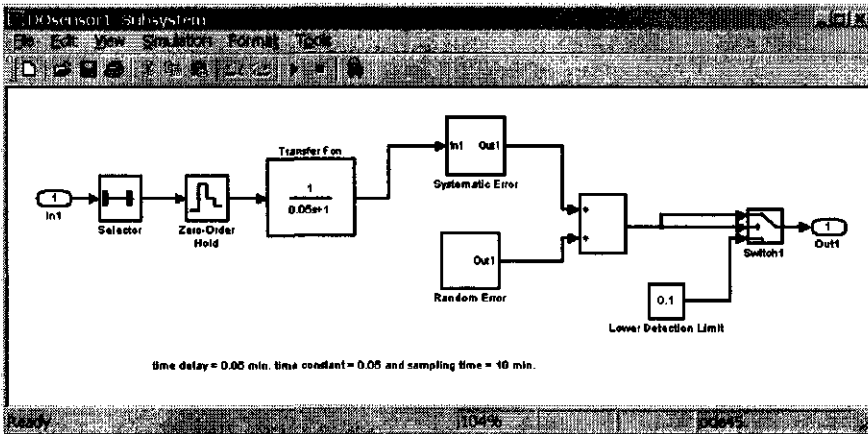


Fig. 1, Matlab/Simulink model of DO sensor type 1

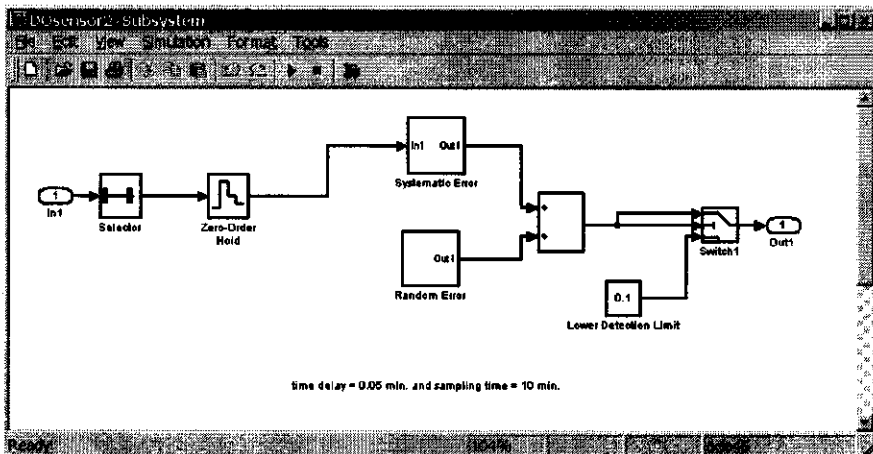


Fig. 2, Matlab/Simulink model of DO sensor type 2

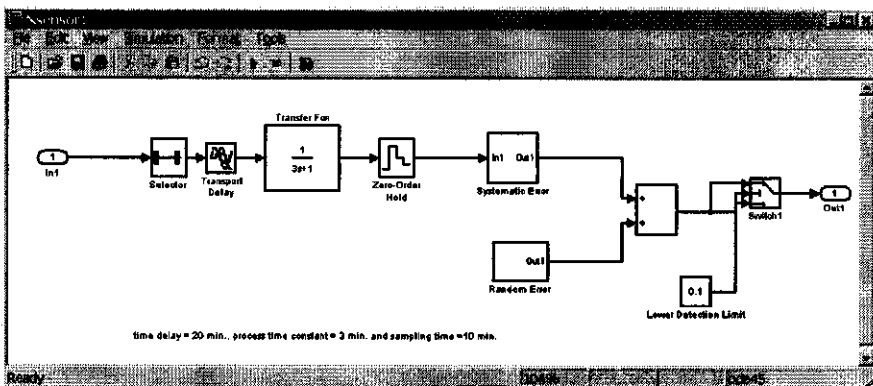


Fig. 3, Matlab/Simulink model of N sensor type 1

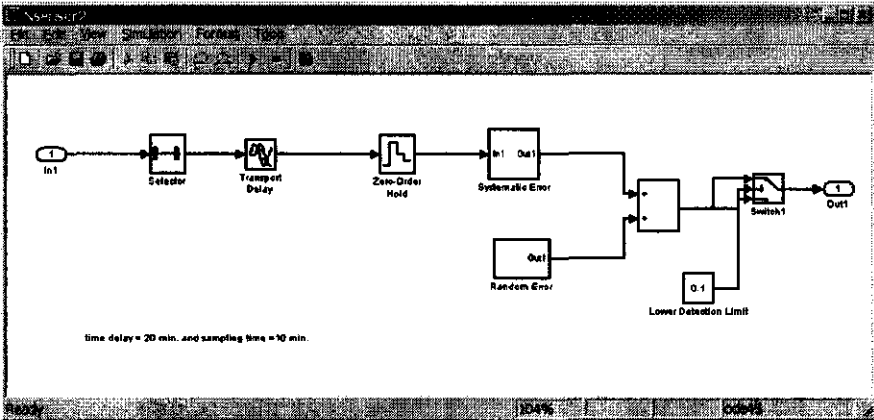


Fig. 4, Matlab/Simulink model of N sensor type 2

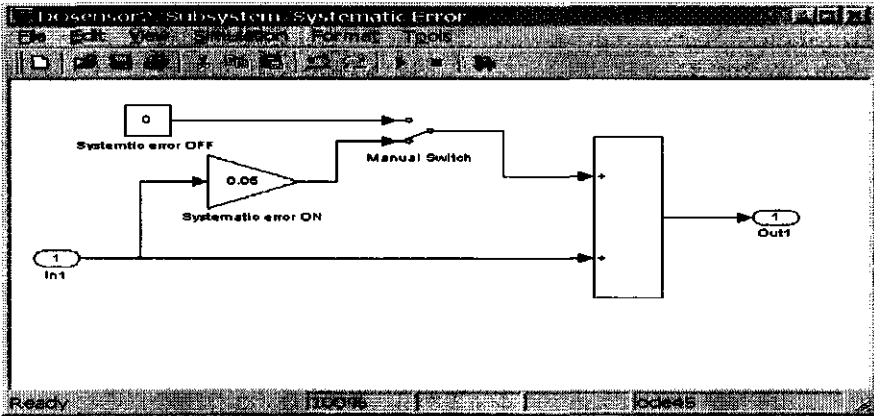


Fig. 5, Subsystem: systematic error.

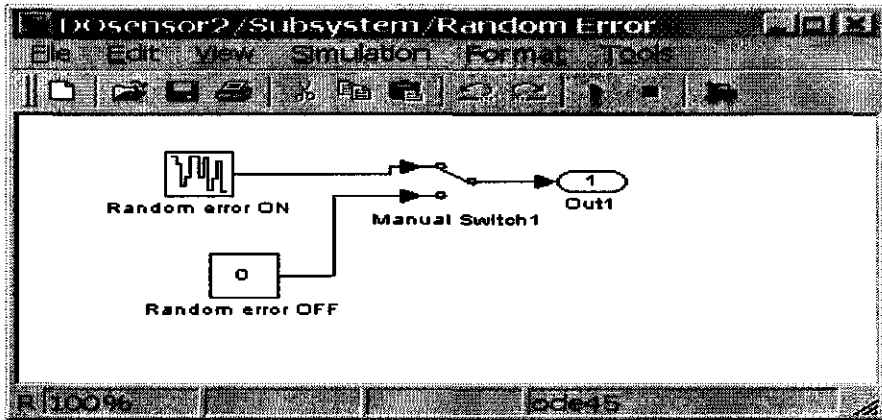


Fig. 6, Subsystem: random error.

In order to make the models more flexible, manual switches are included in the systematic (Fig. 5) and random error (Fig. 6) blocks. Manual switches allow the user to switch these blocks ON or OFF, whenever it is necessary. Because it has been reported that sensor readings are usually a positive value, even when distilled water is used (Wacheux *et al.*, 1996), a lower detection limit block is included in all types of models. Lower detection limit for nutrient sensors reported to range from 0.05 to 2.0 mg/l (Wacheux *et al.*, 1993; Wacheux *et al.*, 1996; Lynggaard-Jensen *et al.*, 1996).

In using these models, the benchmark user has to do the following. First, he has to choose one type of the two types of models proposed here. That is, he has to choose a sensor with or without transfer function block. Secondly, he has to specify values of all parameters used in the model, from transport delay to lower detection limit. For that he is advised to conduct some experiments in order to arrive at realistic values for the parameters. Since this will not be an easy task, a good engineering guess can be a good solution in such cases.

4. References

De Jager, J (1996), Ontwerp en toepassing robuuste ammoniumregeling in een actiefslib-installatie, Doktoraal verslag, Landbouwwuniversiteit Wageningen (in Dutch).

Gernaey, K. (1997), Development of sensors for on-line monitoring of nitrification in activated sludge. Ph.D. thesis Gent University, Belgium.

Kulin, G. W.W. Schuk and I.J. Kugelman (1983), Evaluation of a dissolved oxygen field test protocol, J WPCF 55(2):178-186.

Lynggaard-Jensen, A., N.H. Eism, I. Rasmussen, H. S. Jacobsen and T. Stenstrom (1996), Description and test of new generation of nutrient sensors. *Wat. Sci. Tech.* 33(1):25-36.

Thomsen, H.A., and K. Kisbye (1996), N and P on-line meters: requirements, maintenance and stability. *Wat. Sci. Tech.* 33(1):147-157.

Wacheux, H., S. Da Silva and J. Lesavre (1993), Inventory and assessment of automatic nitrate analysers for urban sewage works. *Wat. Sci. Tech.* 28(11/12):489-498.

Wacheux, H., J. L. Million, C. Guillo and E. Alves (1996), Automatic analysers for wastewater treatment plant: evaluation test at laboratory and field level. *Wat. Sci. Tech.* 33(1):193-201.

Appendix III: Performance Criteria

Performance criteria used in this particular oxidation ditch benchmark are developed by modifying the criteria proposed for benchmarking other activated sludge systems by *COST 624* and *IWA* Respirometry Task-Group. In fact, we have modified the version written by John B. Copp for the *IWA* Respirometry benchmark. The main changes we have made are in the energy equations (aeration energy, *AE*, and pumping energy, *PE*). Further, we have proposed long-term evaluation criteria. In addition, we have considered the part related to the controller assessment to be unnecessary and decided to leave it out.

1.0 Short-term assessment

Short-term assessments are carried out using the data generated during the second week of simulations with the scaled weather files. That is, following the steady state simulations and the 14-day simulation using the scaled dry weather file, each of the three scaled weather files is used to test the dynamics of the system including controller performance and process performance. This is achieved quantitatively through the calculation of a series of composite process variables.

This assessment quantifies the short-term effects of the control strategy on plant performance and it can be divided into three sub-levels: (i) effluent quality index, (ii) effluent violations and (iii) operational costs.

1.1 Effluent Quality Index

Within the context of the benchmark, effluent quality is considered through an effluent quality index (*EQ*), in g/d, which is meant to quantify into one single term the effluent pollution load to a receiving water body. Further, constraints with respect to specific effluent components are defined and the percentage of time that the constraints are not met is to be reported. As well, the methodology for reporting the number of violations also is defined.

Effluent quality (*EQ*), in g/d: calculated as follows by integrating over the period 8 to 14 days ($T = 7$ days):

$$EQ = \frac{1}{T} \int_{-8\text{days}}^{+14\text{days}} [PU_{TSS}(t) + PU_{COD}(t) + PU_{BOD}(t) + PU_{TKN}(t) + PU_{NO}(t)] Q_e(t) dt$$

Table 1, Value of the coefficients (β 's) used in the EQ equation

| | | C-only | Nitrifying | denitrifying |
|--------------------------------------|-----------------|--------|------------|--------------|
| $PU_{TSS}(t) = \beta_{TSS} TSS_e(t)$ | $\beta_{TSS} =$ | 2 | 2 | 2 |
| $PU_{COD}(t) = \beta_{COD} COD_e(t)$ | $\beta_{COD} =$ | 1 | 1 | 1 |
| $PU_{BOD}(t) = \beta_{BOD} BOD_e(t)$ | $\beta_{BOD} =$ | 2 | 2 | 2 |
| $PU_{TKN}(t) = \beta_{TKN} TKN_e(t)$ | $\beta_{TKN} =$ | 0 | 7 | 20 |
| $PU_{NO}(t) = \beta_{NO} NO_e(t)$ | $\beta_{NO} =$ | 0 | 0 | 20 |

The composite variables are calculated as follows:

$$TSS_e = 0.75 (X_{S,e} + X_{BH,e} + X_{BA,e} + X_{P,e} + X_{I,e})$$

$$COD_e = S_{S,e} + S_{I,e} + X_{S,e} + X_{BH,e} + X_{BA,e} + X_{P,e} + X_{I,e}$$

$$BOD_e = 0.25 (S_{S,e} + X_{S,e} + (1 - fp) (X_{BH,e} + X_{BA,e}))$$

$$TKN_e = S_{NH,e} + S_{ND,e} + X_{ND,e} + i_{XB} (X_{BH,e} + X_{BA,e}) + i_{XP} (X_{P,e} + X_{I,e})$$

$$NO_e = SNO_{,e}$$

$$N_{tot,e} = TKN_e + NO_e$$

1.2 Effluent Violations

Included in the performance evaluation is a measure of effluent violations. The violations are calculated for five terms: ammonia, total nitrogen, BOD5, total COD and suspended solids. The effluent constraints on these five terms in units of ($g\ m^{-3}$) are as follows:

Table 2, Effluent constraints

| | C-Removal only | Nitrifying | Denitrifying |
|-----------|----------------|------------|--------------|
| NH_4-N | n/a | <1 | <4 |
| TN | n/a | n/a | <18 |
| BOD_5 | <25 | <25 | <25 |
| Total COD | <125 | <125 | <125 |
| TSS | <30 | <30 | <30 |

The effluent violations are reported through two quantities: (i) number of violations; and, (ii) % time plant is in violation. These quantities are calculated from the output data generated at 15 min intervals [n/a - not applicable].

1.2.1 Number of violations

This quantity represents the number of times that the plant output violates the effluent constraints. An illustrative example is given below.

1.2.2 % time plant in violation

This quantity is a measure of the percentage of the time that the plant output violates the effluent constraints. An illustrative example is given below.

Example 1:

Table 3, Hypothetical data sets used in example 1

| time (hr) | Effluent Suspended Solids (g m^{-3}) | |
|-----------|-------------------------------------------------|--------|
| | case 1 | case 2 |
| 0 | 25 | 25 |
| 0.25 | 34 | 34 |
| 0.5 | 26 | 37 |
| 0.75 | 37 | 26 |
| 1 | 22 | 22 |

Two hypothetical data sets for effluent suspended solids are shown in the Table C2.

In case 1, the number of violations is 2. That is, the effluent suspended solids rose above the effluent constraint twice in this 1 hour period. During that hour, the effluent limit was in violation for 30 minutes (square wave concentrations are assumed, i.e. it is assumed that the effluent suspended solids concentration is 34 g m^{-3} for the entire period from 15 - 30 minutes and 37 g m^{-3} for the period from 45 - 60 minutes); hence the percentage of time in violation is 50.

In case 2, the number of violations is 1. That is, the effluent suspended solids rose above the effluent constraint only once in this hour. The fact that it remained above the constraint for an extended period is irrelevant for this quantity. As in case 1, the effluent limit was in violation for 30 minutes so the percentage of time in violation is also 50 for case 2.

1.3 Operational Costs

The operational costs are considered through three items: sludge production, pumping energy and aeration energy (integrations performed on the data from 8 to 14 days).

1.3.1 Sludge production (in units of kg/d) - [two quantities are calculated here: (i) sludge for disposal; and, (ii) total sludge production]:

(i) Sludge for disposal

$$P_{sludge} = [\Delta M(TSS_{system}) + M(TSS_w)] / T$$

where:

$\Delta M(TSS_{system})$ = change in system sludge mass from beginning of day 8 to end of day 14, i.e. $\Delta M(TSS_{system}) = M(TSS_{reactors}) + \Delta M(TSS_{settler})$

$$M(TSS_w) = 0.75 \int_{=8days}^{=14days} [X_{S,w} + X_{I,w} + X_{BH,w} + X_{BA,w} + X_{P,w}] Q_w(t) dt$$

(ii) Total sludge production

$$P_{total-sludge} = P_{sludge} + M(TSS_e) / T$$

where:

$$M(TSS_e) = 0.75 \int_{=8days}^{=14days} [X_{S,e} + X_{I,e} + X_{BH,e} + X_{BA,e} + X_e] Q_e(t) dt$$

1.3.2 Pumping energy (in units of kWh/d):

$$PE = \frac{1}{T} \int_{=day8}^{=day14} [0.008Q_r(t) + 0.004Q_w(t)] dt$$

where:

PE: total pumping energy, kWh/d.

Q_r : returned sludge recycle, m³/d.

Q_w : waste sludge flow, m³/d.

1.3.3 Aeration energy (AE), in units of kWh/d:

$$AE := \frac{1}{N \cdot T} \int_0^{0+T} \sum_{i=1}^n F_i \cdot k_i \cdot (C_s^* - C_{L,i}) dt$$

where

AE: aeration energy, kWh/d

N: efficiency of the aerator under field conditions (default value for Landy-F aerators is $1.35 \cdot 10^3$ g O₂/kWh).

$AC_{h,i}$: average hourly aeration capacity relative to the aerator full capacity.

F: average daily aeration capacity relative to the aerator full capacity ($F_i = \frac{1}{24} \sum_{j=0}^{24} AC_h$).

- k*: aeration constant ($\text{m}^3 \text{d}^{-1}$), which equals $K_L a \cdot V$
k_La: overall oxygen transfer rate, d^{-1}
V: volume of the aerated compartment, m^3
C_S: oxygen saturation concentration at field temperature, mg/l
C_L: operating oxygen concentration, mg/l
i: number of the aerated compartment, 1...*n*
n: number of aerators in the oxidation ditch

Efficiency under field conditions can be estimated using the following equation:

$$N = N_0 \left(\frac{\beta_o C_{w,alt} - C_L}{C_{S,20}} \right) 1.024^{T-20} \alpha_o$$

where

- N*: $\text{kg O}_2/\text{kWh}$ transferred under field conditions
N₀: $\text{kg O}_2/\text{kWh}$ transferred in clean water at 20 °C and zero dissolved oxygen
C_{w,alt}: oxygen saturation concentration for tap at given temperature and altitude
C_{S,20}: oxygen saturation concentration in tap water 20 °C, mg/l
C_L: operating oxygen concentration, mg/L
T: temperature, °C
 α_o : oxygen-transfer correction factor for wastewater
 β_o : salinity-surface tension correction factor, usually 1.

2. Long-term assessment

Long-term assessments are calculated using the data generated during a period equal or greater than 4-5 times the sludge age. The calculations should be carried out in the same way as for the short-term assessments (see section 1), with the following modifications:

(i) Scale and repeat all weather files many times, according to the needs. Here, scaling is regarding only the average hydraulic load (m^3/d). For example, if your plant has a hydraulic load, which is 20 % (say) higher than that proposed by COST, then multiply the influent flow rate in all COST files by 1.2 (120 %). Regarding the length of the influent file, let us assume that the oxidation ditch at your plant has sludge age of 15 days. Thus, to assess the performance of the plant in period equivalent to 4-5 times the sludge age, you need influent files of length between 60 to 75 days. You can achieve this by repeating the scaled influent files 4 to 5 times.

(ii) Adjust the integration limits, according to the length of the influent file. Here, the integration limits used in the equations for calculating the performance indices (see above), need to be modified, from 8 to 14 days, to new values.

Effect of possible failures of sensors and actuators on the plant performance can also be assessed in this part. However, realistic scenarios of failures for sensors and actuators still need to be developed.

Appendix IV: Description of the benchmarked full-scaled WWTP

The WWTP is located in Rotterdam, The Netherlands (Schieland, 1994). It consists of two main parallel treatment lines. Each treatment line has two primary settlers, one selector, one carousel and secondary settlers. In addition, the plant has a number of sludge treatment units. The plant is designed to treat dry weather flow (DWF) of 5200 m³/hr. The maximum designed flow for this plant is 12800 m³/hr. Below is a brief description of the various units used in the treatment plant.

Primary settlers:

Number = 4

Maximum surface load = 4 m³/m²hr.

Minimum detention time = 0.5 hr.

Depth = 2 m.

Total surface area = 3200 m².

Selectors:

Number = 2

Capacity = 2 x 750 m³.

Detention time (DWF) = 10 min.

Carrousel:

Numbers = 2

Organic load = 0.15 kg BOD₅/d.s.day.

Capacity = 2 x 13000 m³ (each is 406.25m x 8m x 4m deep).

Number of aerators = 2 * 4 pieces (each has maximum capacity of 220 kg O₂/hr.).

Secondary settlers:

Number = 6

Maximum surface load = 0.97 m³/m²hr.

Depth = 2 m.

Diameter = 52.9 m.

Primary thickeners:

Number = 1

Maximum load = 60 kg d.s./m²day.

Depth = 3 m.

Diameter = 16 m.

Secondary thickeners:

Number = 1

Maximum load = 25 kg d.s./m²day.

Depth = 3 m.

Diameter = 23 m.

Sludge digestion tanks:

Number = 2

Diameter = 19 m.

Height = 18 m.

Capacity = 2 x 5092 m³

Detention time = 20 day.

Temperature = 30 °C.

References:

Schieland, H., van (1994), Stikstof (total) verwijdering in relatie tot de voortzetting en intensivering van de procesoptimalisatie op de AWZI Kralingseveer: praktijkonderzoek (fase 2), Technische dienst van Schieland, afdeling afvalwater, onderafdeling zuiveringstechnologie (in Dutch).

Appendix V: Matlab/Simulink model of the full-scale WWTP

1. Simulink Blocks

To model the full-scale oxidation ditch wastewater treatment plant, which is used to develop the benchmarking methodology given in chapter 7, Simulink blocks were used (see Fig. 1). Apart from the input blocks (from work space and constant value) and output blocks (to work space), the blocks given in Fig. 1 represent S-functions (system functions) expressed in Matlab language. To significantly reduce the computational time, C-MEX files were used instead of the ordinary S-function files. C-MEX files are S-function files written in C language and can be executed within Matlab/Simulink environment.

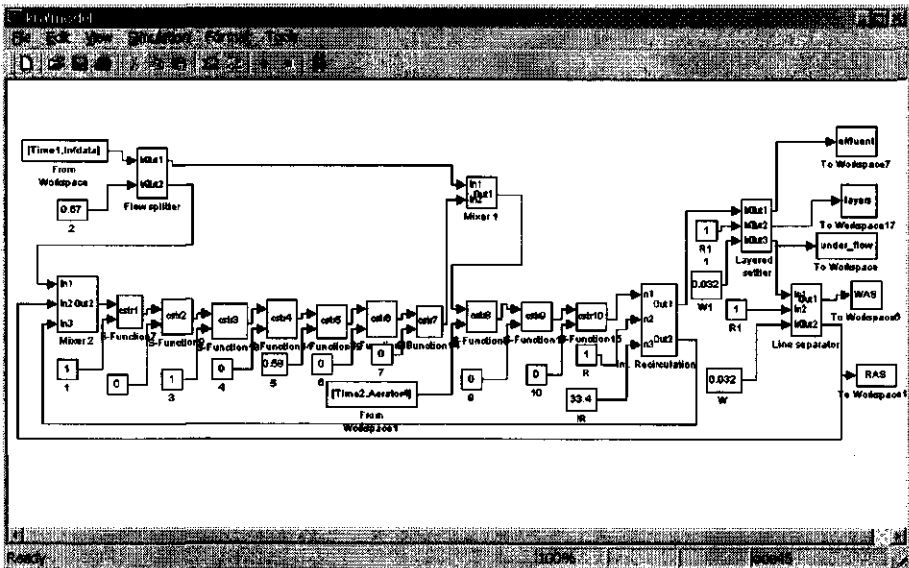


Fig. 1, Matlab/Simulink model of the full-scale oxidation WWTP

As the plant has two parallel treatment lines, only one treatment line was modeled. Treatment units considered in the model were the aeration tank (oxidation ditch) and the secondary settler. As can be seen from Fig. 1, a loop that consists of 10 CSTR's is used to model the hydraulics of the ditch. Biochemical processes are modeled according to activated sludge model (ASM) No. 1 (Henze *et al.*, 1987). Equations used in each of these CSTR's can be found in COST (2000). Fig. 1 also shows that each CSTR has two inputs: a stream coming from the previous CSTR and a predefined aeration rate. Here, the aeration rate is expressed as a ratio to the full aeration capacity of the aerators. For example, one means full aeration capacity, zero means no aeration at all while 0.58 means 58% of the full aeration capacity. Because the aerator 4 is not working at a

constant rate over the day (see Fig. 5 in section 8), the block from work space1 is used to provide the aeration rate. As an example, a C-MEX file of a *CSTR* is given in section 2.

Together with the 10 *CSTR*'s, a flow splitter, two types of mixers (mixer1 and mixer2) and an internal flow recirculation block were also used to model water streams within and around the oxidation ditch. These units are assumed to be ideal. That is, they divide or mix various wastewater streams on volume (i.e. flow, m³/d) basis. The flow splitter was used to divide the influent stream (from workspace block) at a certain ratio between the first aerated compartment (67%) and the fourth aerated compartment (33%).

Mixer 1 was used to mix two streams of wastewater, whereas mixer 2 was used to mix three streams of wastewater. For example, the concentration (*C*) resulted from mixing of two streams was calculated as:

$$C = \frac{Q_1 C_1 + Q_2 C_2}{Q_1 + Q_2} \quad (1)$$

And the flow (*Q*) as:

$$Q = Q_1 + Q_2 \quad (2)$$

Based on the sludge recycle rate (*R*) and the ditch internal recirculation rate (*IR*), the recirculation block divides the effluent of the last *CSTR*, into two streams. The first stream goes to the secondary settler (layered settler), whereas the second stream goes back to the first *CSTR*. The internal recirculation rate (*IR* = 33.4) was calculated based on horizontal velocity equal to 0.3 m/s and channel cross-section equal to 4 m × 8 m.

In Fig. 1, the layered settler block is used to represent the secondary settler. The C-MEX file of this block contains the double-exponential settling velocity model proposed by Takács *et al.*, (1991). Details of the equations used in this model can also be found in COST (2000) website. The layered settler block has three outputs: effluent, layers and under flow streams. The line separator block is used to split the underflow (under_flow) stream into the activated waste sludge (*WAS*) and recirculated activated sludge (*RAS*) streams.

2. An example of the C-MEX files

All C-MEX files of the blocks presented in Fig. 1 were written within Matlab 5.3. Using other Matlab versions this fact should be taken into account. As an example, only the C-MEX file of the *CSTR* is provided here. The same procedure followed in filling-in this template was also used for the other files. Here, the part filled in the C-MEX template is shown in bold.

```

/*
 * sfuntmpl.c: C template for a level 2 S-function.
 *
 * -----
 * | See matlabroot/simulink/src/sfuntmpl.doc for a more detailed
template |
 * -----
 *
 * Copyright (c) 1990-1998 by The MathWorks, Inc. All Rights Reserved.
 * $Revision: 1.18 $
 */

/*
 * You must specify the S_FUNCTION_NAME as the name of your S-function
 * (i.e. replace sfuntmpl with the name of your S-function).
 */

#define S_FUNCTION_LEVEL 2
#define S_FUNCTION_NAME  cstr

/*
 * Need to include simstruc.h for the definition of the SimStruct and
 * its associated macro definitions.
 */
#include "simstruc.h"
#define u(element) (*uPtrs[element])
#define ul(element) (*uPtrs1[element])

#define PARAM1(S) ssGetSFcnParam(S,0)
#define PARAM2(S) ssGetSFcnParam(S,1)

/* Error handling
 * -----
 *
 * You should use the following technique to report errors encountered
within
 * an S-function:
 *
 *         ssSetErrorStatus(S,"Error encountered due to ...");
 *         return;
 *
 * Note that the 2nd argument to ssSetErrorStatus must be persistent
memory.
 * It cannot be a local variable. For example the following will cause
 * unpredictable errors:
 *
 *         mdlOutputs()
 *         {
 *             char msg[256];           {ILLEGAL: to fix use "static char
msg[256];"}
 *             sprintf(msg,"Error due to %s", string);
 *             ssSetErrorStatus(S,msg);
 *             return;

```

```

*      }
*
* See matlabroot/simulink/src/sfunctmpl.doc for more details.
*/

/*=====
* S-function methods *
*=====*/

/* Function: mdlInitializeSizes
=====
* Abstract:
* The sizes information is used by Simulink to determine the S-
function
* block's characteristics (number of inputs, outputs, states, etc.).
*/
static void mdlInitializeSizes(SimStruct *S)
{
    /* See sfunctmpl.doc for more details on the macros below */

    ssSetNumSFcnParams(S, 2); /* Number of expected parameters */
    if (ssGetNumSFcnParams(S) != ssGetSFcnParamsCount(S)) {
        /* Return if number of expected != number of actual parameters
*/
        return;
    }

    ssSetNumContStates(S, 13);
    ssSetNumDiscStates(S, 0);

    if (!ssSetNumInputPorts(S, 2)) return;
    ssSetInputPortWidth(S, 0, 14);
    ssSetInputPortDirectFeedThrough(S, 0, 1);
    ssSetInputPortWidth(S, 1, 1);
/*
    ssSetInputPortDirectFeedThrough(S, 1, 0);
*/

    if (!ssSetNumOutputPorts(S, 1)) return;
    ssSetOutputPortWidth(S, 0, 14);

    ssSetNumSampleTimes(S, 1);
    ssSetNumRWork(S, 0);
    ssSetNumIWork(S, 0);
    ssSetNumPWork(S, 0);
    ssSetNumModes(S, 0);
    ssSetNumNonsampledZCs(S, 0);

    ssSetOptions(S, 0);
}

/* Function: mdlInitializeSampleTimes
=====
* Abstract:
* This function is used to specify the sample time(s) for your

```

```

* S-function. You must register the same number of sample times as
* specified in ssSetNumSampleTimes.
*/
static void mdlInitializeSampleTimes(SimStruct *S)
{
    ssSetSampleTime(S, 0, INHERITED_SAMPLE_TIME);
    ssSetOffsetTime(S, 0, 0.0);
}

#define MDL_INITIALIZE_CONDITIONS /* Change to #undef to remove
function */
#if defined(MDL_INITIALIZE_CONDITIONS)
/* Function: mdlInitializeConditions
-----
* Abstract:
* In this function, you should initialize the continuous and
discrete
* states for your S-function block. The initial states are placed
* in the state vector, ssGetContStates(S) or
ssGetRealDiscStates(S).
* You can also perform any other initialization activities that
your
* S-function may require. Note, this routine will be called at the
* start of simulation and if it is present in an enabled subsystem
* configured to reset states, it will be call when the enabled
subsystem
* restarts execution to reset the states.
*/
static void mdlInitializeConditions(SimStruct *S)
{
    int_T i;
    real_T *x0=ssGetContStates(S);

    real_T icr1=mxGetPr(PARAM2(S))[0];
    real_T icr2=mxGetPr(PARAM2(S))[1];
    real_T icr3=mxGetPr(PARAM2(S))[2];
    real_T icr4=mxGetPr(PARAM2(S))[3];
    real_T icr5=mxGetPr(PARAM2(S))[4];
    real_T icr6=mxGetPr(PARAM2(S))[5];
    real_T icr7=mxGetPr(PARAM2(S))[6];
    real_T icr8=mxGetPr(PARAM2(S))[7];
    real_T icr9=mxGetPr(PARAM2(S))[8];
    real_T icr10=mxGetPr(PARAM2(S))[9];
    real_T icr11=mxGetPr(PARAM2(S))[10];
    real_T icr12=mxGetPr(PARAM2(S))[11];
    real_T icr13=mxGetPr(PARAM2(S))[12];

    x0[0]=icr1;
    x0[1]=icr2;
    x0[2]=icr3;
    x0[3]=icr4;
    x0[4]=icr5;
    x0[5]=icr6;
    x0[6]=icr7;

```

```

x0[7]=icr8;
x0[8]=icr9;
x0[9]=icr10;
x0[10]=icr11;
x0[11]=icr12;
x0[12]=icr13;

}
#endif /* MDL_INITIALIZE_CONDITIONS */

#undef MDL_START /* Change to #undef to remove function */
#if defined(MDL_START)
/* Function: mdlStart
-----
* Abstract:
*   This function is called once at start of model execution. If you
*   have states that should be initialized once, this is the place
*   to do it.
*/
static void mdlStart(SimStruct *S)
{
}
#endif /* MDL_START */

/* Function: mdlOutputs
-----
* Abstract:
*   In this function, you compute the outputs of your S-function
*   block. Generally outputs are placed in the output vector,
ssGetY(S).
*/

static void mdlOutputs(SimStruct *S, int_T tid)
{
int_T i;
int_T width=ssGetInputPortWidth(S,0);
InputRealPtrsType uPtrs=ssGetInputPortRealSignalPtrs(S,0);
real_T *y=ssGetOutputPortRealSignal(S,0);
real_T *x=ssGetContStates(S);
{
y[13]=(*uPtrs[13]);
}
for(i=0;i<13;i++){
*y++=*x++;
}
}

#undef MDL_UPDATE /* Change to #undef to remove function */
#if defined(MDL_UPDATE)
/* Function: mdlUpdate
-----

```

```

* Abstract:
*   This function is called once for every major integration time
step.
*   Discrete states are typically updated here, but this function is
useful
*   for performing any tasks that should only take place once per
*   integration step.
*/
static void mdlUpdate(SimStruct *S, int_T tid)
{
}
#endif /* MDL_UPDATE */

```

```

#define MDL_DERIVATIVES /* Change to #undef to remove function */
#if defined(MDL_DERIVATIVES)
/* Function: mdlDerivatives

```

```

-----
* Abstract:
*   In this function, you compute the S-function block's
derivatives.
*   The derivatives are placed in the derivative vector, ssGetdX(S).
*/
static void mdlDerivatives(SimStruct *S)
{

```

```

    real_T rho1, rho2, rho3, rho4, rho5, rho6, rho7, rho8, p;
    real_T ss,xbh,xs,xl,snh,sl,snd,xnd,so,xba,xp,sno,salk;

```

```

    real_T *dx=ssGetdX(S);
    real_T *x=ssGetContStates(S);

```

```

    InputRealPtrsType uPtrs=ssGetInputPortRealSignalPtrs(S,0);
    InputRealPtrsType uPtrs1=ssGetInputPortRealSignalPtrs(S,1);

```

```

    real_T v=mxGetPr(PARAM1(S))[0];
    real_T ya=mxGetPr(PARAM1(S))[1];
    real_T yh=mxGetPr(PARAM1(S))[2];
    real_T fp=mxGetPr(PARAM1(S))[3];
    real_T ixb=mxGetPr(PARAM1(S))[4];
    real_T isp=mxGetPr(PARAM1(S))[5];
    real_T muh=mxGetPr(PARAM1(S))[6];
    real_T ks=mxGetPr(PARAM1(S))[7];
    real_T koh=mxGetPr(PARAM1(S))[8];
    real_T kno=mxGetPr(PARAM1(S))[9];
    real_T bh=mxGetPr(PARAM1(S))[10];
    real_T etag=mxGetPr(PARAM1(S))[11];
    real_T etah=mxGetPr(PARAM1(S))[12];
    real_T kh=mxGetPr(PARAM1(S))[13];
    real_T kx=mxGetPr(PARAM1(S))[14];
    real_T mus=mxGetPr(PARAM1(S))[15];
    real_T knh=mxGetPr(PARAM1(S))[16];
    real_T ba=mxGetPr(PARAM1(S))[17];
    real_T koa=mxGetPr(PARAM1(S))[18];
    real_T ka=mxGetPr(PARAM1(S))[19];
    real_T sosat=mxGetPr(PARAM1(S))[20];

```

```

real_T kopt=mxGetPr(PARAM1(S)) [21];
real_T m=mxGetPr(PARAM1(S)) [22];

si=x[0];
ss=x[1];
xi=x[2];
xs=x[3];
xbh=x[4];
xba=x[5];
xp=x[6];
so=x[7];
sno=x[8];
snh=x[9];
snd=x[10];
xnd=x[11];
salk=x[12];

p=ul(0);

/* Process rates */
rho1=muh*(ss/(ks+ss))*(so/(koh+so))*xbh;
rho2=muh*(ss/(ks+ss))*(koh/(koh+so))*(sno/(kno+sno))*etah*xbh;
rho3=muu*(snh/(knh+snh))*(so/(koa+so))*xba;
rho4=bh*xbh;
rho5=ba*xba;
rho6=ka*snd*xbh;
rho7=kh*((xs/xbh)/(kx+(xs/xbh)))*((so/(koh+so))+(etah*(koh/(koh+so))*(sno/(kno+sno))))*xbh;
rho8=rho7*xnd/xs;

/* ASM No.1 */
dx[0]=u(13)*(u(0)-x[0])/v;
dx[1]=(u(13)*(u(1)-x[1])/v)-(rho1/yh)-(rho2/yh)+rho7;
dx[2]=u(13)*(u(2)-x[2])/v;
dx[3]=(u(13)*(u(3)-x[3])/v)+((1-fp)*rho4)+((1-fp)*rho5)-rho7;
dx[4]=(u(13)*(u(4)-x[4])/v)+rho1+rho2-rho4;
dx[5]=(u(13)*(u(5)-x[5])/v)+rho3-rho5;
dx[6]=(u(13)*(u(6)-x[6])/v)+(fp*rho4)+(fp*rho5);

dx[7]=(u(13)*(u(7)-x[7])/v)-((1-yh)*rho1/yh)-(rho3*(4.57-ya)/ya)+(p*m*kopt*(sosat-x[7])/v);

dx[8]=(u(13)*(u(8)-x[8])/v)-(((1-yh)*rho2)/(2.86*yh))+rho3/ya;
dx[9]=(u(13)*(u(9)-x[9])/v)-(ixb*rho1)-(ixb*rho2)-((ixb+(1/ya))*rho3)+rho6;
dx[10]=(u(13)*(u(10)-x[10])/v)-rho6+rho8;
dx[11]=(u(13)*(u(11)-x[11])/v)+((ixb-(fp*ixp))*rho4)+((ixb-(fp*ixp))*rho5)-rho8;
dx[12]=(u(13)*(u(12)-x[12])/v)-((ixb*rho1)/14)+(rho2*((1-yh)/(14*2.86*yh)-(ixb/14)))-(rho3*((ixb/14)+(1/(7*ya))))+(rho6/14);

}
#endif /* MDL_DERIVATIVES */

```

```

#undef MDL_TERMINATE /* Change to #undef to remove function */
#if defined(MDL_TERMINATE)
/* Function: mdlTerminate
=====
* Abstract:
*   In this function, you should perform any actions that are
necessary
*   at the termination of a simulation. For example, if memory was
*   allocated in mdlInitializeConditions, this is the place to free
it.
*/
static void mdlTerminate(SimStruct *S)
{
}

/*=====
* See sfuntmpl.doc for the optional S-function methods *
*=====*/

/*=====
* Required S-function trailer *
*=====*/

#ifdef MATLAB_MEX_FILE /* Is this file being compiled as a MEX-file?
*/
#include "simulink.c" /* MEX-file interface mechanism */
#else
#include "cg_sfuns.h" /* Code generation registration function */
#endif

```

5.3 References

COST (2000), www.ensic.u-nancy.fr/COSTWWTP/Benchmark/Benchmark1.htm.

Henze, M., C.P.L. Grady, jr, W. Gujer, G. van R. Marais and T. Matsuo (1987), Activated sludge model no. 1, IAWQ scientific and Technical Report no. 1, IAWQ, London, U.K.

Takács, I., G.G. Patry and D. Nolasco (1991), A dynamic model of the clarification-thickening process, *Wat. Res.* 25(10):1263-71.

Summary

Process complexity and strict effluent standards are the main reasons for the growing interest in the use of advanced control techniques in biological wastewater plants. So far, many control strategies have been proposed. However, few of these have been thoroughly evaluated, either in practical tests or in computer simulations. It is obvious that evaluation of the proposed control strategies by carrying out practical tests is impossible, due to time and money limitations. Thus computer simulations offer a useful approach to solve this problem. However, this approach requires development of a standard simulation procedure and evaluation criteria. That is, development of a whole benchmarking methodology.

The purpose of this study was to develop a benchmarking methodology that can be used to evaluate existing or new control strategies in *oxidation ditch* WWTP's. In this study, the emphasis was on oxidation ditch plants that treat mainly domestic wastewater and perform only carbon oxidation and nitrogen removals. The purpose was achieved by developing a benchmark for a specific full-scale WWTP, located in Rotterdam, The Netherlands, using available real process data. This does not imply that this specific plant located in Rotterdam is the reference plant. Rather the focus was in developing a benchmarking procedure. Hence, for other WWTP's, the same procedure can also be followed.

The main parts of the benchmark are the basic simulation model and the performance criteria. In chapters 2, 3 and 4, the basic simulation model was developed and calibrated. The loop-of *CSTR*'s model, without back flows, was chosen for modeling oxidation ditches because it is simple, realistic, and can be easily used for controller design. In chapter 2, the model was used to estimate the ditch hydraulics and aeration, under clean water conditions. Due to the hyperbolic relationship between $K_L a$ and V_A (the effective volume of the aerated compartment), it was found that it is not possible to individually identify these parameters. However, it was found that the aeration constant $k (= K_L a \cdot V_A)$ can accurately be estimated. In chapter 3, the adequate number of *CSTR*'s needed for modeling an oxidation ditch was investigated. Results obtained have shown that number of *CSTR*'s that are needed for modeling oxidation ditches can be limited to about 10-15 *CSTR*'s. In chapter 4, the developed model was then calibrated, using the response surface methodology (*RSM*), prior to the formal least-square estimation step. *RSM* is based on elliptical analysis of response surfaces. This method was chosen because of the following advantages: (i) it can be used for problems with a multi-objective criterion function, (ii) it is useful in selecting the best identifiable parameters, and (iii) it provides a good initial guess of parameter values.

After developing the basic simulation model, models for *DO* and *N* sensors (Appendix II), and subsequently, performance criteria were also developed (Appendix III). The performance criteria proposed by both COST 624 and IWA Respirometry Task Group were modified to suit oxidation ditch WWTP's. Main modifications were made in the aeration energy (*AE*) and pumping energy (*PE*) equations. The reason for that are the

following. First, oxidation ditches usually use mechanical aerators, which are different from air diffusers adopted by the previously mentioned working groups. Secondly, in an oxidation ditch there is no special pump for internal recirculation, since the mechanical aerators also do this function. In addition, a long-term evaluation criterion was also proposed.

Next, carrying out sensitivity and uncertainty analysis assessed reliability and applicability of the developed model. In chapter 5, a method for studying the effect of parameter variations on the performance indices was illustrated. Short-term results obtained have indicated that *ASM No. 1* parameters that need special attention are: Y_{FH} , K_S , b_{FH} , k_h , η_B , η_h , K_X , μ_A and K_{NH} . In chapter 6, methods for quantifying the effect of various uncertainty sources on the performance indices were demonstrated. Important short-term results obtained are the following. First, due to uncertainty in influent loads and parameter values, large and symmetrical uncertainty ranges around the nominal values are found in the effluent quality and total sludge production indices. Secondly, relatively smaller deviations, however, are found due to uncertainty in the states initial conditions. Thirdly, effect of the additive model structural uncertainty on the performance indices seems to be negligible, when compared to the effect of parameter uncertainty.

In the last part of the thesis, a step-by-step benchmarking procedure was outlined (see section 7.3), and the application of the benchmark was demonstrated (see chapter 8). In section 8.2, the benchmark was used for studying the effect of the horizontal velocity on nitrogen removal processes. In oxidation ditches, aerators have dual function: (i) introducing oxygen into the system, and (ii) creating a horizontal velocity between 0.25 to 0.60 m/s that prevents the organic particles from settling on the channel bottom surface. The study reported in this section shows that, at non-limiting *DO* concentrations, a small change in the horizontal velocity can significantly affect the nitrogen removal processes. Hence, it is suggested that variations in the horizontal velocity should be taken into account when maximizing nitrogen removal efficiency, or to decouple the effects of horizontal velocity and oxygen input, by using air diffusers, which are operated in relation to the *TN* concentration in the effluent, and flow recirculating pumps (boosters) instead of mechanical aerators.

In section 8.3, the benchmark was used for evaluating some basic and advanced control strategies of the plant in Rotterdam, The Netherlands. It was found that the ratio of splitting the influent flow between the first and the fourth aerated compartments of the ditch has no significant effect on the *TN* concentrations in the effluent. Also in this part it has become clear that, for the evaluation of the long-term control strategies, future benchmarks need to be able to assess the performance of the secondary settler.

Finally, in chapter 9, a general discussion about the practical applicability of the developed benchmarking methodology and general conclusions are presented. This chapter ends by listing the following achievements and novelties, which represent the contribution of this thesis:

- In contrast to the set of benchmarks developed elsewhere, the procedure developed here is directed towards benchmarking oxidation ditch WWTP's.
- The introduction of the benchmarking procedure, without trying to define a generic reference plant, allows benchmarking of any specific oxidation ditch WWTP's.
- In comparison to the existing standard methods, a realistic and simple method that can be used in the estimation of the standard oxygen transfer rate (*SOTR*) in oxidation ditches has been derived.
- Short-term, as well as long-term, evaluation criteria for the performance of oxidation ditch WWTP's, have been formulated.
- Systematic procedures for parameter estimation and uncertainty assessment have been developed.

Samenvatting

De complexiteit van het actief-slib proces en de strenge normen voor de kwaliteit van het effluent zijn de belangrijkste motivaties voor de toepassing van geavanceerde regelstrategieën in afvalwaterzuiveringsinstallaties (AWZI's). Verscheidene regelstrategieën zijn hiervoor ontwikkeld door verschillende onderzoeksgroepen. Echter, slechts enkele van deze regelingen zijn daadwerkelijk beoordeeld op hun prestaties met behulp van laboratoriumexperimenten of computersimulaties. Evaluatie van deze strategieën op basis van full-scale/pilot experimenten is dikwijls onmogelijk vanwege de beperkte tijd en beperkte financiële middelen. Computersimulaties zijn daarom een aantrekkelijk alternatief. Evenwel, deze aanpak vereist de ontwikkeling van een "benchmark", oftewel een standaard simulatieprocedure.

Het hoofddoel van deze studie is de ontwikkeling van zo'n benchmark methodologie, die gebruikt kan worden voor de evaluatie van bestaande of nieuwe regelstrategieën in oxidatiesloot AWZI's. In deze studie ligt het accent op de zuivering van huishoudelijk afvalwater, dat is, C-oxidatie en verwijdering van stikstof. Het doel is verder gespecificeerd in termen van de ontwikkeling van een benchmark voor een specifieke AWZI gelegen in Rotterdam, door gebruik te maken van beschikbaar reële proces data. Voor andere AWZI's kan eenzelfde procedure gevolgd worden.

De belangrijkste delen van de benchmark zijn het simulatiemodel en de beoordelingscriteria. In de hoofdstukken 2, 3 en 4 worden de ontwikkeling en calibratie van het basismodel gepresenteerd. Een CSTR-model zonder backflow was gekozen voor de modellering van de oxidatiesloten, omdat dit model-type eenvoudig en realistisch is en gemakkelijk kan worden gebruikt voor regelaarontwerp.

In het hoofdstuk 2 worden de onbekende modelparameters voor de beluchting en de hydraulica van de oxidatiesloten geschat op basis van experimenten met zuiver water. Het bleek niet mogelijk om $K_L a$ en V_A (het effectieve volume van het beluchttingscompartiment) afzonderlijk te identificeren. Er is echter gebleken dat de beluchtingconstante $k (= K_L a \cdot V_A)$ heel precies geschat kan worden. In hoofdstuk 3 wordt beschreven hoe het aantal CSTR's is bepaald dat nodig is voor de modellering van een oxidatiesloot. 10-15 CSTR's bleken voldoende te zijn voor een nauwkeurige beschrijving van een oxidatiesloot.

In hoofdstuk 4 wordt de calibratie van het model besproken. Daartoe is de zogenaamde "Response Surface Method" (RSM) toegepast, gevolgd door een kleinste kwadraten schatting. Deze RSM heeft de volgende voordelen: (i) hij kan gebruikt worden om meer dan één doelfunctie te optimaliseren, (ii) hij maakt duidelijk hoe gevoelig diverse parameters zijn en (iii) hij levert goede beginwaarden op van de te schatten parameters.

Modellen voor de opgelost-zuurstof and N sensoren zijn ook ontwikkeld (Appendix II) en beoordelingscriteria zijn opgesteld (Appendix III). De beoordelingscriteria van de COST 624 en IWA Respirometry Task Group zijn aangepast, zodat ze geschikt zijn voor oxidatiesloten. De belangrijkste modificaties zijn gemaakt in de vergelijken voor beluchtingsenergie (AE) en de pomp-energie (PE). Hiervoor zijn twee redenen te

noemen. Ten eerste worden oxidatiesloten meestal mechanische beluchters gebruikt. Mechanische beluchters verschillen van de bellen-beluchters die worden gebruikt door de bovengenoemde twee groepen. Ten tweede is er in de oxidatiesloten geen speciale pomp nodig voor interne recirculatie, omdat de mechanische beluchters al daarvoor zorgen. Een andere aanpassing die is gedaan, is het kiezen van een langere evaluatietijd.

Vervolgens is de betrouwbaarheid en toepasbaarheid van het ontwikkelde model beoordeeld op basis van een gevoeligheids- en onzekerheidsanalyse. In hoofdstuk 5 wordt een methode beschreven om het effect van variaties in de parameters op de doelfuncties te kunnen bepalen. Uit de verkregen kortetermijnresultaten kan geconcludeerd worden dat de volgende parameters van *ASM No. 1* speciale aandacht behoeven: Y_H , K_S , b_H , k_h , η_D , η_b , K_X , μ_A en K_{NH} . Hierop aansluitend wordt in hoofdstuk 6 een procedure gepresenteerd voor de kwantitatieve beoordeling van de verschillende bronnen van onzekerheid. De belangrijke kortetermijnresultaten zijn de volgende. Ten eerste zijn er grote symmetrische onzekerheidsintervallen gevonden rondom de nominale waarden van het gezuiverde water en slibproductie als gevolg van variaties in het influent. Ten tweede zijn er relatief kleine afwijkingen gevonden als gevolg van variaties in de begintoestand. Ten slotte is het effect van additieve structurele model-onzekerheid op de beoordelingscriteria te verwaarlozen, als dat vergeleken wordt met de effecten van parameter onzekerheid.

In het laatste gedeelte van deze dissertatie wordt een stapsgewijze benchmarking procedure geschetst (paragraaf 7.3) en de toepassing van de benchmark geïllustreerd (hoofdstuk 8). In paragraaf 8.2 wordt de benchmark toegepast om het effect van de horizontale snelheid van stikstofverwijderingsprocessen te bestuderen. In oxidatiesloten hebben de beluchters twee functies: (i) het inbrengen van zuurstof in het systeem, en (ii) het creëren van een horizontale snelheid tussen 0.25 tot 0.60 m/s. Deze snelheid is noodzakelijk om te voorkomen dat slib deeltjes niet bezinken. Deze studie heeft aangetoond dat kleine variaties in de horizontale snelheid aanzienlijke effecten op het stikstofverwijderingsproces hebben. Hierbij is uitgegaan van een niet limiterende opgelost-zuurstof concentratie. Voor een efficiënte verwijdering van de stikstof moet dus rekening worden gehouden met de horizontale snelheid. Anderzijds kan de horizontale snelheid ook onafhankelijk gemaakt worden van zuurstoftoevoer door het gebruik van "boosters" en bellenbeluchters in plaats van mechanische beluchters.

In paragraaf 8.3 wordt de benchmark gebruikt voor de evaluatie van enkele regelstrategieën voor de AWZI in Rotterdam. Dit heeft geleid tot de volgende resultaten. Verandering van de split ratio van het influent tussen de eerste beluchter en de vierde beluchter heeft geen significant effect op de *TN*-concentratie in het effluent. Daarnaast is gebleken dat het belangrijk is om rekening te houden met de nabezinktank in een lange-termijn evaluatie.

Tenslotte worden in hoofdstuk 9 de praktische toepasbaarheid van de ontwikkelde benchmark geëvalueerd en de conclusies van dit onderzoek besproken. Dit hoofdstuk sluit af met een bespreking van de belangrijkste vernieuwende bijdragen van dit onderzoek:

- De ontwikkelde benchmark procedure is speciaal geschikt voor oxidatiesloot AWZI's.
- Het generieke karakter van deze procedure maakt het mogelijk om voor elk type AWZI een benchmark te maken.
- Er is een praktisch toepasbare en eenvoudige methode voor de schatting van de standaard zuurstofoverdracht (*SOTR*) in oxidatiesloten ontwikkeld.
- Korte en lange termijn criteria voor de beoordeling van het gedrag van oxidatiesloot AWZI's zijn geformuleerd.
- Er zijn systematische procedures ontwikkeld voor de schatting van parameters en beoordeling van onzekerheid.

Curriculum Vitae

Abdalla Abdelgadir Ahmed Abusam was born in August 1956 in El-Fashir/Sudan. He received his bachelor degree in Civil Engineering in 1982, from the University of Khartoum. From 1982 to 1984, he worked with the National Cooperation for Water in El-Fashir. In 1985, he joined the Administration for Sanitary Engineering in Khartoum. In 1986, he obtained M.Sc. in Sanitary Engineering from University of Khartoum. At the end of 1988, he traveled to the USA. In January 1989, he started following the Master of Public Health (MPH) program at the University of Illinois at Chicago (UIC), where, in June 1990, he obtained the MPH in Environmental and Occupational Health Sciences. In October 1992, he asked for political asylum in The Netherlands. In August 1995 and after studying the Dutch language for about two years in Rotterdam, he joined Wageningen University, where in 1997 he obtained M.Sc. in Environmental Technology. In June 1998, he started his Ph.D. studies at the Department of Systems and Control Group, Wageningen University. From February 2000 to June 2001, he worked as a scientific researcher by the Department of Systems and Control Group, Wageningen University. Since July 2001, he is with Lettinga Associates Foundation.